This is a preprint draft. The published article can be found at: https://doi.org/10.1016/j.pmatsci.2019.100577

Please cite this article as:
Naser M.Z. (2019). "Extraterrestrial Construction Materials." *Progress in Materials Science*. Vol. 105, 100577. https://doi.org/10.1016/j.pmatsci.2019.100577.

Extraterrestrial Construction Materials

M. Z. Naser, PhD, PE
Glenn Department of Civil Engineering, Clemson University, Clemson, SC, 29634, USA
E-mail: mznaser@clemson.edu, m@mznaser.com, Website: www.mznaser.com

Abstract

In recognition of the 50th anniversary of the first manned lunar landing, the National Aeronautics and Space Administration (NASA), together with the European Space Agency (ESA), revealed plans to resume manned exploration missions and to establish permanent human presence in outposts (habitats) on the Moon and Mars by 2040. In order to promote feasible and sustainable space exploration, these habitats are envisioned to be built from lunar and Martian in-situ resources. Our understanding of such indigenous resources, from materials science, construction and structural engineering points of view, is lacking and continues to hinder further development of Earth-independent habitats. In order to bridge this knowledge gap, a comprehensive assessment on the physical features and property characteristics of extraterrestrial construction materials such as those exploited from the Moon and Mars, mined from near-earth objects (NEOs), or cultured through modern technologies is presented herein. This review explores the suitability of construction materials derived from lunar and Martian regolith along with concrete derivatives, space-native metals and composites, as well as advanced and non-traditional materials for interplanetary construction. This review also identifies processing techniques suitable to produce non-terrestrial construction materials in the alien environment of space (i.e. vacuum, low gravity etc.) and highlights emerging trends and future directions to stimulate further research in this area.

Keywords: Space exploration, extraterrestrial materials, interplanetary construction, processing methods, vacuum, radiation.

This is a preprint draft. The published article can be found at: https://doi.org/10.1016/j.pmatsci.2019.100577

Please cite this article as:
Naser M.Z. (2019). "Extraterrestrial Construction Materials." *Progress in Materials Science*. Vol. 105, 100577. https://doi.org/10.1016/j.pmatsci.2019.100577.

Table of Contents

This is a preprint draft. The published article can be found at: https://doi.org/10.1016/j.pmatsci.2019.100577

Please cite this article as:
Naser M.Z. (2019). "Extraterrestrial Construction Materials." *Progress in Materials Science*. Vol. 105, 100577. https://doi.org/10.1016/j.pmatsci.2019.100577.

Abbreviations

ACI	American Concrete Institute
AI	Artificial intelligence
AIAA	American Institute of Aeronautics and Astronautics
ASCE	American Society of Civil Engineers
ALRS-1	Australian Lunar Regolith Simulant Type 1
ALS	Arizona Lunar Simulant
ASCE	American Society of Civil Engineers
BMG	Bulk metallic glass
BSA	Bovine Serum Albumin
C/C	Carbon/carbon composites
CLRS	Chinese Lunar Regolith Simulant
CNSA	China National Space Administration
DBP	Dibutylphthalate
DCM	Dichloromethane
DMSI	Dry-Mix/Steam-Injection
DSP	Densified with small particle
EGBE	Ethylene glycol butyl ether
ESA	European Space Agency
FJS	Fuji Japanese Simulant
HMP	hot-melt polyamide
ICRP	International Commission on Radiological Protection
IOH	Inorganic-organic hybrid
ISRFE	In-situ repair, fabrication and expansion
ISRO	Indian Space Research Organisation
ISRU	In-situ resource utilization
ISS	International Space Station
JAXA	Japanese Aerospace Exploration Agency
JMSS-1	Jining Mars Soil Simulant Type 1
JSC	Johnson Space Center
KOHLS-1	Korea-Hanyang Lunar Simulant Type 1
LENS	Laser Engineering Net Shaping
MDF	Macro defect free
MLS-1	Minnesota Lunar Simulant Type 1
MLS-2	Minnesota Lunar Simulant Type 2
MMS	Mojave Mars Simulant
NASA	National Aeronautics and Space Administration
NEOs	Near-earth objects
NEU-1	Northeastern University Lunar Simulant Type 1
NU-LHT-1M	Lunar Highlands Type 1M

PE	Polyethylene
PLGA	Polylactic-co-glycolic acid polymer
PMA	Polymer micro-agglomerations
RBC	Regolith Bio-Composite
SEI	Space Exploration Initiative
SHS	Self-propagating high-temperature synthesis
SMAs	Shape memory-alloys
SMCs	Shape memory-ceramics
SMH	Shape memory hybrid
SMMs	Shape memory materials
SMPs	Shape memory-polymers
SNC	Shergotty-Nakhla-Chassigny
SPD	Space Policy Directive
UV	Ultraviolet
VA	Volcanic Ash
XPS	X-ray photoelectron spectroscopy

A Brief History to Modern Space Exploration

Space exploration is the process of investigation and discovery of outer space (beyond Earth's atmosphere) by means of evolving technologies that may include manned or unmanned spacecraft, remote sensing probes etc. While the notion of exploring the outer space dates back to early civilizations, serious attention was first directed towards exploring nearby bodies such as the Moon and Mars [1]. In pursuit of this desire to explore, a series of milestones took place as a result of the extensive research and military efforts that were carried out during 1940-1960's. These events include the successful launch of the first: rocket, *Vergeltungswaffe-2*, to cross the Kármán line and reach space in 1944, satellite (i.e. *Sputnik 1* in 1957), probe to reach the Moon (viz. *Luna 2* in 1959), and interplanetary flyby (in 1962 when *Mariner 2* flyby Venus) [2–4]. Shortly after, the American and Soviet space programs also succeeded to land a number of unmanned spacecraft

This is a preprint draft. The published article can be found at: https://doi.org/10.1016/j.pmatsci.2019.100577

Please cite this article as:
Naser M.Z. (2019). "Extraterrestrial Construction Materials." *Progress in Materials Science*. Vol. 105, 100577. https://doi.org/10.1016/j.pmatsci.2019.100577.

and rovers on the Moon and Mars, commissioning a new era of space exploration (see Fig. 1). A natural successor to these efforts was to send manned missions and astronauts to low Earth orbit.

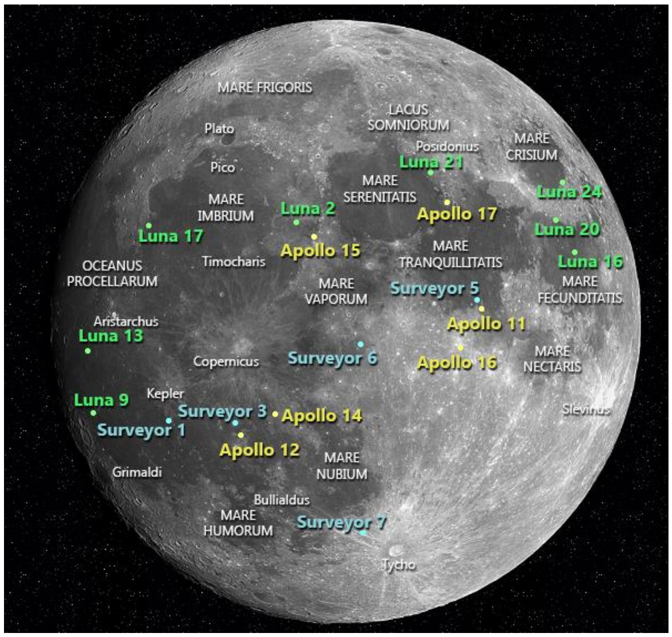

(a) Selected landing sites on the Moon (American missions; *Apollo* and *Surveyor* missions, Russian missions; *L*

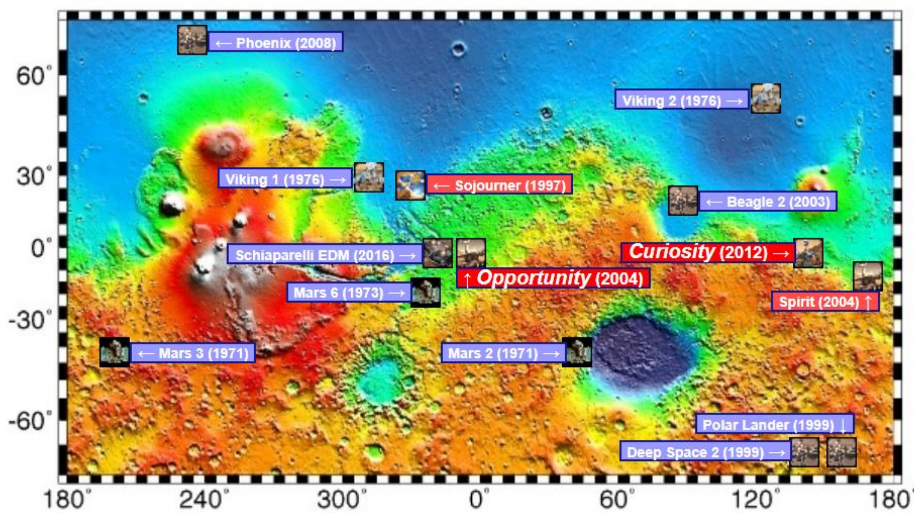

(b) Selected landing sites on Mars (American missions; *Vikings, Phoenix, Sojourner, Curiosity, Opportunity, Spirit, Deep Space 2, Polar Lander*, Russian missions; *Mars 2* and *3*, European missions; *Schiaparelli* and *Beagle 2*) – Red label; Rover, Blue label; Lander

Fig. 1 Selected landing sites on the Moon and Mars (Courtesy of NASA)

The 1960's witnessed the first time humans have been into space, when Yuri Gagarin completed an orbit of Earth in 108 minutes in *Vostok 1* spacecraft in 1961. He was followed by Alexey Leonov who was the first human to walk in space when he exited the *Voskhod 3KD's* capsule for a 12 minute spacewalk in 1965 [5]. This decade also marked an intense period where the American and Soviet space agencies pursued a transition from short-term manned orbital missions and spacewalks to extended crew landings and on-site stays. In 1969, this goal was fulfilled when the crew of Apollo 11 successfully landed on the Moon and then returned safely to Earth. This landing was followed by five manned landings (Apollo 12, 14, 15-17). These missions shared common objectives; to explore features of the Moon, examine its environment and assess the feasibility of establishing a lunar outpost.

The next logical step to follow up on the success of Apollo missions was to design and found a permanent and functional base on the Moon. According to Ganapathi et al. [6], the development of a lunar base was expected to proceed in five stages spanning over a 10-year period. The first stage started by an initial lunar landing in the 1969-71, followed by a Moon exploration stage in 1972-74, then experimentation and prototyping of a number of base designs in 1974-1976, lunar resource utilization in 1976-1978, and advanced resource exploitation in 1978-1980. Unfortunately, the political climate after the last lunar landing in 1972, i.e. cold war, oil crisis, and NASA's reprioritization towards *Skylab* – a low Earth orbit research space station, was not very supportive of continuing manned exploration missions. This, when combined with the realization that many technical challenges associated with establishing a lunar base were not effectively addressed, have halted manned missions to the Moon. As a result, research efforts in the early 1980's were heavily directed towards developing strategies to overcome some of the unresolved challenges such as radiation effects, physical and psychological issues relating to long-term stays in space, and most of all exploring in-situ resources for utilization in order to allow feasible and self-sustaining space exploration [7].

In-situ resource utilization (ISRU) is defined as an operation that collects and processes indigenous resources encountered during the course of human (or robotic) space exploration in order to minimize Earth-dependency. The first documented discussion of this concept was aimed at providing solutions to produce propellant fuel using Martian local resources to return to the Earth after an extended exploration mission. According to Steinhoff [8], ISRU has the potential of reducing overall space exploration costs by a factor ranging between 10 to 50 times. This concept was then extended to collect resources for building a permanent lunar/Martian outpost and then expanded into *in situ repair, fabrication and expansion (ISRFE)* which capitalizes on the need for means that allow quick repairs of habitats in case of emergencies, as well as feasible and smooth expansion from outposts and habitats into colonies [9].

In 1989, President Bush initiated the *Space Exploration Initiative (SEI)* and committed to returning to the Moon as well as to exploring Mars. During this period of time, the space community was divided between those who pursued Moon colonization and those who seek to find a home on Mars [10]. Whereas the Moon represents the ideal test bed for examining human capability to function and live in space as transportation to (and from) the Moon requires less energy, time, and cost than that required to reach Mars (i.e. flight duration is about 3 days to the Moon and can take up to 300 days to Mars) [11]. It is still of equal importance to note that the extreme environment of the Moon (i.e. lack of atmosphere, low gravity, heavy radiation etc.) creates additional complexities that have yet to be resolved. On the other hand, the rationale behind pursuing Mars as an alternative to the Moon arises from the more favorable conditions present on the Martian surface (e.g. reduced radiation, improved gravity and atmosphere/environmental conditions). In fact, Paine [12] projected that the first manned mission to Mars can take place by 2015. Paine also predicted that the first Martian base would be ready by 2035 and that the population on Mars would reach 10,000 and 100,000 people by 2065 and 2085, respectively. Thus, the red planet was further examined in 1996 through a series of successful landings including *Pathfinder* and *Sojourner*.

Until the mid-1990's, most of space exploration efforts were mainly carried out by the American and Russian space agencies. In 1998, and as a result of international co-operation efforts between North America, Russia, Japan and the European Union, the *International Space Station (ISS)* was launched into Earth orbit. This station, fitted with a space-based research laboratory, provides a platform in which up to six astronauts can live and conduct research for extended durations [13]. It is worth noting that the ISS has been continuously occupied for the last 17 years with international crews and is expected to continue to operate until 2028.

The decade spanning over the late 1990s and 2000s, perceived a global and growing interest in space exploration. For a start, NASA launched *Spirit* and *Opportunity* rovers in 2003 to further explore the environment and surface of Mars in more detail. In 2007, the *China National Space Administration (CNSA)* became the third agency to send a spacecraft to the Moon when *Chang'e 1* orbited, mapped and finally *hard-landed* (crashed) on the Moon surface. *Tiangong-1*, a space station and research laboratory, was also launched by CNSA and orbited the Earth from 2011 to 2018 [14]. The Chinese space program announced timelines for future missions including plans for sample returns from the Moon (*Chang'e 5* in 2019) and a manned lunar landing by 2036.

In similar efforts, *Chandrayaan-1* was launched by the *Indian Space Research Organisation (ISRO)* and successfully landed on the Moon in 2008 [15]. The objective of this probe was to prepare a three-dimensional atlas of the Moon as well as to perform chemical and mineralogical mapping of the lunar surface. The success of this mission has paved the way for *Chandrayaan-2*; which is planned to take place by the end of this year.

The last decade witnessed the rise of privately funded space programs and organizations (i.e. *SpaceX*, *Blue Origin*) aimed at establishing commercial space exploration and interplanetary transportation using cutting edge technologies such as reusable launching systems, autonomous retrieval systems etc.) [16,17]. These organizations/corporations also intend at establishing privately owned space manufacturing industries and mining colonies. Earlier this year, SpaceX's *Falcon Heavy*, which has the highest payload capacity of any currently operational launch vehicle, was successfully tested. This rocket measures at 70 m tall, with three boosters containing 27 engines, and is capable of transporting 63.8 tons into low Earth orbit or delivering 16.8 tons to Mars. Falcon heavy is to be succeeded by the next generation fully reusable rocket; the *Big Falcon Rocket*, in early 2020's. The BFR will have a height of 106 m with payload capacity from Earth to Mars of 150 tons and from Mars to Earth of 50 tons[1] [18].

Although most of the aforementioned research and exploration efforts were tailored towards exploring the Moon and Mars, the last few years also noted the discovery of a number of exoplanets and Super-Earths, such as *Kepler-452b* and *Gliese 667 Cc*. These exoplanets, while seeming to have more preferable atmosphere and host much more Earth-like conditions [19,20],

[1] *Saturn V* remains the tallest (110 m) and most powerful rocket ever to carry humans beyond Earth's orbit and to the Moon during the Apollo era. Saturn V had a full capacity of 11.8 tons [436].

Please cite this article as:
Naser M.Z. (2019). "Extraterrestrial Construction Materials." *Progress in Materials Science*. Vol. 105, 100577. https://doi.org/10.1016/j.pmatsci.2019.100577.

they however, are positioned at a much farther distance than the Moon or Mars and have not been fully investigated for possible manned missions. At the same time, concepts to modify the atmosphere of the Moon or more possibly Mars, through *terraforming* (or *Earth-shaping*), has been proposed [21]. Terraforming is the practice of engineering a space body's atmosphere in terms of temperature, pressure, or ecology into that of the Earth. Regrettably, terraforming of the Moon or Mars can take thousands of years and may not be practical with current technologies [22]. As a result, present research efforts continue to be focused on developing strategies and solutions to mitigate the harsh environment of the Moon and Mars.

The current administration has re-established the main objectives of its space program in 2017 when President Trump signed the *Space Policy Directive (SPD)*, and said

> *"It [SPD] marks a first step in returning American astronauts to the Moon for the first time since 1972, for long-term exploration and use. This time, we will not only plant our flag and leave our footprints -- we will establish a foundation for an eventual mission to Mars, and perhaps someday, to many worlds beyond."*

At the time of this review, plans to resume manned missions to the Moon in the next decade (possibly by 2024), to orbit Mars, and finally to land on Mars by 2030s have been announced by the National Aeronautics and Space Administration (NASA) as well as the European Space Agency (ESA) [23]. Announcements made by the aforementioned agencies as well as their international peers, seem to converge on the notion that lunar and Martian habitats could be established as early as 2040.

This review is motivated by the notion that in order to realize permanent and Earth-independent space habitats within the next two decades, serious inertia is to be directed towards developing novel, and preferably extraterrestrial, construction materials. In order to promote feasible and self-sustaining habitats, this review emphasizes the role of in-situ resources, and as such, explores the suitability of materials derived from lunar and Martian resources (regolith and rocks) along with concrete and metallic derivatives, advanced composites, modern and non-traditional materials for interplanetary construction. To provide a thorough assessment, processing techniques required to fabricate the aforementioned construction materials in space are reviewed and emerging trends and future directions to stimulate and accelerate research in this area are highlighted.

Space Environment and Resources

The space hosts a multitude of unique environments and conditions that are fundamentally dissimilar to those on Earth. Some of these environments include hard vacuum, extreme radiation, temperature fluctuation, weak atmosphere and low gravity, as well as space debris effects [24]. A comparative discussion of these environments and conditions is discussed herein.

Space Environment

Both the Moon and Mars host hostile environments. These environments arise from key differences in the characteristics of the Moon and Mars. A transitory description of these environments is of importance to identify abnormalities and critical factors that could potentially hinder future space exploration efforts; and by extension the realization of space habitats. For a start, Table 1 shows that both the Moon and Mars are of much smaller mass than that of the Earth and due to their smaller size, the Moon and Mars also have lower gravity than the Earth's (estimated at about 16.7% and 38% of that on the Earth, respectively). These low gravity levels, and the fact that these bodies seem to lack active tectonic plates, produce insignificant Moonquakes and/or Marsquakes [25]. In one study, Oberst and Nakamura [26] estimated that a lunar habitat could experience a shallow Moonquake of magnitude greater than 4.5 only once in 400 years. On the other hand, Marsquakes are a bit more frequent and active than the Moon. It is worth noting that most of the observed Moonquakes and Marsquakes are a result of geo-physical processes such as cracking caused by contraction from thermal cycles, burst of underground magmas and meteoritic impacts which can reach a speed of 20-70 km/s (72×10^3-252×10^3 km/hr) [27].

Table 1 Differences between Earth, Moon, and Mars [28,29].

Parameter	**Earth**	**Moon**	**Mars**
Mass (kg)	5.9×10^{24}	7.3×10^{22}	6.4×10^{23}
Diameter (km)	12742	3474	6779
Surface area (km^2)	196.9×10^6	37.9×10^6	144.8×10^6
Surface gravity (m/s^2)	9.81	1.62	3.71
Seismic energy (J/yr)	$10^{17\sim18}$	$2.0\times10^{10\sim14}$	-
Atmospheric pressure (kPa)*	101.3	3×10^{-13}	0.7
Main composition**	N_2, O_2	He, Ar	CO_2, Ar
Surface temperature extremes (°C)	-89.2 to 56.9	-171 to 111	-143 to 35
Diurnal cycle (hrs)	23.9	656	24.7
Orbital period (days)	365.3	29.5	687
Average radiation level (mSv)	2.4	380	100
Distance from Earth (km)	-	384.4×10^3	54.6×10^6
Flight duration from Earth (days)	-	~3	100-300

*1 kPa = 7.5 torr., **N_2: Nitrogen, O_2: Oxygen, He: Helium, Ar: Argon, CO_2: Carbon dioxide

The low gravity of the Moon and Mars also imposes other adverse effects such as weak atmosphere which causes low atmospheric pressure, extreme temperature cycles, and weak shielding to *space weathering*, i.e. radiation and micrometeorite. For example, the Moon does not have an atmosphere and hence its surface is calm as it experiences a negligible pressure estimated at 3×10^{-13} kPa. The Martian atmosphere, on the other hand, mainly comprises of carbon dioxide and nitrogen, and is about 1 percent as dense as that on Earth (atmosphere at surface is equivalent to that at an altitude of 30,000 m on Earth) [30]. Due to Mars' weak atmosphere, strong wind formation is not common and can only reach a maximum speed of 100 km/hr at specific locations.

The weak lunar atmosphere also causes rapid diurnal temperature fluctuations of about 5°C/hr. Moreover, lunar surface temperature can range from 111°C to −171°C, resulting in major thermal expansion/contraction and thermal cycling effects. This diurnal cycle on the Moon is 27.3 Earth (or sidereal) days, almost evenly split between 14 days in daylight and 14 days on nighttime. On Mars, however, temperature change is much less severe with an average temperature around -125°C near the poles and 20°C near the equator. This warm temperature at the equator can fall to about -73°C during nighttime. The duration of a solar day on Mars, *Sol*, is much closer to Earth (i.e. one day on Mars lasts 24 hours, 37 minutes, and 22 seconds as compared to 23 hours, 56 minutes, and 4.1 seconds on Earth) [31,32]. On a similar note, the orbital period of the Earth completes every 365.3 days, while it takes 29.5 and 687 days on the Moon and Mars, respectively.

The space around the Moon and Mars contains different types of radiation sources [33]. Of interest to this review are three types of radiation: solar wind, galactic cosmic rays, and solar cosmic rays (which are quite rare but intense). Space radiation comprises mainly of protons, electrons, and some heavier nuclei. Depending on their intensity, the radiation energies can span up to eight orders of magnitude; reflecting the level of solar activity due to irregular emission of energetic particles [24]. Radiation particles continuously interact with the surfaces of the Moon and Mars and may penetrate depths that vary from micrometers to several meters. The radiation levels on the Moon and Mars are quite high reaching 380 and 100 mSv, respectively [34].

Fortunately, the thick atmosphere of Earth negates most of the adverse effects of space weather. This atmosphere primarily consists of oxygen and nitrogen, carbon dioxide, neon, etc., and manages to minimize extreme temperature fluctuation and radiation effects arising from solar flares and galactic cosmic radiation formed by supernovas [35]. The atmosphere of Earth also provides adequate pressure level (≈101.3 kPa) and acts as an effective shield against micrometeorites impact. As a result, radiation levels on Earth's surface remain practically low (of about 1~2.4 mSv) as compared to the Moon or Mars[2].

The harsh nature of lunar and Martian environments is unfavorable to human life, and to materials as well. From a materials science perspective, weak gravity/weightlessness not only influences materials formation, but also its fundamental processes such as multiphase flow, surface wetting and interfacial tension, as well as constituent properties including mass transport and heat from fluid to solid state (solidification), both of which affect microstructure and pore development. Similarly, severe vacuum conditions cause materials to outgas and release volatiles (molecules) which accelerate material deterioration and fluid loss [36,37]. In the case where vacuum conditions are combined with ultraviolet (UV) radiation, the net effect of these actions causes oxygen vacancies in oxides, leading to significant color changes. This is especially true in most non-metallic materials (i.e. polymers) which experience damage either through cross-linking (hardening) or chain scission (weakening) [38].

Space Resources

The Moon and Mars, as well as near-Earth objects (NEOs) have an abundance of resources; most notably trapped ice pockets (water), metals, minerals, rare substances, Helium-3 etc. These resources could be directly utilized in-situ or harvested and transported either back to Earth, a space mining station, or to the Moon/Mars for processing and further utilization [39].

[2] Note: the recommended maximum dose of radiation is 0.05 Sv/yr [35].

From this work's perspective, any effort to expand the footprint of humankind without utilizing extraterrestrial resources will be, as was the Apollo program, self-limiting, and by today's measures, disappointing [40]. Hence, exploration missions should strive to achieve self-sufficiency through capitalizing on space resources. This section highlights a variety of space resources that could serve as construction materials whether directly or through minimum processing. A detailed discussion on physical and engineering properties of these materials is presented in a later section.

Lunar and Martian In-Situ Resources

Much of the present knowledge on lunar and Martian resources is derived from remote sensing operations, coupled with analyses of returned samples (i.e. oil and rocks) such as those collected by Luna or Apollo missions. The returned lunar samples, estimated at 382 kg, were collected from nine sites at the lunar near-side[3] covering both the *Maria* and *Highlands*[4] (see Table 2). Those samples present a limited geographical area estimated at 6% of the total lunar face [41]. While actual samples have not been returned from Mars as of yet, landed rovers continue to map and closely analyze indigenous resources on the red planet.

The Moon and Mars are mainly covered with fines, commonly referred to as *regolith*. While the term soil is sometimes used synonymously with regolith, this term actually refers to finer fractions (of diameter <10 mm) of the unconsolidated fragments and materials the covers the

[3] The near side of the Moon is the lunar hemisphere that is permanently turned towards the Earth, whereas the opposite side is the far side of the Moon.

[4] The Maria (plural of Mare, *sea*) are plain surfaces of somewhat darker color made of solidified *basaltic* lava from earlier periods of active lunar volcanism. The Maria are lower in altitude than the Highlands and occupy about 15% of the lunar near face. The Highlands, which are often called *terrae* (singular terra, from the Latin for *Earth*), have a lighter color and were formed during the time interval from about 4.5 Gy to about 3.9 Gy ago [437]. The main composition of Highlands is largely *anorthosite*; an igneous rock that forms when volcanic lava cools slowly (than in the case of basalts).

lunar and Martian surface. The lunar and Martian regolith has two potential applications, first as a building material or as raw material for construction- or industrial-based processes.

Table 2 Apollo missions return samples [24,42] (refer to Fig. 1a for location of key sites)

Mission	Landing site	Latitude	Longitude	Sample return (kg)
Apollo 11	Mare Tranquilitatis	0.67 N	23.49 E	21.7
Apollo 12	Oceanus Procellarum	2.94 S	23.45 W	34.4
Apollo 14	Fra Mauro	3.67 S	17.46 E	42.9
Apollo 15	Hadley Rile	26.11 N	3.66 E	76.8
Apollo 16	Descartes	8.60 S	15.31 E	94.7
Apollo 17	Taurus-Littrow	20.17 N	30.80 E	110.5
Luna 16	Mare Fecunditatis	0.68 S	56.30 E	0.101
Luna 20	Mare Fecunditatis	3.57 N	56.50 E	0.055
Luna 24	Mare Crisium	12.25 N	62.20 E	0.170

Regolith is formed from a collection of effects namely, *comminution* (breakage of rocks into smaller particles due to meteorites and micrometeorites impact, *agglutination* – welding minerals and fragments by glassy melts resulting from micrometeorite impacts, and *solar wind spallation* (as a result of high energy particles sputtering) and hence most grains comprising regolith contain about 1000 angstrom thick radiation-damaged rims of various solar-wind implanted atoms (i.e. hydroxyl radical, •OH) [43,44]. *Fragmentation* is another highly abrasive process worthy of mentioning. This process yields fine dust of small size of less than 3-10 μm. Space weathering effects do not only form the lunar and Martian regolith, but also continue to change its characteristics and properties over time. A thorough examination of space weathering effects is avoided herein for brevity as it can be found in Taylor et al. [45] as well as McKay et al. [46].

Apollo astronauts have reported that the lunar dust tends to levitate due to electrostatic potentials produced by photoelectron effects [47]. The Martian dust, on the other hand, is of a disc-shape with an aspect ratio of 0.1. The fine particles of Martian dust (0.1-10 μm) remain suspended in the atmosphere and give Mars its red color [48]. Overall, the depth of the lunar regolith layer varies between 3-20 m and can reach about 60 m in Highlands [49]. On the other hand, Gilmore [50] estimated that the Martian regolith can reach much deeper depth of about 90-113 m. Figures 2a, b and c show lunar soil and rock samples collected by Apollo 11 and 16. A photograph of Martian regolith, as captured by Mars rover *Curiosity* in 2012, is also presented in Fig. 2d.

This is a preprint draft. The published article can be found at: https://doi.org/10.1016/j.pmatsci.2019.100577

Please cite this article as:
Naser M.Z. (2019). "Extraterrestrial Construction Materials." *Progress in Materials Science*. Vol. 105, 100577. https://doi.org/10.1016/j.pmatsci.2019.100577.

(a) Lunar sample no. 67075 (Cube edge is 10 mm)

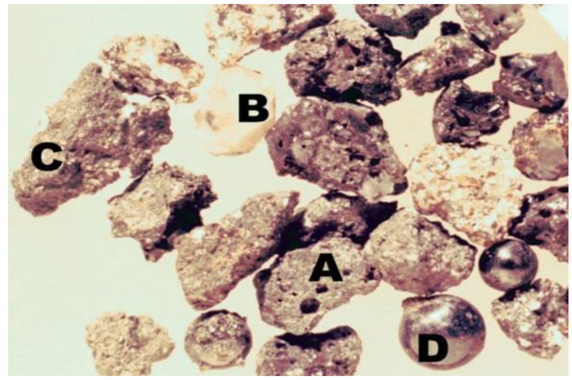

(b) Fragments of the main types of lunar rocks: basalt (A), anorthosite (B), and breccia (C), glass spherules (D).

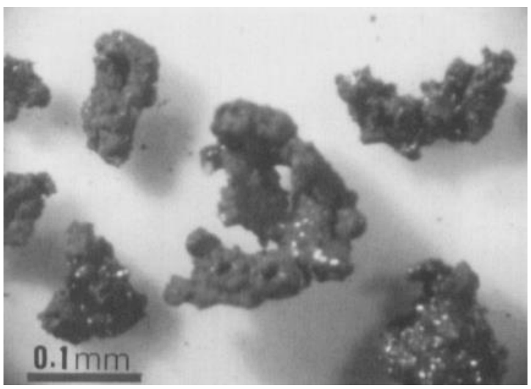

(c) Microscope photograph of agglutinates separated from Apollo 11 soil sample no. 10084, (NASA Photo S-69-54824)

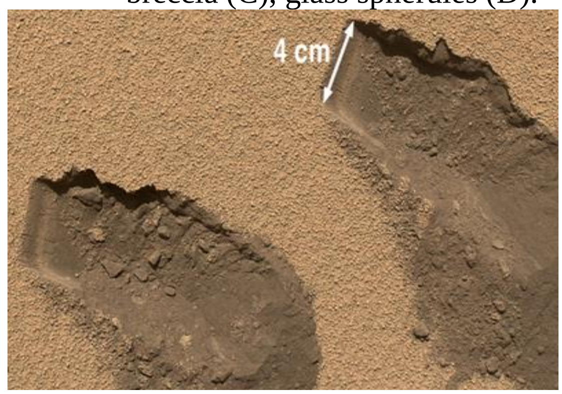

(d) Martian soil

Fig. 2 Samples of lunar and Martian soil and rocks (Courtesy of NASA)

A number of researchers analyzed lunar soils (and rocks) collected by NASA such as Ryder and Norman [51], Fruland and Reimold [52], as well as Morris et al. [53] (see Table 3 and supplementary illustration in Fig. 3). These studies have shown that collected regolith and rocks comprise of high amounts of silica (SiO_2) and alumina (Al_2O_3) of about 46.61-47.1% and 9.3-21.4% of weight, respectively. These samples also contained moderate amounts of calcium oxide (CaO) estimated at 7.78-11.64%. Results of remote sensing carried out by *Viking*, *Pathfinder*, *Opportunity*, and *Curiosity* probes on Mars noted the availability of high amounts of SiO_2, as well

This is a preprint draft. The published article can be found at: https://doi.org/10.1016/j.pmatsci.2019.100577

Please cite this article as:
Naser M.Z. (2019). "Extraterrestrial Construction Materials." *Progress in Materials Science*. Vol. 105, 100577. https://doi.org/10.1016/j.pmatsci.2019.100577.

as Al_2O_3, ranging approximately from 43.4-55% and 7.2-12.4%, respectively as well as noted the presence of a lower concentration of CaO than that on the Moon (refer to Fig. 3 and Table 3). It should be remembered that the presence of aforementioned constituents promotes production of cementitious-based construction materials. A dedicated discussion on this aspect is presented in a subsequent section.

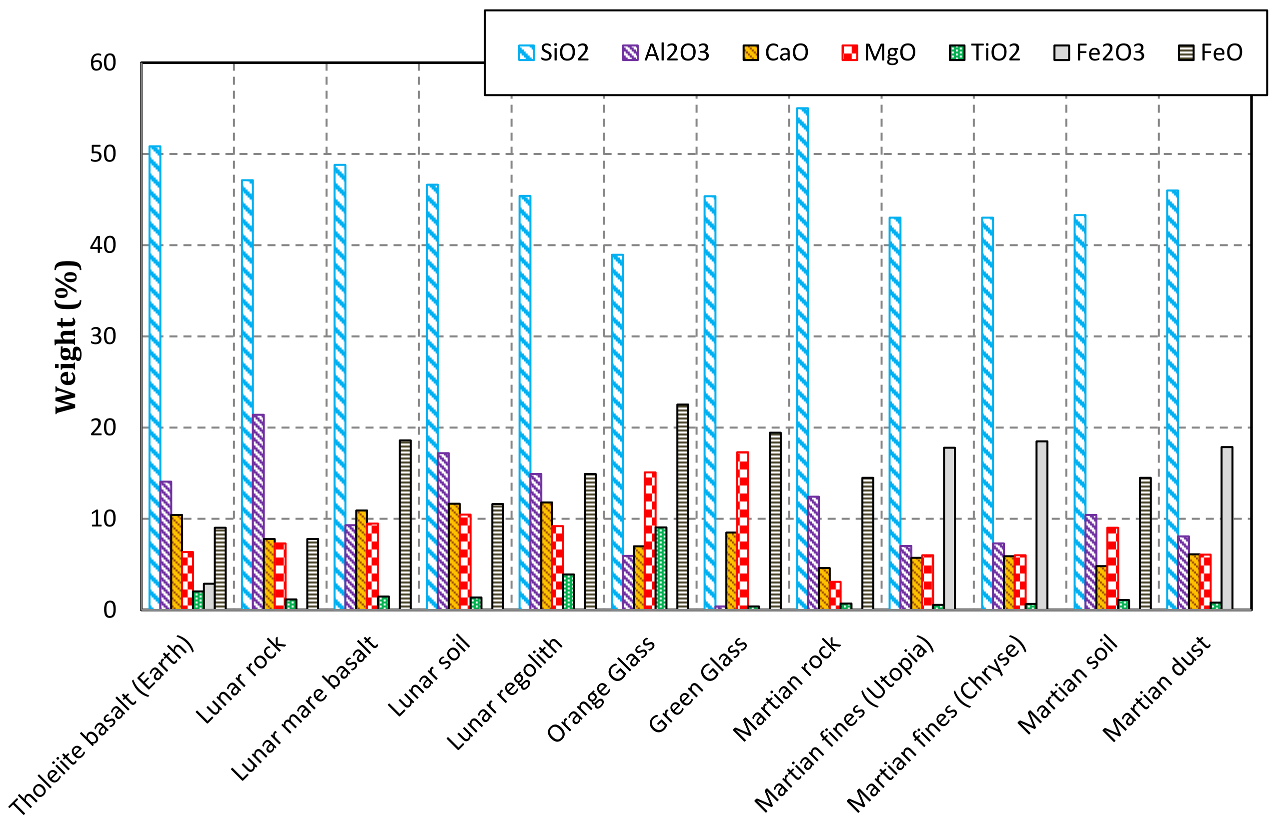

Fig. 3 Comparison in chemical contents of Earth, lunar and Martian in-situ resources

This is a preprint draft. The published article can be found at: https://doi.org/10.1016/j.pmatsci.2019.100577

Please cite this article as:
Naser M.Z. (2019). "Extraterrestrial Construction Materials." *Progress in Materials Science*. Vol. 105, 100577. https://doi.org/10.1016/j.pmatsci.2019.100577.

Table 3 Chemical content of Earth, lunar and Martian soil, rock, and dust samples

	Earth	**Lunar materials**								**Martian materials** [54]			
Constituent	**Basalt**	**Rock***	**Mare basalt****	**Soil****	**Regolith****	**Regolith (Highland)**	**Yellow-brown glass#**	**Orange glass** [55]	**Green glass** [56]	**Rock+**	**Surface fines++**	**Surface fines+***	**Dust**
SiO_2	50.83	47.10	48.8	46.61	45.4	45.5	42.7	38.94	45.38	55.0	43.0	43.0	43.4-48.6
Al_2O_3	14.07	21.40	9.30	17.18	14.9	24.0	8.68	5.94	0.38	12.4	7.0	7.3	7.2-8.3
FeO	9.0	7.78	18.6	11.62	14.1	5.9	22.4	22.51	19.44	14.5	-	-	-
Fe_2O_3	2.88	-	-	-	-	-	-	-	-	-	17.8	18.5	17.5-18.2
MgO	6.34	7.29	9.46	10.46	9.2	7.5	12.5	15.10	17.29	3.1	6.0	6.0	6.07.5
CaO	10.42	7.78	10.9	11.64	11.8	11.8	8.45	6.99	8.49	4.6	5.7	5.9	5.8-6.3
K_2O	0.82	0.48	0.03	0.20	-	-	0.06	0.07	0.02	1.4	<0.15	<0.15	0.1-0.3
Na_2O	2.23	0.70	026	0.46	0.6	-	0.60	-	-	4.2	-	-	1.3-2.2
TiO_2	2.03	1.16	1.46	1.36	3.9	0.6	3.75	9.04	0.38	0.7	0.56	0.66	0.6-1.1
P_2O_5	-	0.42	0.03	-	-	-	-	-	-	-	-	-	-
MnO	0.18	0.11	0.27	0.16	-	-	0.35	-	-	0.5	-	-	-
Cr_2O_3	-	0.25	0.66	0.25	-	-	-	-	-	-	-	-	-
SO_3	-	-	-	-	-	-	-	-	-	-	8.1	6.6	5.4-7.2

*Obtained from Apollo 14, **Obtained from Apollo 15 [57], #Obtained from Apollo 15, +Obtained from Pathfinder mission, ++From Utopia location, +* From Chryse location.

When meteorites (or micrometeorites) impact the lunar surface, the energy dissipating from this impact often melts surrounding regolith. The same could also occur due to volcanic eruptions on the Moon or more commonly on Mars. The melted regolith, if cooled rapidly can turn into *glass* [58]. A variety of glass is found in the lunar soils, most notably in samples collected by the crews of Apollo 15 and 17. In fact, astronauts from Apollo 15 and 17 collected brown-yellow, green, and orange soil samples with varying glass contents in the range of 6-92% of total weight (see Table 3 for composition of glasses). The green glass was analyzed and found to be of primitive basaltic composition, while the orange and brown-yellow glass was formed through Mare basalt eruption. In the case where melted regolith is left to slowly cool down, this melt tends to crystallize instead of turning into glass. This crystalized melt is referred to as *cast regolith* [59]. Figure 4 shows selected samples of lunar glass and cast regolith collected by the Apollo missions. The following section shows how both glass and cast basalt have superior mechanical properties.

(a) Glass-coated basalt melt sample no. 64455

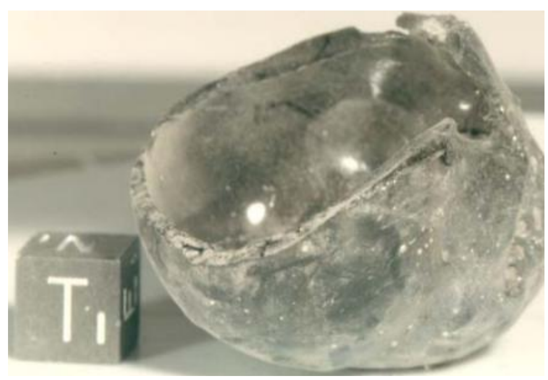

(b) Green glass sample no. 65016 (Cube edge is 10 mm)

Fig. 4 Samples of basaltic melt and glass (Courtesy of NASA)

Another resource that could potentially be utilized in constructions on the Moon or Mars is *sulfur*; given its abundance on the Moon and Mars (in the form of the mineral troilite, FeS) [60]. Depending on its crystal form, sulfur melts at 112.8°C (orthorhombic) or 119°C (monoclinic), begins to turn viscous at about 160°C, and boils around 444.6°C [61]. These features of sulfur allow its ease of processing in lunar and Martian environments and integration into binding of non-hydraulic construction materials as well as production of sulfuric acid (H_2SO_4) frequently used in extraction of metals. While sulfur is available in partial amounts on the Moon (reaching a maximum of 0.27% in high-titanium Mare basaltic lavas), sulfur is much more available on Mars with amounts reaching a minimum of 1-3% by soil/regolith weight [62].

Experiments carried out under vacuum ($< 2\times10^{-6}$ torr) by Gibson and Moore [63] on samples obtained from Apollo 15 and 16 indicate that 12-30% of the total sulfur in lunar regolith can be extracted at 750°C. At higher temperatures reaching 950°C, 50-70% of sulfur can be extracted, and a much higher volume of sulfur (up to 85-95%) can also be extracted at temperatures close to 1100°C. Based on findings of Gibson and Moore [63], Vaniman et al. [60] estimated that thermal processing of mildly crushed regolith of a volume of 1000 m^3 could yield one ton of sulfur. Sulfur can also be extracted from regolith through oxidation of troilite (FeS) to magnetite (Fe_3O_4) which yields SO_2 [64]. Sulfur is also a by-product of oxygen and water production from Martian calcium sulfate dihydrate, $CaSO_4{\cdot}2H_2O$, and anhydrite ($CaSO_4$). This process can yield sulfur in masses up to 10 percent of the mass of oxygen produced such that:

$$CaSO_4 \cdot 2H_2O \rightarrow CaSO_4 + 2H_2O \rightarrow CaO + SO_2 + {}^{1}\!/_{2}\, O_2 \qquad \textit{Eq. 1}$$

$$SO_2 \rightarrow S + O_2 \qquad \textit{Eq. 2}$$

Reactions presented in Eqs. 1 and 2 show that while extracting sulfur, lime (CaO) can also be produced as part of this reaction. Using this technique can result in energy-efficient production of cementitious sulfur-based extraterrestrial construction materials[5].

Binder [65], Happel [66] and Fairén et al. [67] managed to examine a number of actual lunar regolith samples, as well as the data obtained from the Martian surface and noted the abundant presence of *metals* such as magnesium, aluminum, iron, and titanium (see Fig. 5). Fortunately, obtaining these minerals does not require dedicated mining as the processes necessary to extract oxygen or water from lunar and Martian regolith also produce metals at the same time. Still, metals are not often produced in pure conditions but rather in the form of oxides (refer to Table 3), thus a challenge of extracting these metals from chemically bonded oxides could potentially arise. Once extracted, these metals can be used in construction and structural applications on the Moon and Mars.

[5] It is worth noting that the vast majority of the 64×10^6 metric tons of sulfur produced worldwide is a byproduct sulfur from refineries utilizing the *Claus* process in which gases with an H_2S content of over 25% are processed to recover sulfur such that: $2H_2S + 3O_2 \rightarrow 2SO_2 + 2H_2O$ *and*, $4H_2S + 2SO_2 \rightarrow 3S + 4H_2O$. Sulfur can also be extracted through mediated bacteria as proposed by White and Hirsch [438].

This is a preprint draft. The published article can be found at: https://doi.org/10.1016/j.pmatsci.2019.100577

Please cite this article as:
Naser M.Z. (2019). "Extraterrestrial Construction Materials." *Progress in Materials Science*. Vol. 105, 100577. https://doi.org/10.1016/j.pmatsci.2019.100577.

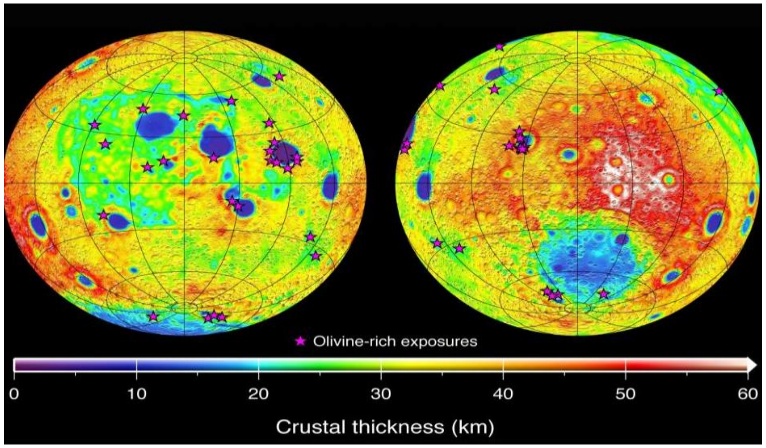

(a) Distribution of olivine (magnesium iron silicate (Mg, Fe_2SiO_4) in lunar crust - stars are locations obtained by Japanese spacecraft Kaguya)

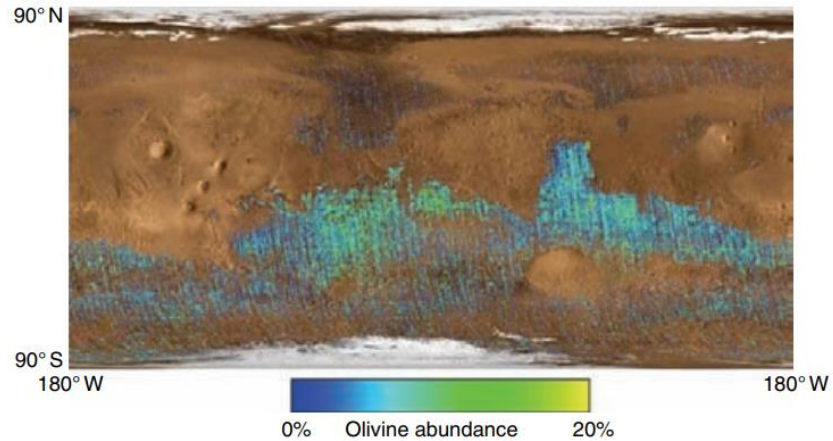

(b) Mineral map of olivine on Mars

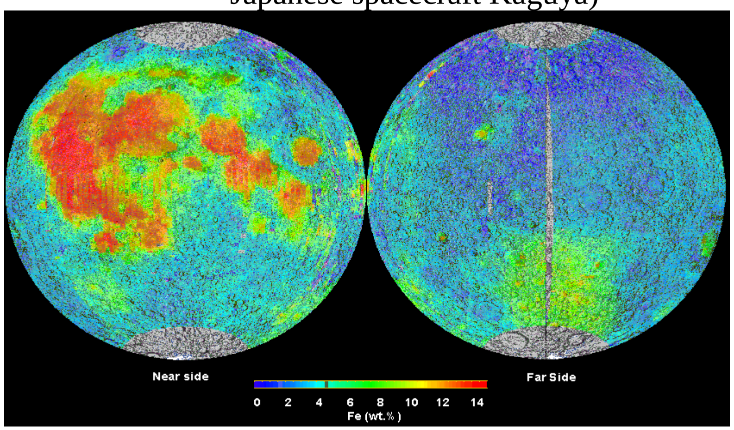

(c) Concentration of iron in the lunar surface.

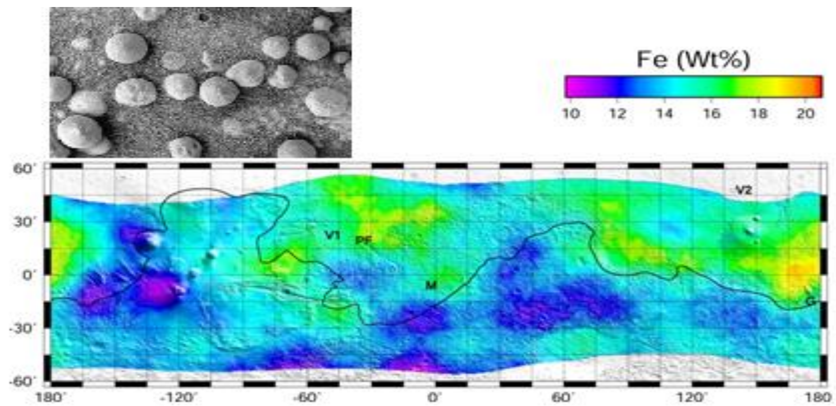

(d) Iron distribution on Mars (top insert shows iron ore found at the Meridiani landing site). – top left insert (not to scale)

This is a preprint draft. The published article can be found at: https://doi.org/10.1016/j.pmatsci.2019.100577

Please cite this article as:
Naser M.Z. (2019). "Extraterrestrial Construction Materials." *Progress in Materials Science*. Vol. 105, 100577. https://doi.org/10.1016/j.pmatsci.2019.100577.

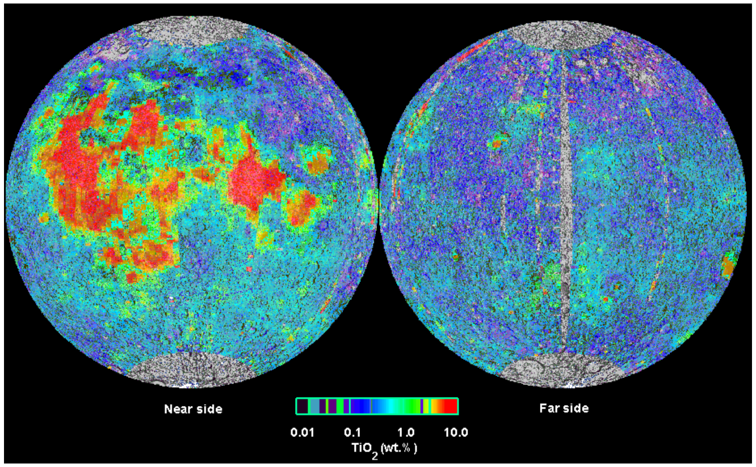

(e) Concentration of titanium in the lunar surface

Fig. 5 Metal content on the Moon and Mars (Courtesy NASA/JPL-Caltech/Cornell as well as NASA/JPL/University of Arizona)

More specifically, Papike et al. [68] and McCallum et al. [69] observed high concentration of magnesium oxide reaching about 47.1 wt.% in the naturally occurring compound; olivine (i.e. magnesium iron silicate (Mg, Fe_2SiO_4)). This popularized the merit of extracting magnesium for use in construction purposes. Magnesium can be extracted through a carbothermal process that yields carbon monoxide, hydrogen, and magnesium oxide (see Eq. 3). Landis [70] noted that magnesium can also be obtained by refining olivine to a mixture of CaO and MgO (see Eq. 4). The *Pidgeon* method is an energy efficient process often used to produce magnesium on Earth and can be applied on the Moon and Mars as well. This process involves heating dolomite ore via a reduction reaction with ferrosilicon (FeSi) to high temperatures in order to evaporate magnesium and then cool it down to obtain magnesium metal as shown in Eq. 5.

$$Mg_2SiO_4 + 2CH_4 \rightarrow 2CO + 4H_2 + 2MgO \qquad Eq.3$$

$$2MgO + 2CaO + Si \rightarrow 2Mg + 2Ca_2SiO_4 \qquad Eq.4$$

$$2MgO + 2CaO + FeSi \rightarrow 2Mg + Ca_2SiO_4 + Fe \qquad Eq.5$$

Another equally promising metal for extraterrestrial construction is aluminum. Aluminum is the third most abundant metal on the Moon and can be found in the form of aluminum oxide (Al_2O_3) with concentrations as high as 15% in lunar Highlands and 24-33% in lunar feldspar ($KAlSi_3O_8$ – $NaAlSi_3O_8$ – $CaAl_2Si_2O_8$) [65,71]. Aluminum can be extracted through breaking down anorthitic plagioclase ($CaAl_2Si_2O_8$) or plagioclase (CaAl,NaSi)$AlSi_2O_8$, which contains 19.4% aluminum, through a carbothermal reduction reaction [72]. Other processes may also include, carbochlorination process. This process magnetically separates regolith to remove ilmenite ($FeTiO_3$), which is then electrostatically separated to isolate anorthite in a carbochlorination unit where it can be further processed, such that:

$$CaAl_2Si_2O_8 + 8C + 8Cl \rightarrow CaCl_2 + 2AlCl_3 + 2SiCl_4 + 8CO \qquad Eq.\ 6$$

The produced aluminum chloride ($AlCl_3$) is condensed and mixed with alkali and alkaline chlorides for aluminum extraction by electrolysis. It is interesting to note that the alkali and alkaline chlorides, which are to be brought from Earth, can be recycled, and used in future processes – favoring the adoption of electrolysis. Landis [70] examined the extraction of aluminum via a fluoridation process and vacuum pyrolysis (see Eq. 7). Other processes, including acid digestion of regolith, were also proposed [73].

$$Al_2O_3 + 3F_2 \rightarrow 2AlF_3 + 3/2O_2 \qquad Eq.7$$

Opportunity rover found iron ores on Mars of approximately 50% hematite by weight; the mineral form of ferric oxide (Fe_2O_3) (see top left insert in Fig. 5d). Extraction of iron from silicate minerals or the oxide-based mineral ilmenite can be energy intensive. However, iron extraction is stipulated to be a natural by-product of producing oxygen through a number of processes such as ilmenite reduction (as shown in Eq. 8) or carbothermal reduction as can be seen in Eq. 9.

$$FeTiO_3 + H_2 \rightarrow Fe + TiO_2 + H_2O \qquad Eq.8$$

$$FeTiO_3 + 4C \rightarrow Fe + TiC + 3CO \qquad Eq.9$$

Similar to aluminum, the fluoridation process can also be used to extract iron (see Eq. 10). The product of the fluoridation process is a fluoride salt, which can be purified and then reduced to iron.

$$2FeO + 3F_2 \rightarrow 2FeF_3 + O_2 \qquad Eq.10$$

Reactions presented in Eqs. 8 and 9 show that titanium dioxide (TiO_2) and titanium carbide (TiC) can be by-products of iron extraction. Thus, titanium which has favorable structural-based properties can be produced and used in extraterrestrial construction. Titanium has higher yield strength and is of a much lighter density as compared to iron. Titanium is also available in the form of ilmenite ($FeTiO_3$) and can be extracted through ilmenite reduction, using hydrogen as a reducing agent as shown in Eq 8. Titanium can also be produced through a dedicated electro-chemical process such as described by Schwandt et al. [74] as well as fluoridation [70]. Fluoridation of titanium would require additional processing to recuperate titanium from the distilled titanium tetrafluoride through a reaction with potassium such that:

$$TiO_2 + 2F_2 \rightarrow TiF_4 + O_2 \qquad Eq.11$$

$$TiF_4 + 4K \rightarrow Ti + 4KF \qquad Eq.12$$

Near-Earth objects (NEOs)

Near-Earth Objects (NEOs) are small bodies such as comets and asteroids. These bodies are often nudged, by means of gravitational forces generated from nearby larger bodies (planets), into orbits allowing them to be in the vicinity of Earth. NEOs can be classified according to their compositions into three groups, C-type, S-type, and M-type. C-type NEOs are primarily made of carbonaceous rocks and contain up to 22% water. These NEOs are very dark (least reflective) with an albedo of 0.03-0.09. C-type asteroids inhabit the main belt's outer regions and are the most abundant type (approximated at nearly 75% of the total asteroid population). S-type NEOs are typically made of stony materials and make up to 15-17% of population of NEOs. They are mainly consisting of iron- and magnesium-silicates and due to their relatively higher density, these NEOs dominate the inner asteroid belt. On the other hand, M-type NEOs contain heavy metals of more than 90% metallic nickel-iron-cobalt alloys and hence are very reflective with an albedo of 0.10-

0.18. These NEOs occupy the main belt's middle region [75]. According to NASA, the number of discovered NEOs exceeds 15000, with an average of 30 new discoveries added each week [76].

Lewis [77] and O'Leary [78] reported that some NEOs contain free metals at a concentration about 100 times that in the lunar or Martian soil and may also offer substances that are rare[6] or absent on the Moon or Mars (see Fig. 6). The fact that contents of plotted NEOs contain large amounts of S, SiO_2, CaO and metals, far exceeding that on the Earth, Moon or Mars, emphasizes the merit of *NEOs mining*; a process of harvesting mineral ores using manned and/or unmanned mining stations. In one study, O'Leary [78] detailed plans for a three-year space mining operation and promised to return 100×10^3 metric tons of free metals, 50×10^3 metric tons of water, 20×10^3 metric tons of carbon compounds. In his work, O'Leary [78] estimated that the energy required to produce aluminum for space construction purposes from lunar regolith is 15-25 times higher than that needed to produce the same metal from an asteroid. This heavily favors the merit of NEO mining.

[6] Such as rare-earth elements as well as platinum (which can be used for power generation in space). Concentration of platinum on Earth is about 7.1 ppb, on the Moon ≈15 ppm, on Mars ≈ 17 ppb, and in iron NEOs of about 63.8 ppm [115,439,440].

This is a preprint draft. The published article can be found at: https://doi.org/10.1016/j.pmatsci.2019.100577

Please cite this article as:
Naser M.Z. (2019). "Extraterrestrial Construction Materials." *Progress in Materials Science*. Vol. 105, 100577. https://doi.org/10.1016/j.pmatsci.2019.100577.

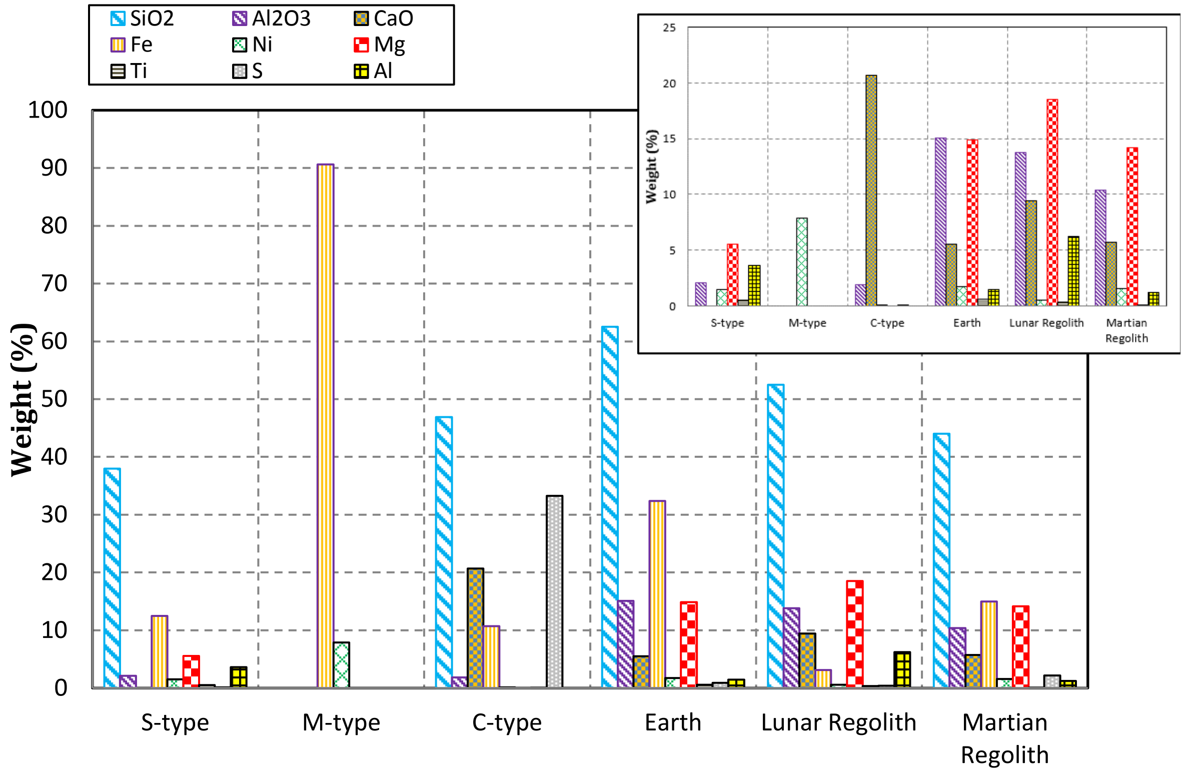

Fig. 6 Mineralogical and chemical content of NEOs, lunar and Martian resources

Brophy et al. [79] estimated that a typical NEO (asteroid) with 7 m diameter and a mass ranging between 250 to 1000 metric kg can be mined for various elements that could be used as construction materials in addition to other necessary compounds for survival and power generation such as water and plutonium. Zacny et al. [80] stipulated that extracting regolith dust (or powder) from NEOs could be directly used for additive manufacturing of structural components (such as beams and trusses). In a more recent announcement, NASA estimated that asteroid *2012 DA14*, with a diameter 45 m and mass of 130×10^3 metric tons, can be harvested for $65 billion of water, and $130 billion in minerals [80]. Table 4 lists some of the NEOs suitable for the mining process.

Table 4 NEOs for mining process [81]

NEO	Estimated value (US$)	Composition
Anteros	5570 billion	Magnesium silicate, aluminum, iron silicate
Ryugu	95 billion	Nickel, iron, cobalt, water, nitrogen, hydrogen, ammonia
1989 ML	14 billion	Nickel, iron, cobalt
2001 SG10	4 billion	Nickel, iron, cobalt

The first step to realize asteroid mining for extraterrestrial construction is to identify possible mineral-rich NEOs that travel at relatively low speeds (preferably in the range of 5-8 km/s). Once a candidate NEO is identified, mining stations can trace and capture such a NEO for mining purposes (see Figure 7). When a NEO is captured, minerals and materials can then be mined and harvested. For example, NEOs with loose surface materials can be scraped using robotic attachments. Metals could also be collected using stationary or dynamic suction tubes or large magnets. Heating, together with mounding, can be used to extract minerals rich in nickel and iron. Tunnelling, through cutters/drillers, to mine NEOS, is another mean of extracting minerals. Other geo-physio-chemical methods could also be applied to mine compounds, elements, and de-alloy metals.

This is a preprint draft. The published article can be found at: https://doi.org/10.1016/j.pmatsci.2019.100577

Please cite this article as:
Naser M.Z. (2019). "Extraterrestrial Construction Materials." *Progress in Materials Science*. Vol. 105, 100577. https://doi.org/10.1016/j.pmatsci.2019.100577.

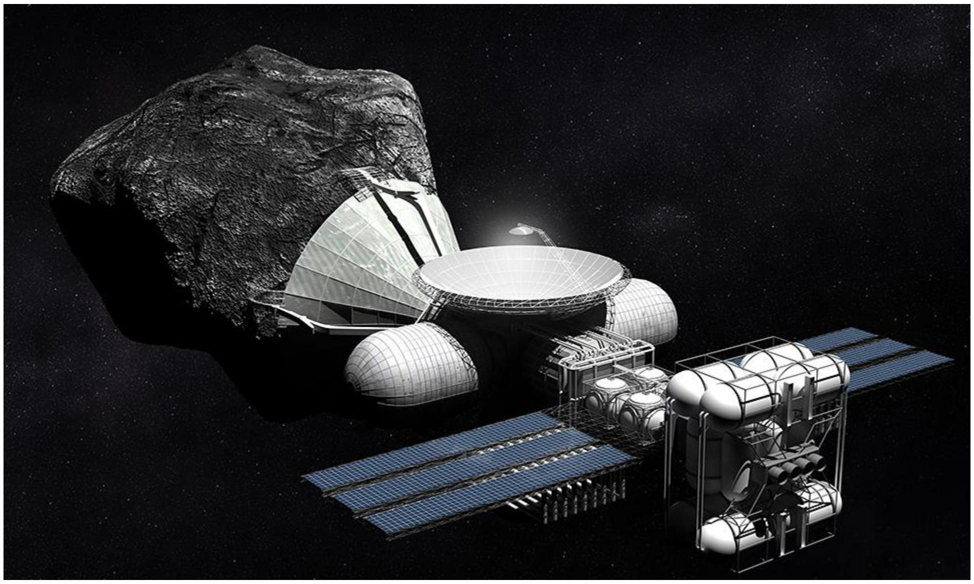

Fig. 7 Illustration of NEO mining station (Courtesy of Deep Space Industries)

To promote NEOs mining, NASA, among other agencies such as the American Institute of Aeronautics and Astronautics (AIAA) and American Society of Civil Engineers (ASCE), hosted number of conferences and workshops dedicated to developing enabling technologies to identify, trace, capture and transport NEOs. NASA and the Japanese Aerospace Exploration Agency (JAXA) also commissioned pilot missions for NEOs exploration. For instance, NASA's Galileo mission visited two asteroids in the inner edge of the main, belt namely, *951 Gaspra* and *243 Ida*. In 2010, the Japanese *Hayabusa* mission managed to successfully land on the asteroid *Itokawa*. Despite major technical difficulties, Hayabusa managed to collect 1500 grains of dust particles (with ranging sizes of 10-100 µm). A sample of dust particle collected by Haybusa is shown in Fig. 8. In 2016, NASA launched *OSIRIS-Rex* mission to study asteroid *101955 Bennu*, with a mass and diameter of 6.0×10^{10} kg and 492 m, respectively, and then return a sample to Earth by 2023. NASA also revealed new plans to robotically capture and transport small to medium-sized NEOs to low Earth orbit for mining [81].

This is a preprint draft. The published article can be found at: https://doi.org/10.1016/j.pmatsci.2019.100577

Please cite this article as:
Naser M.Z. (2019). "Extraterrestrial Construction Materials." *Progress in Materials Science*. Vol. 105, 100577. https://doi.org/10.1016/j.pmatsci.2019.100577.

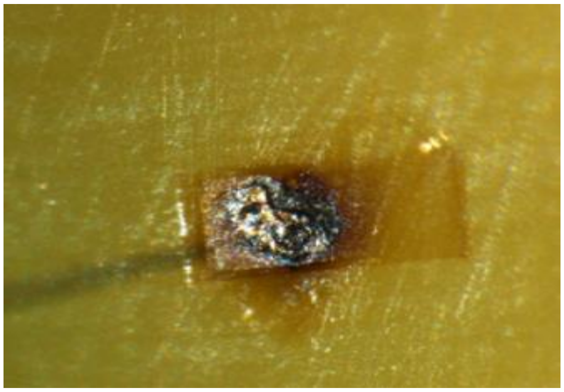

(a) Electron microscope photo

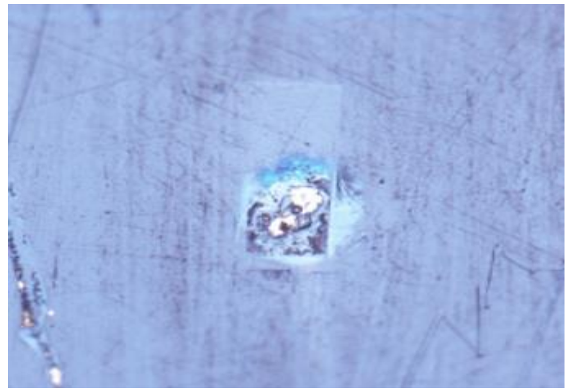

(b) optical microscope photo

Fig. 8 Sample of dust particles from Itokawa asteroid (sample no. RA-QD02-0027 (Courtesy of JAXA)) – size of sample = 91 μm, scale: unknown.

While Hayabusa remains the only mission to return a sample from a NEO back to Earth, much of our knowledge of substances from NEOs is either gathered by means of remote sensing technologies or in rare cases through analysis of meteorites fallen to Earth. Some of these meteorites were tracked down, found and then examined to understand their composition and origin. Table 5 breaks down the composition of some of lunar and Martian meteorites. It can be seen that there is good resemblance between lunar and Martian compositions as well as that of retrieved meteorites especially with regard to the presence of high amounts of silica, magnesium and iron oxides[7]. This observation agrees with those made by other studies such as by Lewis [82], Korotev [83] and Rubin and Ma [84]. Figure 9 shows a sample of rock originating from the Moon, *Miller Range 05035*, and recovered from Antarctica in 2005. This figure also shows a sample from a Martian meteorite, *Nakhla* is which fell in Egypt and was retrieved in 1911. Nakhla belongs to the Shergotty-Nakhla-Chassigny (SNC) group which is thought of to represent the surface of Mars,

[7] As a result, Landis [441] and West and Clarke [442] examined the feasibility of mining meteoritic steel as a construction resource on Mars.

This is a preprint draft. The published article can be found at: https://doi.org/10.1016/j.pmatsci.2019.100577

Please cite this article as:
Naser M.Z. (2019). "Extraterrestrial Construction Materials." *Progress in Materials Science*. Vol. 105, 100577.
https://doi.org/10.1016/j.pmatsci.2019.100577.

as their oxygen isotope ratios are not terrestrial and contain trapped gasses that closely resemble the Martian atmosphere [85–88].

Table 5 Composition of lunar and Martian meteorites

Constituent	**Lunar origin**		**Martian origin**					
	Soil [57]	**Miller Range 05035** [89]	**Regolith**	**Calcalong Creek** [90]	**Yamato 793169** [91]	**Nakhla**	**Shergotty**	**Chassigny**
SiO_2	46.61	48.39	43.3	47.3	43.59	49.33	51.36	38.16
Al_2O_3	17.18	10.50	10.4	20.5	12.89	1.64	7.06	0.69
FeO	11.62	20.70	14.5	9.66	21.42	21.7	19.41	27.10
MgO	10.46	5.90	9.0	7.51	5.75	11.82	9.28	31.6
CaO	11.64	13.70	4.8	12.9	13.25	14.30	10.0	0.60
K_2O	0.20	0.01	0.7	0.24	0.13	0.16	0.18	0.041
Na_2O	0.46	0.21	5.1	0.44	0.40	0.56	1.29	0.13
TiO_2	1.36	0.90	1.1	0.77	1.52	1.64	0.87	0.10
P_2O_5	-	0.02	-	0.16	0.29	0.10	0.80	0.058
MnO	0.16	0.33	0.5	0.14	0.18	0.55	0.525	0.526
Cr_2O_3	0.25	0.30	-	-	-	-	0.203	0.63

Compositions of Nakhla, Shergotty, Chassigny obtained from [92]

This is a preprint draft. The published article can be found at: https://doi.org/10.1016/j.pmatsci.2019.100577

Please cite this article as:
Naser M.Z. (2019). "Extraterrestrial Construction Materials." *Progress in Materials Science*. Vol. 105, 100577. https://doi.org/10.1016/j.pmatsci.2019.100577.

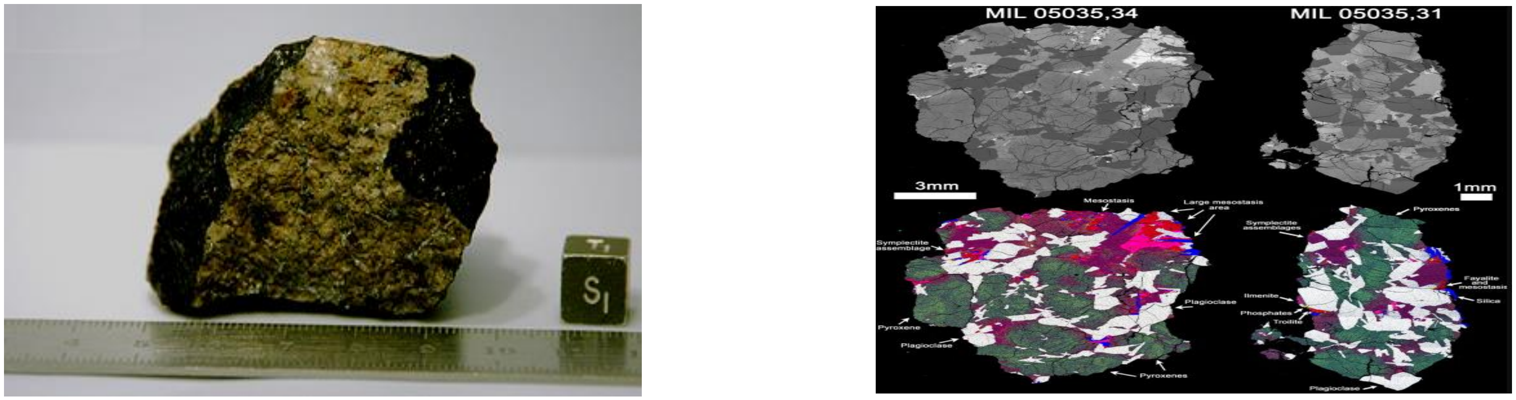

(a) Lunar meteorite - Miller Range 05035 (left), and microscopic view of sample (right). Colors correspond to: white represents high levels of aluminum; red represents iron; green represents magnesium; pink represents titanium; blue represents silicon. [89]

(b) Martian meteorite - Nakhla meteorite (left), and microscopic view of sample (right) - Courtesy of Chatzitheodoridis et al. [93]
Fig. 9 Samples of recovered lunar and Martian meteorites (meteorites images are courtesy of NASA)

This is a preprint draft. The published article can be found at: https://doi.org/10.1016/j.pmatsci.2019.100577

Please cite this article as:
Naser M.Z. (2019). "Extraterrestrial Construction Materials." *Progress in Materials Science*. Vol. 105, 100577. https://doi.org/10.1016/j.pmatsci.2019.100577.

Properties of Extraterrestrial Construction Materials

The Moon, Mars and NEOs hold a variety of resources that can directly be used in construction or can be processed to yield construction materials. This section reviews properties of construction materials obtained from space native resources as well as Earth-derivative building materials specifically developed for extraterrestrial construction purposes. The processing techniques associated with some of these materials, such as sintering and cold-pressing etc., are discussed in the following section.

Regolith Derivatives

Regolith

While r*egolith* is considered to be the most abundant resource with the highest potential for utilization on the Moon and Mars, there is limited information on the physical, thermal and mechanical properties of regolith [93]. Observations taken by researchers who analyzed returned lunar samples have noted that loose regolith is a relatively dense material, having a density that varies from 1500 kg/m^3 at the lunar surface to 1660 kg/m^3 at a depth of 60 m [94]. Mitchell et al. [94] analyzed core samples obtained from the landing site of Apollo 15 and derived a relation for the density of lunar regolith, ρ, as a function of depth, Z. This relation, as well as others reported by Carrier et al. [95] are presented in Eqs. 13-15:

$$\rho\ (gm/cm^3) = \rho_o + k\ln(Z+1) \qquad Eq.13$$

$$\rho\ (gm/cm^3) = 1.92 + \frac{Z+12.2}{Z+18} \qquad Eq.14$$

$$\rho\ (gm/cm^3) = 1.39Z^{0.056} \qquad Eq.15$$

where, ρ_o and k are fitting coefficients equals to 0.80-1.38 and 0.225 and 0.121, respectively. Z is measured in centimeters.

In a similar manner, rovers roaming the surface of Mars have reported that the density of Martian regolith also varies but on a much wider range between 1000 to 1900 kg/m^3 [96]. Due to the dense nature of regolith, the use of loose regolith for shielding purposes (to cover habitats from effects of radiation and micrometeoritic impacts) has been proposed over the past few decades [97,98]. These proposals estimated that a shielding layer of 3-5 m could be sufficient to prevent most adverse effects of long term exposure to lunar radiation as well as to dissipate impact energy from fallen micrometeorites. In the case of Mars, Ortiz et al. [99] proposed the use of 1 m thick layer or Martian regolith, due to the presence of a weak atmosphere (as oppose to lack of one on the Moon) as well as the possibility of Martian regolith to contain light elements (such as H, C or N) as these prove to be effective at stopping neutrons produced by primary cosmic rays.

In a notable study, Gromov [96] presented a comparison between the physical properties of lunar and Martian regolith. This comparison revealed that lunar and Martian regolith have an average grain size ranging from 40 to 270 μm and 70-800 μm, respectively. Gromov also reported that lunar soils have an average cohesion, angle of internal friction, and bearing capacity of 2.35 kPa, 18.5°, and 31 kPa, respectively. These properties were estimated at 0.75 kPa, 25° and 55 kPa for the Martian soil.

Khoshnevis et al. [93] showed that due to its poor thermal properties, a shielding layer of regolith could also act as a thermal barrier against extreme temperature fluctuations occurring on the Moon and Mars. The poor thermal properties arise from the fact that at low temperatures and atmospheric pressure, the small physical contacts between grains limit heat conduction and lead to extremely low bulk thermal conductivity. Langseth et al. [100] and Jakosky [101] estimated thermal conductivity of regolith to be as low as 0.001 W/m.K but averages between 0.9-1.6 W/m.K for lunar and 0.02-0.105 W/m.K for Martian regolith [93]. The specific heat of lunar regolith is 750-1000 J/kg.°C and is slightly higher than the specific heat of Martian regolith (500-600 J/kg.°C) [102]. In most studies, the thermal properties of regolith were shown to be a function of the microstructure and temperature of regolith, T. Colozza [103] derived two expressions (Eq. 16 and 17) to evaluate temperature-dependent thermal conductivity, k, and specific heat, c, for lunar regolith. In the meantime, expressions for thermal properties of lunar and Martian regolith are rare (see Eq. 18 for specific heat capacity obtained from Kieffer [104]), [105,106],

$$k_{Moon}\ (W/m.K) = 1.281\times10^{-2}+4.431\times10^{-2}T^{3} \qquad \text{Eq. 16}$$

$$c_{Moon}\ (J/kg.K) = 1848.5+1047.41\log(T) \qquad \text{Eq. 17}$$

$$c_{Mars}\ (J/kg.K) = 6.087\times10^{-2}(T-220) \qquad \text{Eq. 18}$$

From mechanical and geotechnical aspects, regolith particles are shown to be much sharper than their terrestrial counterparts. This sharpness arises from the nature of regolith formation, i.e. space weathering. The specific surface area of lunar regolith is high and measures at about 0.5 m^2/g which is about eight times larger than an assemblage of spheres with an equivalent particle size distribution [107]. Thus, it can be inferred that lunar regolith has high porosity (40-50%) and this has been reported in number of studies [107,108].

The sharp nature of regolith particles, when combined with favorable conditions, show that regolith can be pressed into blocks forming strong material with good interlocking properties [95,108]. This can be true, especially in the case of the Martian regolith. Depending on the location of where regolith is collected, Martian regolith can hold up to 3% of weight in water content. When cold-pressed, this regolith can form building blocks without any additives, referred to as *duricrete*

[109]. The pressing of regolith is often undertaken through mechanical pressure (of a magnitude of 9.8 MPa) [110]. The cold-pressed bricks can reach a compressive strength of 5 MPa.

Other than utilizing loose or cold-pressed regolith, lunar and Martian regolith can also be processed through melting, heating, or binding with additives [111]. This processing yields construction materials with much improved mechanical properties that can bypass those produced on Earth [66]. For instance, regolith can be melted through subjecting it to elevated temperatures or microwave-heating energy at 1200-1500°C. The melt can then molded into structural components (i.e. beams). Regolith can also be molded into pellets, bricks, or cylinders and then heated (sintered) to temperatures lower than its melting temperature (~1000-1200°C) [112]. While heating without the application of an external stress can remove much of the porosity in regolith, the fact of the matter is that the production of construction material with low permeability often requires the application of external stressing (in the range of few to hundreds of MPa). Simonds [112] expects that regolith collected from non-Mare sites can be readily heated since its glass component crystallizes slowly at temperatures at which glasses flow than Mare soil glasses. The cooled regolith, referred to as *cast regolith*, is a dense material that can be formed into building bricks or panels and be used in construction of civil infrastructure/habitats.

Taylor and Meek [107] showed that melting lunar regolith was possible due to the high presence of nanophase Fe^0; particles of iron with grain sizes less than 100 nm. Happel [66] reported that cast regolith has superior mechanical properties (i.e. stiffness, compressive and tensile strengths of 100 GPa, 538 and 34.5 MPa, respectively). As a result of its dominant-compressive nature of cast regolith, this material is expected to be adequate in compression-based (pre-stressed) structures. Due to its high density (reaching 3000 kg/m^3), structural panels made of cast regolith may have adequate radiation and thermal shielding properties. Cast regolith also has good toughness and abrasion resistance.

Taylor [113] reported that lunar regolith contains, on average 25% to 30% of agglutinates (i.e. lithic minerals and glass fragments embedded in a glass matrix). This also agrees with findings from Happel [66] who also reported that mature regolith, in some areas, could consist of 40% of glass and may reach 60% of sample weight. Hence, glass can also be mechanically collected from regolith or produced in-situ if melted regolith is cooled rapidly. This glass could be used to manufacture a variety of building elements (such as transparent components). With reported modulus of elasticity and bending strength of 450 GPa and 377.5 MPa, lunar and Martian glass could also be used to fabricate a variety of structural components such as bars, cables as well as reinforcing fibers. These products could be used as stand-alone structural members and could also be used to reinforced regolith and cementitious-based construction materials (duricretes). Table 6 lists thermal and mechanical properties of lunar and Martian regolith based construction materials.

Table 6 Properties of lunar and Martian materials made of in-situ resources

Property	**Lunar glass** [66,113,114]	**Lunar cast regolith** [113,115]	**Martian regolith** [93,113]
Compressive strength (MPa)	-	538	-
Tensile strength (MPa)	0.7-3000	34.5	-
Density (kg/m^3)	2700	900-3000	1000-1900
Modulus of elasticity (GPa)	450	100	-
Thermal coefficient of expansion	-	8×10^{-6}	-
Bending strength (MPa)	125-630	-	-
Fracture toughness (MPa.m$^{0.5}$)	2.5	2.0	-
Specific heat (J/kg°K)	-	672.4	500-600
Thermal conductivity (W/m°K)	-	0.0011	0.02-0.105

This is a preprint draft. The published article can be found at: https://doi.org/10.1016/j.pmatsci.2019.100577

Please cite this article as:
Naser M.Z. (2019). "Extraterrestrial Construction Materials." *Progress in Materials Science*. Vol. 105, 100577. https://doi.org/10.1016/j.pmatsci.2019.100577.

Cast and Sintered Basalt

With minimum processing to regolith, *cast basalt* can be produced. Cast basalt is a black, amorphous and homogeneous solid with glassy features. This cast basalt can be produced through melting or sintering. Dalton and Hohmann [116] showed how lunar regolith can be melted at high temperatures (~1320-1350°C). The molten regolith can then be controlled slowly cool down to 800°C to prevent bursting and imperfections arising as a result of annealing. After reaching 800°C, the melt can be further cooled to ambient conditions to solidify, turning into cast basalt within 24 hours. Given that the specific heat, latent heat of fusion and melting point of basalt are 0.8J/g.°C, 340 J/g and 1200°C, respectively, Binder et al. [117] estimated that it can take 1.3×10^3 MJ to melt one ton of regolith into cast basalt.

Cast basalt can be molded into bricks or plate-like structural members (slabs). Fibers can also be drawn from molten basalt at temperature range of 1250-1375°C. These fibers have an estimated tensile strength of 2-2.9 GPa and modulus of elasticity of 80 GPa [118]. Blacic [119], on the other hand, reported that lunar glass can be processed from cast basalt. Lunar glass can have high strength, reaching about 3.4 GPa. According to Rogers and Sture [120], melting regolith can produce a variety of engineering materials with high strength, and low variability in properties. Molten (liquid) cast basalt can also be used to weld (join) structural members in place; a feature that can allow in-situ repairs [117].

Similar to regolith, basalt can also be sintered when subjected to a source of energy such as that generated in a solar furnace supplemented with mechanical pressure of about 98 MPa [121]. Allen et al. [121] carried out thirty tests on sintered basalt. The basalt was first pressed at 324 MPa and then heated to 1000-1150°C in a furnace filled with argon to simulate the lunar environment as well as to prevent oxidation of grain surfaces. The outcome of these tests is depicted in Fig. 10. A closer look into this figure shows that sintering, in the case of basalt, is very dependent on the attained peak temperature. For instance, the strength of sintered basalt increases from 3.4 to 14.47 MPa when regolith is sintered at 1000°C as opposed to 1100°C, respectively. Further, sintered specimens seem to be slightly dependent on the duration of sintering as most specimen reached up to 90% of their maximum strength within the first 30 minutes. Hence, sintering can be a quick method for fabricating structural components on the Moon and Mars.

This is a preprint draft. The published article can be found at: https://doi.org/10.1016/j.pmatsci.2019.100577

Please cite this article as:
Naser M.Z. (2019). "Extraterrestrial Construction Materials." *Progress in Materials Science*. Vol. 105, 100577. https://doi.org/10.1016/j.pmatsci.2019.100577.

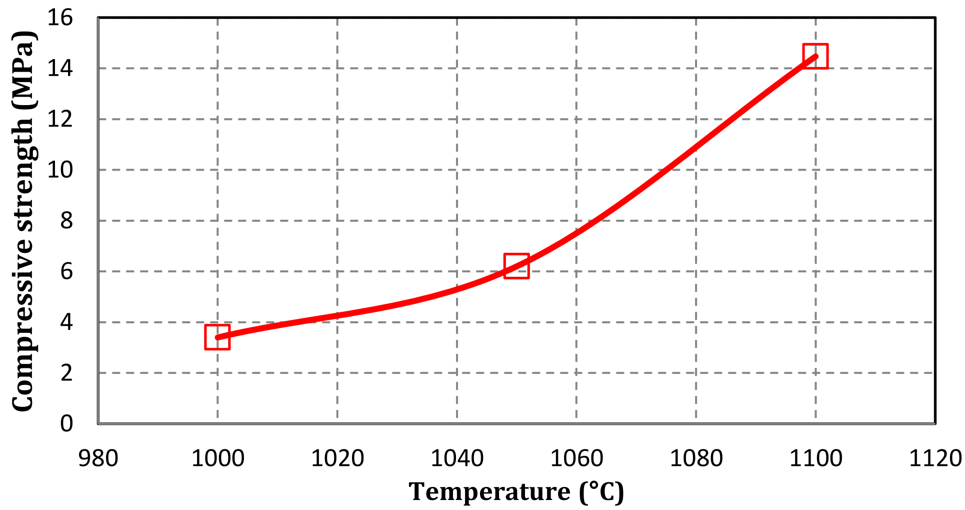

(a) Effect of sintering temperature

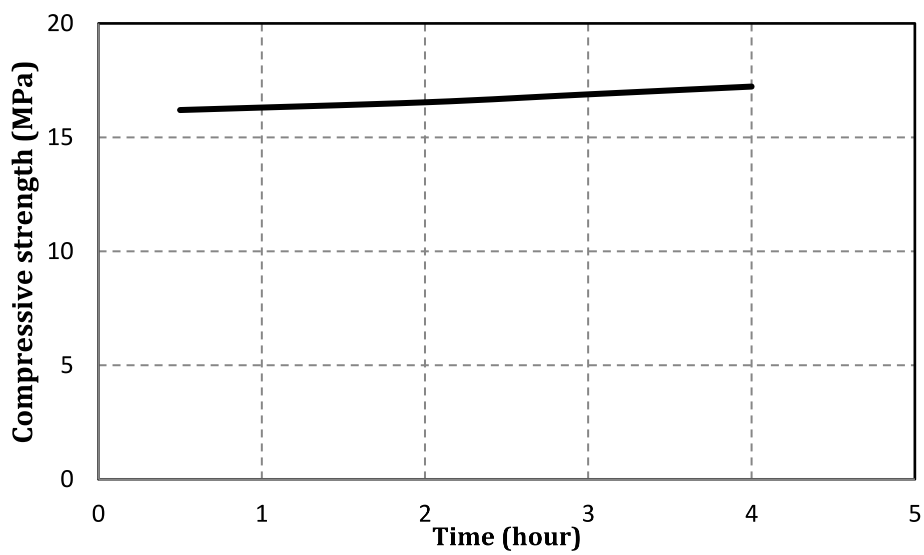

(b) Effect of sintering duration

Fig. 10 Results of tests on sintered basalt (from Allen et al. [121])

Table 7 lists properties of melted and sintered basalt. It can be seen that the density of cast basalt is relatively high, reaching a density of 3000 kg/m^3. Happel [66] reported that cast basalt has a high compressive strength to tensile strength ratio (approximated at a 1:15 ratio). Since cast basalt has a compressive strength ranging between 162-490 MPa, then the tensile strength of cast basalt can be estimated to be in the range of 10.8-32.7 MPa. Both of these properties exceed that of commonly used concretes.

Overall, basalt has high resistance to chemicals and abrasion effects but could be of a brittle nature under tensile actions [122]. Like other construction materials, cast basalt also has few limitations. Some of these limitations include high thermal conductivity and large shrinkage deformations during the cooling process which may induce thermal cracking. Surprisingly, the high hardness of cast and sintered basalt makes consequent processing (i.e. cutting and drilling) nearly impossible [123]. As such, care and precision in manufacturing/processing of cast and sintered basalt is warranted.

This is a preprint draft. The published article can be found at: https://doi.org/10.1016/j.pmatsci.2019.100577

Please cite this article as:
Naser M.Z. (2019). "Extraterrestrial Construction Materials." *Progress in Materials Science*. Vol. 105, 100577. https://doi.org/10.1016/j.pmatsci.2019.100577.

Table 7 Properties of cast and sintered basalt as reported in the literature.

Property	**Lunar origin**					**Martian origin**	
	Cast Basalt				**Sintered basalt**		
	Rogers and Sture [120]	**Dalton and Hohmann** [116]	**Kopecky and Voldan** [126,127]	**Capps and Wise** [128]	**Allen et al.** [121]	**Cast Basalt** [93,124]	**Basalt** [125]
Compressive strength (MPa)	300-550	392-490	399-501	162-203.5	3.4-14.47	162-490	-
Tensile strength (MPa)	36	24.5-34.3	25-35	10-14.25	-	10	14
Density (kg/m^3)	2900-3000	-	-	-	-	2900-3000	-
Modulus of elasticity (GPa)	110	-	-	-	-	-	73
Thermal coefficient of expansion (°C^{-1})	7.8×10^{-7}	7.8×10^{-7}	78×10^{-7}	-	-	$7.7\text{-}8.6 \times 10^{-6}$	-
Bending strength (MPa)	-	39.2-44.1	39-46	16.25-18.30	-	40	-
Hardenss (Moh)	-	8-9	-	-	-	-	-
Specific heat (J/kg°K)	-	837.4	-	-	-	500-800	-
Thermal conductivity (W/m°K)	8×10^{-6}	9.3×10^{-4}	-	-	-	0.02-0.105	-

Lunar and Martian Simulants

Due to the scarcity and limited accessibility to actual regolith as well as NASA's policy of limiting destructive tests on lunar samples, a number of lunar and Martian *simulants* were developed over the years[8]. Simulants are synthesized soils of terrestrial origin, formed with approximate mineralogy, physical and engineering properties as well as particle sizes to that of actual lunar and Martian regolith [129,130]. Table 8 lists a few lunar and Martian simulants commonly used by researchers and will be further discussed and referred to throughout this review [57,131]. This table also compares the chemical composition of the listed simulants. Judging by these compositions, one can see that while the listed simulants seem to have similar chemical composition, they vary slightly in their origin and contents of Fe_2O_3 and MgO (in lunar simulants) as well as Al_2O_3 and Fe_2O_3 (in Martian simulants).

[8] While simulants were developed to simulate lunar and Martian regolith, these simulants are still made of terrestrial materials. The discussion on differences between regolith and simulants is spared herein as findings of various studies, some of which were commissioned by international space agencies (i.e. NASA, JAXA), have shown lunar and Martian simulants to share enough resemblance to that of lunar and Martian regolith from materials science, construction, geotechnical and structural engineering perspectives [131,133]. As such, this review is carried out following judgment of notable studies in this field in which regolith simulants are assumed to be replicas of regolith. Still, to maintain transparency, this review distinguishes wherever simulants were used to produce or fabricate construction materials. Interested readers are encouraged to review the following resources to gain in-depth understanding of the history, development and suitability of simulants in mimicking lunar and Martian indigenous resources [131–136].

This is a preprint draft. The published article can be found at: https://doi.org/10.1016/j.pmatsci.2019.100577

Please cite this article as:
Naser M.Z. (2019). "Extraterrestrial Construction Materials." *Progress in Materials Science*. Vol. 105, 100577. https://doi.org/10.1016/j.pmatsci.2019.100577.

Table 8 Description of commonly used simulants [131–136]

Simulant	Origin	Remarks
JSC-1	From volcanic ash of basaltic composition.	One of the first lunar simulants to go in mass production. No longer available.
JSC-1A/AF/1AC	From volcanic ash deposited near Flagstaff, Arizona, USA.	The JSC-1 series is the most known simulants produced. It resembles low titanium Mare. It contains a high glass fraction as it is chemically similar to Apollo sample no. 14163.
FJS-1	From basaltic lava available near Mt. Fuji, Japan,	Mixed with crushed ilmenite and/or olivine.
DNA	Based on natural volcanic material to be found close to the Bolsena Lake (Italy).	-
NU-LHT-1M	From a combination of Stillwater Norite, Anorthosite, and Hartzburgite, and Twin Sisters Dunite.	Based on the average chemical composition of Apollo 16 regolith samples.
ALRS-1	Sourced from a basalt quarry in Kulnura, New South Wales.	Produced at the University of New South Wales and was specifically developed to test regolith sintering.
VA	From volcanic ash.	Contains augite, ferroan forsterite.
NEU-1	Prepared from cinder and basalt near Jinlong Peak in Jinlin Province, China.	-
ALS	Made of crushed rock from the Pomona basalt flow near Hanford, WA.	It was created as a Mare soil simulant to develop structural materials and ceramic composites.
MLS-2	A successor to MLS-1. Developed as a Highlands simulant by grinding up an anorthosite from the Duluth Gabbro Complex.	Produced in very small quantities.
KOHLS-1	-	-
CLRS	CLRS-1 is described as a low-Ti mare simulant, and CLRS-2 as a high-Ti mare simulant.	Produced by the Chinese Academy of Sciences.
JMSS-1	From mechanically crushing Jining basalt, a Miocene aged unit located in the North China craton.	-
JSC-Mar1/1A	A fine soil obtained from a Hawaiian cinder cone. (<1mm size fraction of altered volcanic ash).	-
MMS	Originates from the Saddleback volcanic formation located in the Western Mojave Desert near the town of Boron, California.	-

This is a preprint draft. The published article can be found at: https://doi.org/10.1016/j.pmatsci.2019.100577

Please cite this article as:
Naser M.Z. (2019). "Extraterrestrial Construction Materials." *Progress in Materials Science*. Vol. 105, 100577. https://doi.org/10.1016/j.pmatsci.2019.100577.

Constituent	Lunar simulants												Martian simulants		
	JSC-1	**JSC-1A**	**FJS-1**	**DNA**	**NU-LHT-1M**	**ALRS-1**	**VA**	**NEU-1**	**ALS**	**MLS-2**	**CLRS-2**	**KOHLS-1**	**JMSS-1**	**JSC-Mars-1**	**MMS**
SiO_2	47.71	46.67	49.10	41.9	47.6	42.36	43.4	44.92	48.0	48.3	41.89	54.56	49.28	34.5-44	49.40
Al_2O_3	15.02	15.79	16.20	17.8	24.4	13.48	15.3	17.23	13.5	32.4	13.41	16.73	13.64	18.5-23.5	17.10
FeO	7.35	8.17	8.30	10.5	4.30	-	9.75	13.09	7.0	0.45	15.90	-	-	2.5-3.5	-
Fe_2O_3	3.44	12.5	4.80	0.0	-	12.55	2.75	-	1.9	-		-	16.00	9-12	10.87
MgO	0.18	9.39	3.80	9.60	8.5	10.23	6.8	4.37	4.3	0.15	7.06	2.32	6.35	2.5-3.5	6.08
CaO	10.42	9.90	9.10	11.4	13.1	8.61	11.1	9.44	8.3	16.0	9.70	5.44	7.56	5-6	10.45
K_2O	0.82	0.78	1.00	0.60	-	1.49	1.7	3.01	0.5	0.06	0.78	3.38	1.02	0.5-0.6	0.48
Na_2O	2.70	2.83	2.80	0.7	1.4	3.29	4.5	3.97	2.7	2.42	2.34	2.28	2.92	2-2.5	3.28
TiO_2	1.59	1.71	1.90	1.60	-	2.73	2.9	2.87	1.6	0.03	7.62	0.70	1.78	3-4	1.09
P_2O_5	0.66	0.71	0.44	0.00	-	0.53	0.9	0.54	-	-	0.25	0.21	0.30	0.7-0.9	0.17
MnO	-	0.19	0.19	0.10	-	0.18	0.2	0.34	0.20	-	0.20	0.18	0.14	0.2-0.3	0.17
Cr_2O_3	0.04	-	-	0.20	-	-	-	-	-	-	-	-	-	-	0.05

JSC: Johnson Space Center, FJS: Fuji Japanese Simulant, NU-LHT-1M: Lunar Highlands Type 1M, ALRS-1, Australian Lunar Regolith Simulant Type 1, VA, volcanic Ash, NEU-1: Northeastern University Lunar Simulant Type 1, MLS-2: Minnesota Lunar Simulant Type 2, ALS: Arizona Lunar Simulant, CLRS-2: Chinese Lunar Regolith Simulant Type 2, KOHLS-1: Korea-Hanyang Lunar Simulant Type 1, JMSS-1: Jining Mars Soil Simulant Type 1, MMS: Mojave Mars Simulant.

*Sum of FeO and Fe_2O_3

This is a preprint draft. The published article can be found at: https://doi.org/10.1016/j.pmatsci.2019.100577

Please cite this article as:
Naser M.Z. (2019). "Extraterrestrial Construction Materials." *Progress in Materials Science*. Vol. 105, 100577. https://doi.org/10.1016/j.pmatsci.2019.100577.

Similar to regolith, simulants can be melted when heated to above the liquidus temperature (roughly 1300°C) and produce cast regolith-like products. Bodiford et al. [137] also reported the successful development of glass rebars (with diameters of 9.5-12.5 mm) and fibers (with diameters of 0.01- 0.76 mm) from molten JSC-1 regolith simulant (see Fig. 11). These products can be used as tension-carrying members or internal reinforcement for structural members. Fabes et al. [138] also investigated the production of differently shaped construction materials, other than cylinders/bricks. In their work, these researchers showed the feasibility of heating lunar and Martian simulants to form a melt of desired homogeneity and viscosity. Once cast and cooled down to room temperature, the cast melt can form building blocks, monolithic glasses, glass fibers, and glass-ceramics. These products became glass bars (with surface flaws and unflawed) and glass fiber (unflawed) – see Table 9.

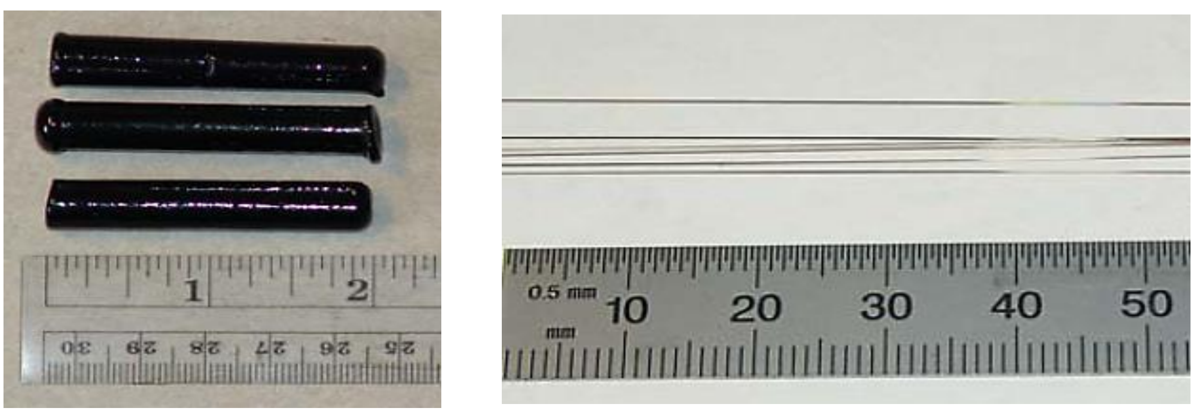

(a) Glass rebars (b) Glass fibers

Fig. 11 Construction materials obtained from molten JSC-1 regolith simulant (Courtesy of NASA)

Table 9 Mechanical properties of lunar glass, fiber, and cables [71,139]

Property	**Glass bar (with surface flaws)**	**Glass bar (unflawed)**	**Glass fiber (unflawed)**	**Glass cables**
Bending strength (MPa)	125	360	630	690
Young's modulus (GPa)	450	-	-	-
Fracture Toughness (MPa.m$^{0.5}$)	2.5	-	-	-

Sintering simulants can also be carried out through solar, microwave, or laser energy [107,140,141][142]. In one study, Meurisse et al. [143] studied the mechanical properties of cylindrical structural members made by sintering of two different lunar simulants, JSC-1A and DNA. In this work, the lunar simulants were first pressed at 255 MPa and then sintered for a duration of three hours at a heating rate of 400°C/hr. Sintering of JSC-1A cylinders was performed at 1100°C in vacuum and 1125°C in air while sintering DNA cylinders was performed at slightly lower temperatures of 1070°C in vacuum and 1100°C in air (due to the higher amount of albite, Na-rich plagioclase mineral, with low melting point, that reduces overall heat required to sinter DNA simulant). Meurisse et al. [143] reported that cylinders sintered in air generated a distinctive reddish color, while those sintered under vacuum developed a black color to them. This was attributed to the fact that sintering in air can cause some of the minerals containing iron (olivine, pyroxene) to slightly decompose, thus leaving some free iron available to react with the surrounding oxygen from the atmosphere. As a result of this reaction, hematite (i.e. rust) is therefore formed in a quantity sufficient to give such red color to the sample [144].

A common trend observed by Meurisse et al. [143] was that vacuum-sintered cylinders made of DNA simulants had lower densities (2266 kg/m^3) and higher porosities (18.2%) than those made of JSC-1A simulant (2542 kg/m^3 and 12.8%). Furthermore, DNA samples had an increase in mechanical properties when sintered in air (i.e. the stiffness increased from 16 to 31 GPa and the compressive strength also increased from 95 to 213 MPa). On the other hand, the porosity in JSC-1A samples was lower in cylinders sintered in vacuum than those in air (12.8 vs. 22.7%). As a result, the stiffness of these samples increased from 18 to 24 GPa; and the compressive strength also increased, from 98 to 152 MPa when compared with samples sintered in air. These differences in simulants were attributed to variation in mineral and glass compositions between DNA and JSC-1. The outcome of this study shows the feasibility of sintering simulants (and by extension regolith) as well as the effect of varying sintering conditions (i.e. air vs. vacuum) on sintered construction materials.

Song et al. [145] examined pore formation and thermal conductivity of CLRS-1 under vacuum conditions while being heated to 1100°C. These researchers reported that sintering of CLRS-1 has led to developing porous samples with an average density of 1190 kg/m^{-3} and low thermal conductivity (measured at 0.265 Wm^{-1} K^{-1} and 0.359 Wm^{-1} K^{-1} at lunar and Earthly conditions, respectively). On the other hand, Liu et al. [146] managed to sinter small-sized samples made of CLRS-2 through a two-stage heat treatment process (in air atmosphere). In the first stage, samples were subjected to 450°C and were kept for two hours to ensure complete pyrolysis. Then, in the second stage, samples were sintered at 1150°C for 4 hours. It is worth noting that both the heating and the cooling rate in these stages was kept at 2°C/min. The compressive and flexure strength measured in these sintered samples were reported at 428.1 ± 39.7 MPa and 129.5 ± 13.6 MPa, respectively. Dou et al. [146] also explored sintering of CLRS-2. These researchers sintered two types of samples; one at 1100°C and the second at 1150°C under an air or argon-controlled atmosphere. Dou et al. [146] noted that air-sintered samples (at 1150°C) showed the highest mechanical properties due to undergoing high shrinkage, thus forming glassy phase and dense structure.

Indyk and Benaroya [147] also investigated the direct use of a sintered lunar simulant to fabricate cylindrical structural members (i.e. to replicate short columns). In their investigation, two batches of lunar regolith simulant JSC-1A, having varying porosities of 1.44% and 11.78%, were selected for analysis. Lunar simulants were first pressed at a low pressure of 4 MPa and then oven-fired at 1120°C for 15 minutes [148]. The sintered cylinders had a height of 19 mm and a diameter of 12 mm (see Fig. 12a). The cylinders were measured for density and then subjected to compressive loading. The density and compressive strength of sintered cylinders with low porosity were measured at 2700 kg/m^3 and 218.8 MPa, respectively. In the case of sintered cylinders with low porosity, the aforementioned properties were reported at 2000 kg/m^3 and 84.6 MPa. Overall, the average toughness of all specimen was reported at 3.2 MJ/m^3.

This is a preprint draft. The published article can be found at: https://doi.org/10.1016/j.pmatsci.2019.100577

Please cite this article as:
Naser M.Z. (2019). "Extraterrestrial Construction Materials." *Progress in Materials Science*. Vol. 105, 100577. https://doi.org/10.1016/j.pmatsci.2019.100577.

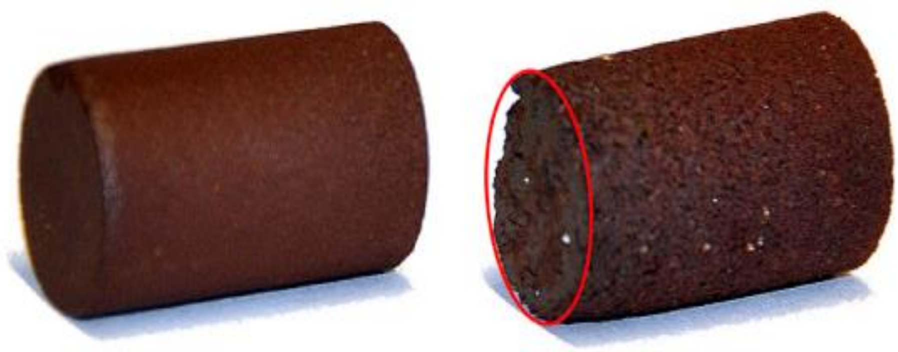

(a) Photograph of samples fabricated by Indyk and Benaroya [147], (left) is 1.44% porosity and (right) is 11.78% porosity

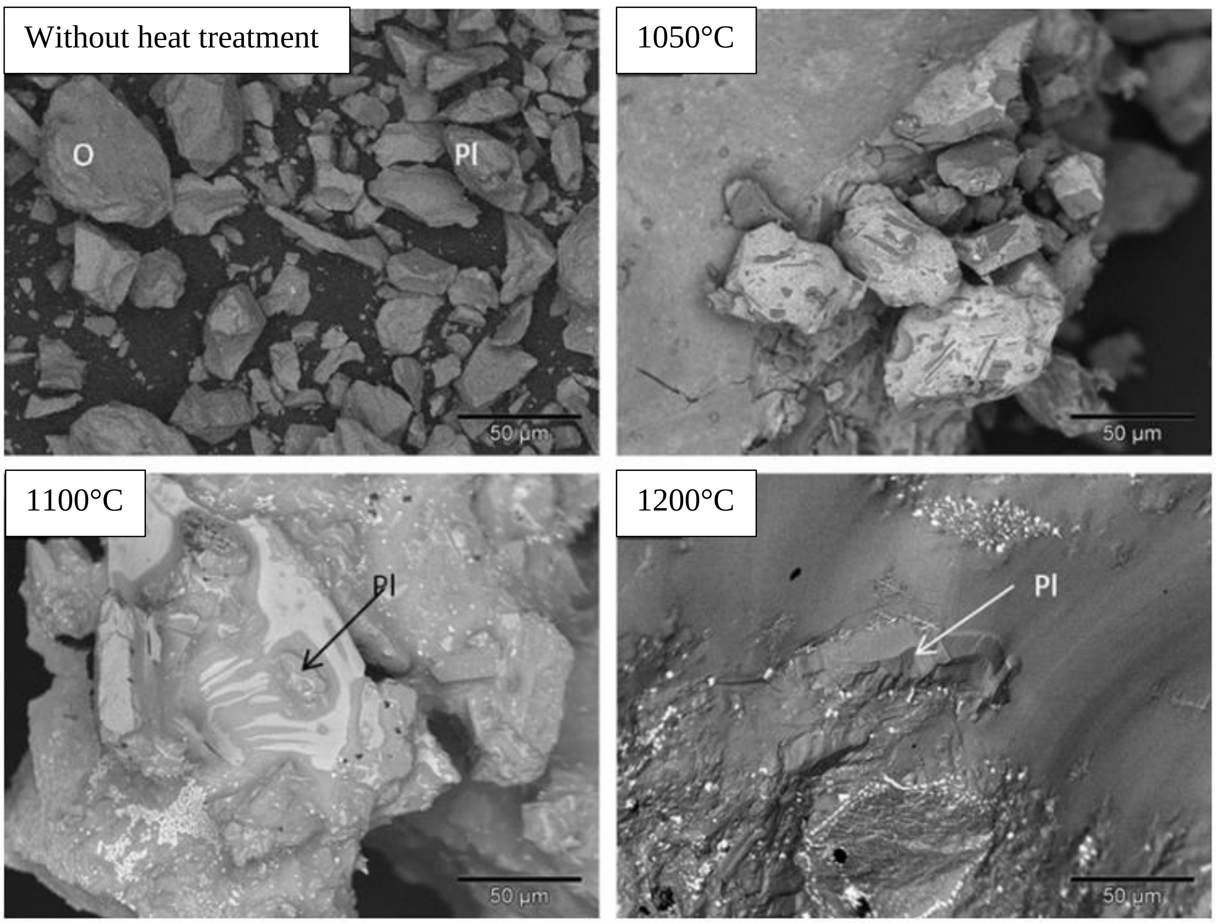

(b) Simulant JSC-1A after ambient condition; at 1050°C; at 1100°C; at 1200°C; individual particles are labeled Pl for plagioclase, O for olivine, and Py for pyroxene (Courtesy of NASA) – scale = 50 µm.

Fig. 12. Photographs and microstructures of sintered lunar simulant

In a separate study, Hintze and Quintana [149] reported that JSC-1A starts to sinter at 1150°C and this sintering completes at 1200°C. Images of heated and treated samples were taken by scanning electron microscopy (SEM) at elevated temperatures of 1050, 1100 and 1200°C through which these researchers traced microstructural changes of sintered lunar simulant JSC-1A, similar to that tested by Indyk and Benaroya [147], (see Fig. 12b). Upon visual comparison of collected images, these researchers noted that iron-containing minerals were affected first at temperatures starting at 1050°C which likely initiated the sintering process. At 1100°C, iron-rich crystals were developed and were reported to concentrate, primarily on the edges of (and within) melted areas of the lunar simulant.

Other researchers also carried out similar tests with the goal of achieving construction materials from lunar and Martian simulants but with improved properties [150–152]. For example, Gualtieri and Bandyopadhyay [150] investigated the possibility of sintering lunar regolith made of a mixture of simulants (namely, JSC-1, JSC-1AF, and JSC-1AC). In this study, cylindrical dies of 12.7 mm and 7 mm diameter, and a height to diameter ratio varying between 1.5:1 and 2:1 were pressed to approximately 145 MPa and then heated at 1200°C for 20 minutes to sinter. Two types of sintered samples were produced with relatively low porosity ranging from 92 to 99%. These samples were then tested under compression loading and evaluated for hardness. It was noted that sintered samples with low and high porosity failed at 232 and 103.2 MPa and had a modulus of elasticity of 10.9 and 5.98 GPa, respectively. The average hardness of all sintered samples was reported at 1027 $HV_{0.1}$.

In a notable study, Meek et al. [151] applied microwave energy to heat three different lunar simulants similar to lunar soils collected in Apollo missions (11, 15, and 16). The simulants were first compacted at 4.8 MPa and then isostatically pressed through a rubber sleeve up to 344.7 MPa. These simulants were sintered at temperatures of 1000-1204°C for durations between 5-45 minutes reaching 1000°C within the first few minutes of sintering. Once the sintering process was completed, the sintered specimens were left to cool and their physical and mechanical properties were measured. Table 10 lists properties of selected samples (the complete set of measured data can be found in Ref. [151]). Observations from comparing samples obtained by Apollo 11 show that the mechanical properties of sintered simulants through microwave energy seem to improve with rise of temperature and duration of sintering.

Table 10 Properties of sintered simulants as reported by Meek et al. [151]

No.	**Sintering temperature (°C)**	**Sintering time (min)**	**Compressive strength (MPa)**	**Modulus of elasticity (MPa)**	**Elongation**
A11	1000	5	27.6	238.1	0.116
A11	1038	20	50.1	480.0	0.105
A16	1204	45	307.9	772.7	0.40

Allen et al. [153] proposed a novel design for a microwave furnace that can be used to fabricate bricks from lunar regolith/simulants. Using this furnace and by sintering two lunar simulants (MLS-1 and the JSC-1) at temperatures between 1000-1125°C for 0.5-3 hours, Allen et al. [154] were able to sinter building bricks of relatively large dimensions measured at 79×55×36 mm. In a separate study, Allen [154] also carried out a more extensive experimental program by testing 36 cylinders made from MLS-1 simulants. These cylinders were heated in a transient manner for 85 min, then held at a temperature of 980°C for 35 min. After which, specimens were slowly cooled by ramping down the microwave energy over several hours. Allen [154] reported that the bricks produced were free of cracks, with compressive strengths reaching 7.6 MPa. While this compressive strength may seem low for terrestrial construction, this strength would theoretically satisfy most loading conditions in a lunar structure (due to much lower gravity on the Moon).

The application of laser sintering, specifically through Laser Engineering Net Shaping (LENS), to simulants as an enabling technology for additive manufacturing for extraterrestrial construction was examined by Krishna Balla et al. [140]. These researchers used a laser of 2.12 J/mm density to melt JSC-1AC lunar simulant at a rate of 20 mm/s. This process successfully managed to fabricate solid cylinders with a height of 25–30 mm and a diameter of 8-10 mm. A similar approach was applied by McLemore et al. [155,156] to produce metallic parts from lunar and Martian simulants. McLemore et al. [155,156] carried out a feasibility study to sinter a Lunar Highland Type Medium NU-LHT-1M lunar simulant using an electron beam melting process to melt fine powders of the simulant in a layer-by-layer manner. Unfortunately, Krishna Balla et al. [140] and McLemore et al. [155,156] did not examine structural performance nor report mechanical properties of these sintered components.

In lieu of sintering, the use of heat or UV cured solvent-free polymers can be used to solidify (or stabilize) lunar and Martian simulants. Hintze and Quintana [149,157] compared the behavior of solar-sintered lunar simulant; JSC-1A, to that of a composite made by mixing the same simulant with UV cured polymer. While sintered simulants achieved a bearing strength of 0.89-2.13 MPa, specially designed solvent-free polymer of 200 μm thickness led to developing weak components achieving a relatively low strength of 0.68 MPa. Tests to measure abrasion resistance were carried out by gun-spraying 500g of silicon carbide media at different samples. While both sintered and polymer-cured specimens lost about 10-12% of their total mass, sintered simulants were reported to experience 1-2% less loss in mass. Hintze et al. [149,157] noted that the concept of polymerizing regolith was promising and recommended developing new heat or UV cured solvent free polymers to improve overall performance of solidified components.

In a similar study, Gosau [158] mixed urethane resins with JSC-1A lunar regolith simulant to stabilize lunar regolith for the construction of launch pads. The polymerized cylinders were tested under compressive loading and achieved a strength of 4.7 MPa. Bodiford et al. [137] noted efforts to investigate combining regolith and binders to fabricate structural components. In these efforts, polyethylene powder (ranging from 10% to 50% by weight) was first mixed with JSC-1 simulant and then compacted and subjected to a pressure and temperature of 204°C to develop polyethylene-based structural blocks.

Corrias et al. [159] investigated triggering chemical reactions to solidify lunar simulants. These researchers examined the feasibility of fabricating cylinders out of lunar and Martian regolith simulant through chemical reaction under vacuum conditions. Using JSC-1, JSC-Mars and MMS simulants, cylindrical pellets of 11 mm diameter and height of 25 mm were fabricated by mixing minerals with a reducing agent to ignite a thermite reaction. These specimens achieved an average compressive strength of 26 MPa which is comparable to ordinary concrete. Hobosyan and Martirosyan [160] carried out similar tests in on samples made by mixing lunar simulant (JSC-1A) with 12% aluminum and 1.5% Teflonand (by weight). These samples were then tested at close-to vacuum conditions (10^{-3} torr). The finished solid samples measured at 13 mm in diameter and 3 mm in height. These samples had an average porosity of 50%. Unfortunately, these researchers did not report mechanical properties of the samples produced.

In a recent study, Jakus and colleagues [161,162] proposed an approach for developing lunar and Martian-based inks that can be used in additive manufacturing to print structural members. These inks are developed from 90% lunar and Martian simulants, i.e. JSC-1A and JSC Mars-1A, and 10% of bio-derived polylactic-co-glycolic acid (PLGA) polymer. Despite being in liquid form, Jakus et al. [161,162] showed that structural components can be accurately printed with a deposition rates of 1–150 mm/s through 300 μm to 14 mm diameter nozzles. The printed components can instantly dry and when tested under low gravity conditions can achieve large elastic deformations (15-20%) prior to failure. The tensile strength of lunar and Martian ink can reach 0.3 and 1.2 MPa, with stiffness that also varies between 8-13 and 2-3 MPa, respectively. While the developed inks have significantly low strength, from structural and construction points of views, this study marks one of the promising efforts towards developing novel concepts for additive printing using in-situ resources.

NEOs Derivatives

Fallen fragments of NEOs, together with dust particles collected by the Hayabusa mission, constitute the only materials available on Earth that provide an approximate indication of characteristics of NEOs. The chemical and physical properties of those pieces offer imperative clues to understanding not only the formation of NEOs, but also to developing insights into mining and utilizing NEOs for extraterrestrial construction applications [163]. According to Flynn et al. [164] and Marvin [171], the first identification of fallen meteorites dates back to Chaldni in 1794 [165], as well as to Biot [166] who documented retrieval and measurement of asteroidal samples near l'Aigle, France in 1803. Over the last 200 years, a handful of studies managed to physically test material properties of fallen meteorites [77,167]. This section overviews some of these properties from a construction/structural engineering standpoint.

Given the extreme diurnal temperature that could occur on the lunar or Martian surface, thermal properties of construction materials are of great interest as these can help estimate temperature progression within space habitats. These properties (i.e. thermal diffusivity, thermal conductivity, and heat capacity) are also critical to get a grasp on in the pursuit of mining NEOs as to properly select appropriate processing and extraction techniques. While direct measurements of thermal properties of meteorites has been very limited [164], a classic study carried out by Yomogida and Matsui [168] measured the thermal diffusivity of twenty asteroidal samples over the temperature range 173-226°C and under a vacuum of less than 7.5×10^{-4} torr. These values were then used to calculate thermal conductivity and heat capacity of parent NEOs.

Figure 13 plots a scatter showing variation in thermal conductivity and specific heat as a function of temperature as measured by Yomogida and Matsui [168] and Opeil et al. [169]. These works revealed that the average thermal diffusivity is in the range of $2\text{-}34\times10^{-7}$ m^2/s while the heat capacity and thermal conductivity average at 497-600 J/Kg.°C and 2-3 W/m.°C, respectively. Flynn et al. [164] noted a strong correlation between the thermal conductivity, k, and porosity, P, of NEO and derived an expression for this relation (see Eq. 19). Another expression was also developed for specific heat, C_p, as a function of temperature, T (see Eq. 20). A thorough review on properties of various types of meteorites, from a geological perspective, can be found in [164,170,171].

$$k\ (W/m.K) \approx 0.11\times(1\text{-}P)/P \qquad \text{Eq. 19}$$

$$C_p\ (J/Kg.K) = 2.82T - 8.1 \qquad \text{Eq. 20}$$

This is a preprint draft. The published article can be found at: https://doi.org/10.1016/j.pmatsci.2019.100577

Please cite this article as:
Naser M.Z. (2019). "Extraterrestrial Construction Materials." *Progress in Materials Science*. Vol. 105, 100577. https://doi.org/10.1016/j.pmatsci.2019.100577.

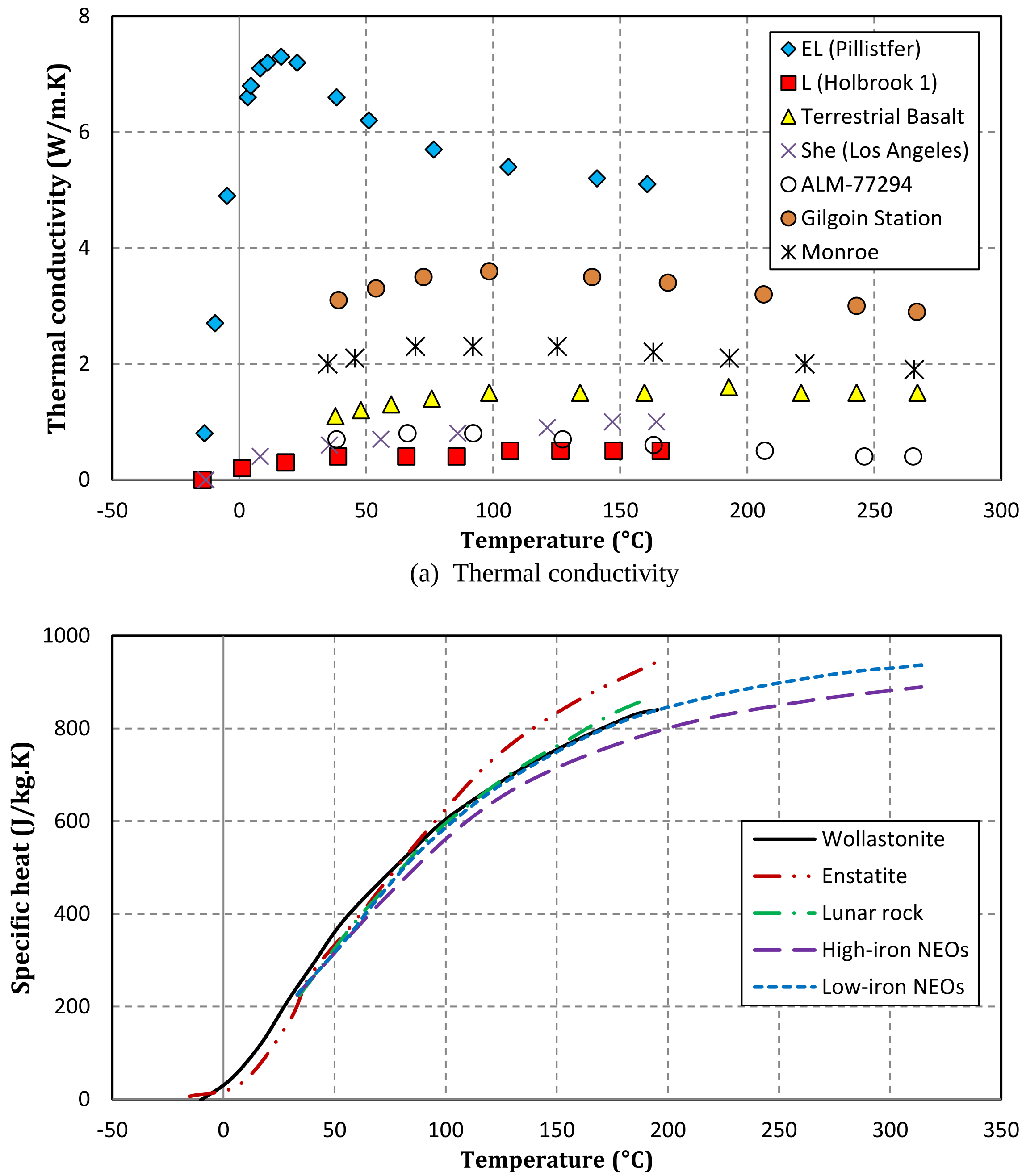

(a) Thermal conductivity

(b) Specific heat

Fig. 13 Reported scatter of thermal properties of NEOs [168,169]

A few studies examined the mechanical properties of a number of meteorites by carrying out simple tests of a compression/tensile nature. Unfortunately, most of these tests did not follow a standardized procedure nor had a specific (unified) test set-up [164]. Perhaps a serious limitation that is common in these tests is the fact that tested specimens were of different sizes and were also loaded at varying loading rates. In one notable case, several research groups tested strength properties of samples selected from the same *Tsarev* meteorite[9] and reported compressive and tensile strengths ranging from 157-465 MPa and 16-62 MPa, respectively [172,173].

Building on our previous discussion, and as one would expect, the reported average strength of stony meteorites is lower than that of iron meteorites [164]. On average, samples obtained from stony NEOs were measured with a compressive strength of 6-260 MPa [167]. Petrovic [174] compared mechanical properties of iron and stony NEOs and showed how iron-based meteorites can have a compressive strength of twice as much as that of stony meteorites. He reported the average compressive strength for iron-based and stony meteorites at 430, and 200 MPa, respectively.

Buddhue [175] measured the compressive strengths of 8 stone meteorites that fell in North America and reported a wide range that varied between 6.2-381 MPa; with one sample measuring at 405 MPa without failing as the hydraulic testing machine reached its maximum capacity. On the other hand, McKay et al. [167] examined samples from iron-based origin meteorites. In their work, these researchers reported a compressive strength varying between 100-360 MPa [167]. In a different study, Flynn et al. [164] compared the average compressive and tensile strength of high-iron content meteorites (200 ± 82 MPa, and 33 ± 8 MPa, respectively) to that of low-iron content meteorites (averages at 149 ± 116 MPa and 21 ± 12 MPa). Popova et al. [176] reported comparable

[9] Found in Russia in 1968. This meteorite comprised of 28 pieces with a total mass slightly exceeding 1131 kg.

values to Flynn [164] for the average of compressive and tensile strength for intact meteorites to be at 217 ± 134 MPa, and 30 ± 17 MPa, respectively.

Petrovic [174,177] also reported both the elastic and shear modulus of major minerals in high concentrations in meteorites, such as forsterite, fayalite, and enstatite, at 204, 140 and 180 as well as 82.2, 52.9, and 74.6, respectively. By means of elastic wave testing, Yomogida and Matsui [168] measured the Young's modulus, of twenty NEOs; eleven of which were retrieved from Antarctica. The stiffness of these samples varied between 9.53-138.7 GPa. They also reported the intrinsic density of meteorites with high-iron concentration to be slightly higher (3800 kg/m^3) than that of low-iron concentration (3600 kg/m^3).

Gordon [178] examined the meteorite *Gibeon*[10] and reported that the properties of retrieved metals are less sensitive to rise in temperature and increase in strain rate than that in pure iron and this weak sensitivity to temperature can be beneficial in construction of interplanetary construction where high thermal fluctuations occurred. The strength and ductility of these metals were found to be 320 MPa and 19%, respectively. Rudge [179] reported that the composition of a sample cut from the *Winburg*[11] meteorite, measuring 127 mm with 19 mm square cross section, was 90.7% of iron soluble in dilute sulphuric acid, 7% of nickel, 1.87% iron insoluble in dilute sulphuric acid and 0.55% of carbon and other trace elements. The measured mechanical properties of this sample were 20 MPa for compressive strength[12], 140 MPa for tensile strength and 200 GPa for modulus of elasticity.

[10] Found in Namibia around 1836-1838 and had a massive mass close to 26000 kg.
[11] Found in South Africa in 1881 (with a mass of 50 kg).
[12] Based on reported sample size of 18×7×8.7 mm and loaded to 31.3 kN.

It can be inferred that most of the aforementioned studies mainly reported thermal properties (i.e. thermal conductivity and specific heat) as well as mechanical properties (such as strength, and Young's modulus). Unfortunately, other properties of interest with regard to construction and structural engineering such as stress-strain response, thermal expansion, deformation properties (i.e. creep etc.) were rarely reported. Despite this wide range, the measured data points still provide a glimpse into the composition and behavior of construction materials to be mined from NEOs. Readers requiring specific properties such as grain density, porosity, acoustic and magnetic features of fallen NEOs are encouraged to review the works of Flynn et al. [164] and Popova et al. [176].

Concrete and Concrete-like products

A quick comparison between the chemical content of regolith, blast furnace slag, and cement slag shows how close the composition of regolith is to cement (see Table 11). As the lunar and Martian surface is rich of regolith, this resource can form the main ingredient for development of cementitious construction material [7,24]. Thus, *concrete* can be efficiently (and also cheaply) produced to fabricate space habitats, launching pads, repair damaged structural components and perhaps expand such settlements into colonies. This, when combined with our extensive knowledge on the behavior and design of concrete structures for extreme conditions, i.e. nuclear power plants etc., as well as concrete's ease of processing, shaping and fabrication[13], inherent resiliency, and overall characteristics demonstrate the merit of using extraterrestrial concrete as a construction material on the Moon and Mars [180–182].

Table 11 Composition of terrestrial and non-terrestrial cementitious materials

[13] Energy processing of concrete, glass, and mild steel is approximately 3.4, 50, and 300 GJ/m^3, respectively [118].

Constituent	**Portland Cement** [183]	**Blast-furnace slag** [184]	**Lunar regolith** [185]	**Lunar regolith (Highlands)** [185]	**Martian regolith** [186]
SiO_2	20.0	34.4	46.0	44.1	43.0
CaO[14]	63.0	39.5	10.9	17.6	6.0
Al_2O_3	6.0	11.1	12.5	29.2	7.5
FeO	2.7	0.5	17.2	4.2	-
MgO	1.5	11.4	10.4	3.9	6.0
TiO_2	-	-	2.8	0.3	0.7

Concrete comprises of coarse and fine aggregates, sand, and admixtures that are bonded together with a paste (cement and water). Typical water-to-cement ratio for traditional concrete varies between 0.4-0.5. As cement only requires 0.2-0.25 to fully hydrate, the excess water, referred to as free water, is added to improve workability of the concrete mix. Once mixed, concrete hardens over time through an exothermic, water-activated chemical reaction referred to as hydration. This hydration reaction occurs between calcium silicates and the water and continues for several days and can take up to 28 days to reach full strength. This reaction chemically bonds the water to cement particles and grow crystals that further bond with other particles [187]. This reaction, or heat of hydration, *H*, can be best illustrated through Eq. 21.

$$H = 500P_{C_3S} + 260P_{C_2S} + 866P_{C_4AF} + 624P_{SO_3} + 1186P_{FreeCaO} + 850P_{MgO} \qquad Eq.21$$

where P_i is the weight ratio of i-th compound in terms of the total cement content [188], C_3S is tricalcium silicate, C_2S is dicalcium silicate, C_4AF is tetracalcium aluminoferrite, SO_3 is sulfur trioxide, *CaO* is calcium oxide (lime) and *MgO* is magnesium oxide (periclase). A more in depth discussion that cover various properties, characteristics, processing and manufacturing of traditional concrete can be found elsewhere [189,190].

[14] The deficiency of CaO in lunar and Martian regolith implies less hydraulic activity but this can be partially countered by the presence of high amount of Al_2O_3 as well as addition of binders.

Materials science enthusiasts and readers with structural/construction engineering background are well aware that concrete, despite its positive attributes, still suffers from certain aspects that could inhibit its use in lunar and Martian environments. Perhaps the major limitation that casts a shadow over adopting concrete as the primary choice for a construction material in space is the need for water for hydration, mixing, and curing the concrete. Other limitations also include the naturally low tensile strength, vulnerability to shrinkage, instability, and tendency to outgas under vacuum. Fortunately, a number of past and recent studies have been dedicated to developing solutions to overcome some of the aforementioned limitations [191,192]. In fact, in the late 1980s the American Concrete Institute (ACI) commissioned a special committee (ACI SP-125) to develop feasible strategies/techniques to enable production of concrete and construction of concrete-based structures on the Moon in support of the NASA and President Bush's administration vision. As a result of these pioneering works, new and modified concrete types were developed. This section highlights the potential of various types of concrete derivatives and concrete-like products as construction materials for extraterrestrial applications as well as novel efforts undertaken to improve performance of concrete in space.

Ordinary Concrete

Ordinary concrete is a type of concrete commonly used in day-to-day applications and does not involve complex mix design nor specialized equipment for production. The early works of Lin et al. [180,193] in the 1980's showcased the feasibility of using ordinary (or traditional) concrete as the main construction material on the Moon (assuming that aggregates could be obtained through physical processing of lunar rocks and cement could be produced through high-temperature processing of regolith). In a later study, Lin et al. [180] went on to carry out a preliminary design of a three-level space habitat as well as a lunar facility (plant) for fabricating concrete.

Lin et al. [194] also investigated the thermal properties of concrete in order to examine the effect of diurnal temperature changes on the development of thermal stresses. These researchers reported that concrete has a relatively low coefficient of thermal expansion (~5.4×10^{-6} °C^{-1}) and also reported that diurnal fluctuations on the Moon can generate thermal stresses of low magnitude (~0.21 MPa) which is much lower than the tensile strength of ordinary concrete (~3-6 MPa)) [194]. In the event where thermal stresses were found to be high, and to overcome the development of thermal cracks, Lin et al. [195] proposed the use of pre-fabricated structural panels made of concrete due to its high tensile strength and quality control.

The success of aforementioned works led NASA to award Lin and his co-workers [196] 40 grams of actual lunar regolith (collected from the Apollo 16 mission) to investigate the performance and physical properties of concrete made of lunar regolith through a series of destructive and non-destructive tests. To compile with the limited quantity of soil, small concrete cubes (having dimensions of 12.5 mm and 25 mm) and beams (3×14.7×80 mm) were fabricated. These samples where then tested in compression and the stress-strain response of a sample made of lunar regolith was compared to that of a sample made of a lunar simulant. This lunar simulant was made of natural Ottawa sand and crushed glassy rhyolite of acid volcanic nature consisting of low calcium, high sodium, and high potassium. Analysis of these tests showed that the mechanical properties of lunar concrete were much improved over that of plain concrete (see Fig. 14). Lin et al. [196] reported stiffness, compressive and tensile strength of lunar concrete samples at 21.4 GPa, 75.7 and 8.3 MPa, respectively. These researchers also noticed that the mechanical behavior of these samples was governed by distribution of grain size, angularity of grains, and porosity. As a side note, Lin and his colleagues stipulated that the improved response of lunar concrete can be credited to the presence of 100 ppm of solar-wind and noble gases such as helium and argon commonly available in lunar regolith. Given the fact that these tests were carried out in the 1980s, the mechanical performance of fabricated concrete seems comparable to that used nowadays.

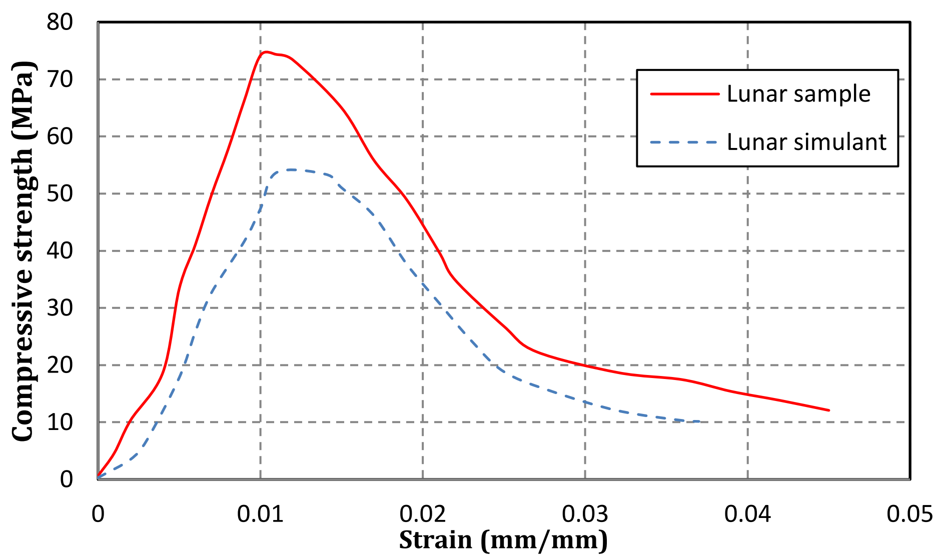

Fig. 14 Measured stress-strain response of concrete samples tested by Lin et al. [196]

The use of ordinary concrete for lunar and Martian construction was also investigated by Ishikawa et al. [192] as well as Swint and Schmidt [197]. Similar to Lin et al. [193], Ishikawa et al. [192] also advocated production of pre-fabricated concrete. Through mixing cement with cold/iced water, precast concrete can be produced without the need for specialized curing or processing chambers. In a separate work, Swint and Schmidt [197] proposed a predictive design algorithm capable of optimizing concrete mix for lunar construction. This algorithm was first developed through a combination of material tests and computer models and then optimized through tests on 18 possible combinations that accounts for several types of plasticizers, condensers, and reinforcement types (i.e. steel wire, aluminum wire, and glass fiber) with the goal of minimizing the amount of needed water for production of concrete on the Moon [197].

Other efforts worthy of mention include those carried out by Mishulovich et al. [198] who explored the use of heating a mix of anorthite and calcium oxide to form a material analog to Portland cement. This material was melted at 1450°C and then quenched to form a clinker which was eventually ground into cement. Concrete cubes, made of this cement, reached a compressive strength of 39 MPa. The feasibility of using cementitious material from basalt, a common material on the Moon, was also examined by Mishulovich et al. [198]. This basalt-based cementitious material, when cured at 100°C and 100% humidity, can achieve a compressive strength of 49 MPa.

In theory, the low gravity conditions on the Moon generate loading effects of a tensile nature that are generally of low magnitude as compared to the tensile strength of concrete. In the event where the tensile strength of concrete might not be sufficient, concrete can be strengthened through addition of internal (or external) reinforcements [199,200]. A proposal to manufacture discrete steel reinforcement through treating lunar ilmenite was also pointed out by number of researchers [201,202]. For instance, Tucker et al. [202] proposed the use of smeared reinforcement in terms of fiber glass. Other solutions specifically tailored to improve tensile strength of concrete and reduce its susceptibility to cracking include the use of concrete that utilizes high performance cements [203,204]. This concrete type can achieve high compressive strength (250-300 MPa) while also maintaining high fracture energy (0.04-0.2 kJ/m^2). Table 12 shows how compressive and tensile strengths of various concretes can change depending on the type of additives and reinforcement. While the compressive strength of such concretes seems to significantly vary over a wide range (i.e. 14.6-300 MPa), the tensile strength on the other hand does not vary by much and can still be crudely be estimated at 10% of compressive strength, f_c', or $\sqrt{f_c'}$.

Table 12 Physical and mechanical properties of ordinary concretes suitable for lunar construction

Property	**Ordinary concrete** [180,196]	**Lunar concrete** [205]	**Fiber-reinforced concrete** [204]
Compressive strength (MPa)	35-85	14.6-75.5	250-300
Modulus of elasticity (GPa)	28-35	21.4	40-50
Tensile strength (MPa)	3.5-6	8.3	-
Flexural strength (MPa)	6-9	-	4-150
Thermal expansion (°C^{-1})	-	5.4×10^{-6}	-
Strain at failure (%)	0.2-0.3	-	0.3
Fracture energy (J/m^2)	-	-	40-200

A few researchers went on to examine the performance of ordinary concrete under simulated space environments (i.e. low gravity, vacuum) [205–208]. In one particular study, Cullingford and Keller [206] examined the behavior of ordinary concrete in vacuum of 3×10^{-6} torr and noted the quick outgassing of free water from concrete under vacuum conditions (of about 0.04% per day which is ~3-4 times higher than that at ambient conditions). They estimated the evaporation coefficient attributable to the vacuum's effect on concrete to be 1.59×10^{-7}. Cullingford and Keller also observed that concrete reaches a stable outgassing rate of 10^{-6} torr·l/cm^2·sec within 73 hours of exposure to vacuum conditions. The fact that the observed compressive strength did not decrease under vacuum but rather slightly improves suggests that cement dehydration does not occur (see Fig. 15a). This research indicated that concrete could properly be designed to be stable under vacuum if this outgassing rate is taken into consideration.

This is a preprint draft. The published article can be found at: https://doi.org/10.1016/j.pmatsci.2019.100577

Please cite this article as:
Naser M.Z. (2019). "Extraterrestrial Construction Materials." *Progress in Materials Science*. Vol. 105, 100577. https://doi.org/10.1016/j.pmatsci.2019.100577.

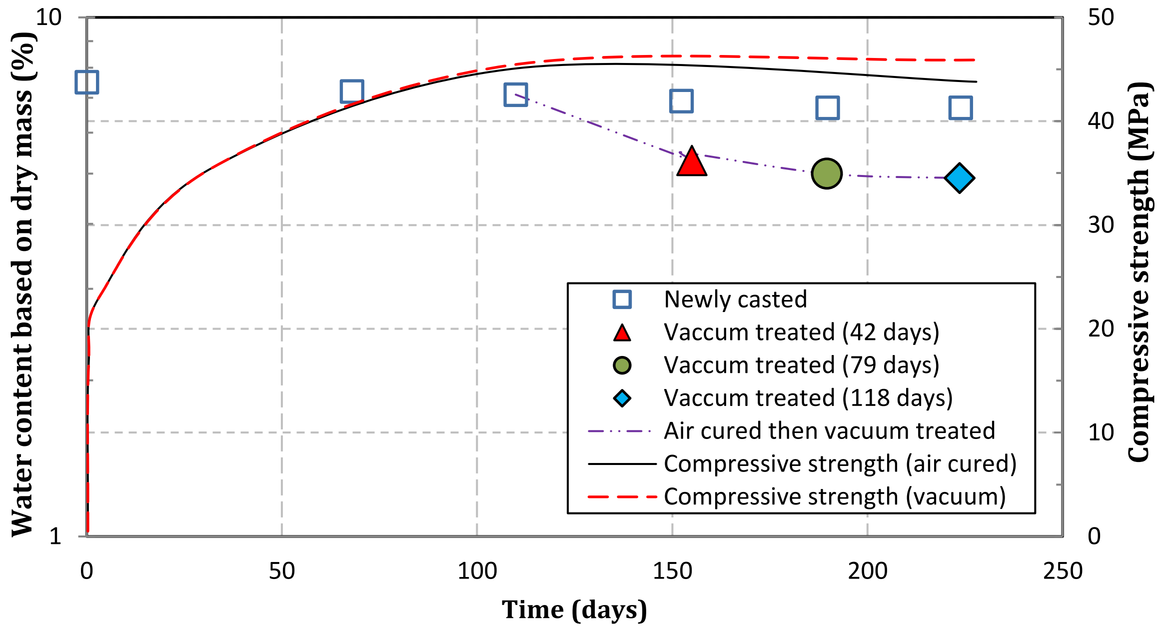

(a) Cullingford and Keller [206]

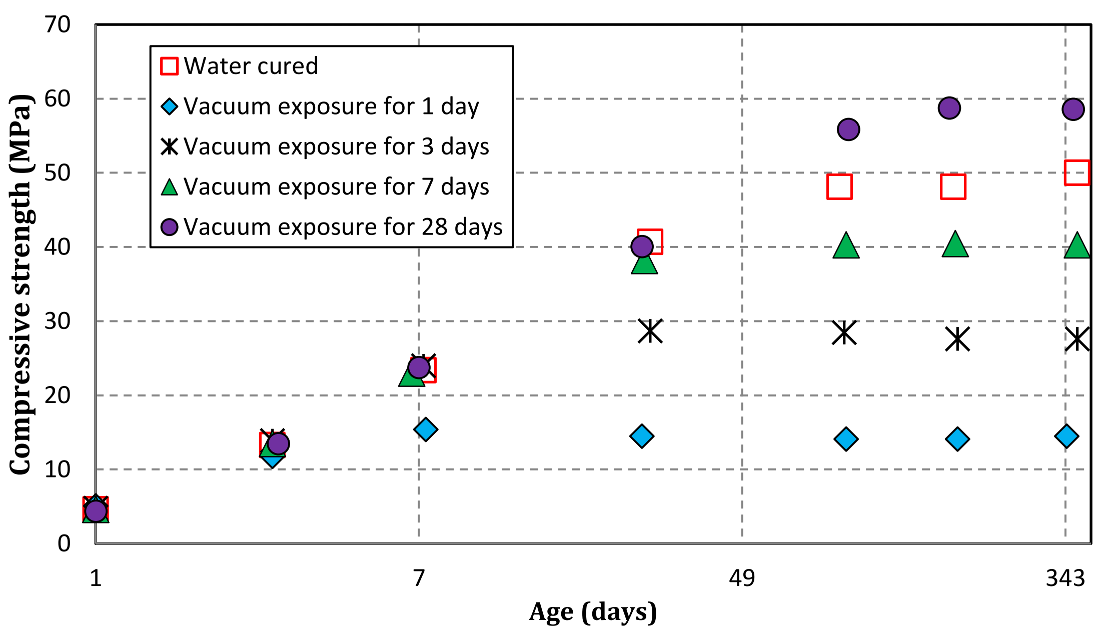

(b) Kanamori et al. [207]

Fig. 15 Effect of cure setting on water content of concrete (based on dry mass) and compressive strength of cylinders.

Similarly, Kanamori et al. [207] reported an interesting behavior in concrete specimens exposed to vacuum of magnitude of one torr. In this experiment, concrete cylinders were pre-cured in water for 1, 3, 7 and 28 days before being exposed to vacuum for a duration varying between 2 days to 1 year. In this work, Kanamori et al. [207] noted that water-cured specimens for 28 days achieved higher compressive and flexural strengths after 1 year exposure to vacuum than those cured in water (see Fig. 15b). This behavior has been attributed to the continuing hydration of cement due to the presence of water in gel and capillary pores. In addition, the drying effect increases the interfacial strain energy between the hydrated cement particles and the water accompanying the decrease in moisture content of the sample.

In contrast, Namba et al. [208] noted that if ordinary concrete is left to harden under vacuum, the effect of vacuum is of a negative effect and cannot be neglected. This is ascribed to the rapid off-gassing rate of moisture and air bubbles which eventually creates a porous structure that weakens the mechanical properties of concrete. However, they also noted that concrete can retain 89.2% and 96.4% of its compressive strength and theoretically all of its weight if concrete was pre-cured for 11 to 24 hours, respectively, before exposure to vacuum. In the same study, Namba et al. [208] also showed that low gravity causes significant segregation in concrete mix originating from the difference in specific gravity of constituent materials and can limit development of dense concrete. The effect of low gravity on compressive strength of concrete can be estimated using the flowing expression:

$$f_c'(g) = 3.69\, log(G) + 27.67 \qquad \textit{Eq. 22}$$

where, $f_c'(g)$ is the compressive strength with respect to a given gravity level, G.

This is a preprint draft. The published article can be found at: https://doi.org/10.1016/j.pmatsci.2019.100577

Please cite this article as:
Naser M.Z. (2019). "Extraterrestrial Construction Materials." *Progress in Materials Science*. Vol. 105, 100577. https://doi.org/10.1016/j.pmatsci.2019.100577.

Horiguchi et al. [205] further investigated the behavior and curing of ordinary concrete and mortar along with those made of lunar simulants[15] under vacuum conditions. Cubic samples, with sides of 40 mm, were made with a 1-to-2 cement/sand ratio and wet-mixed or steam-cured and left to cure. Once cured, the samples were placed in a sealed chamber to simulate vacuum conditions of magnitude of 10^{-4} torr. These concrete cubes where exposed to 28 days of vacuum after which they were tested under compression loading. The compressive strength of wet-cured and steam-cured concrete cubes made of lunar simulant was 14.6 and 24.3 MPa, respectively. This was about 58% higher than that measured in cubes made of Portland cement and exposed to the same vacuum conditions. Horiguchi et al. [205] also examined the effect of long term exposure to vacuum for 9 months. It is interesting to note that not only did the steam-cured samples outperform those made of wet-cured Portland cement, but in spite of the vacuum maintained a steady pore area of about 7 m^2/g (as oppose to 26 m^2/g in wet-cured samples) was observed.

One of the early studies to propose the use of ordinary concrete on Mars was conducted by McKay and Allen [209]. These researchers argued that despite the relatively low CaO content (of about 4.6-5.3% of weight), approximately one half that of common lunar basaltic rocks, the indigenous materials on Mars could be better suited for concrete than those on the Moon due to the high amount of silica and carbonates in some locations in the Martian soil [210]. Perhaps one of the key aspects in the case of using concrete on Mars, is the availability of large, close to surface, ice pockets which can be mined for water.

Despite the positive outcome of aforementioned studies, a key limitation that seem to hinder the use of concrete as a construction material on the Moon, and to some extent on Mars, is

[15] The lunar simulant used in this program was made of Anorthite rocks from Hokkaido, Japan.

the necessity of water to carry out hydration process and cure concrete. Thus, research efforts were directed towards developing solutions that do not necessarily require water to produce concrete or concrete derivatives[16]. Some of these efforts led to the development of novel cements such as those known as macro defect free (MDF) and densified with small particle (DSP) cements which minimizes the quantity of required water for hydration and mixing as compared to that of regular cement [118]. Young and Berger [211] showed that the integration of special cements into the concrete mix can optimize particle size and distribution which reduces voids between grains, and thus the need for water during concrete mixing from 40-50% to 10-18%. Table 13 show properties of typical MDFs and DSPs as collected from a number of resources [212,213].

Table 13 Typical mechanical properties of cement-based particles

	Macro defect free (MDF)	**Densified with small particle (DSP)**
Water/cement ratio (%)	10	18
Compressive strength (MPa)	300	250
Flexural strength (MPa)	150	40
Modulus of elasticity (GPa)	50	40
Fracture energy (J/m^2)	200	40

While the above solutions successfully managed to reduce the required water for concrete, the availability of water (despite being in small quantities) seems to be a prerequisite for production of concrete. From a space exploration perspective, the production of water, on the other hand, is vital for human survival and it would perhaps be poor judgment to direct the use of such a scare resource from human consumption to construction of settlements. Although contemporary remote sensing efforts have indicted the possibility of water reservoirs near the poles of the Moon and

[16] Other efforts targeted developing sophisticated concrete fabrication processes. For example, Lin et al. [180,193] developed a unique concrete fabrication process that uses water steam to initiate hydration. A complete discussion on this process is spared to the following section.

Mars [214,215], this presents two issues; first, it restricts the location of space habitat to pole areas and hence hinder flexibility of long-ranged surface exploration missions, second; in case such water is not easily accessible or if mined water is of poor quality, then water is to be refined on-site or imported from Earth, and third; an investigation on the suitability of such water in concrete production has not be conducted as of yet. Since, importing water for this purpose defies the notion for Earth-independent space exploration as well as principles of ISRU, a number researchers started exploring technologies to develop *waterless* or *non-hydraulic concretes* through the use of novel additives or binders.

Polymer Concrete

In order to produce non-hydraulic concrete for space construction, a number of alternatives were recently explored. One such alternative is the use of thermoplastic and/or thermosetting polymers to develop *polymer concrete*. The development of polymer concrete dates back to the late 1950s as a replacement for ordinary concrete to be used in remote and/or extreme constructions [216][17]. This type of concrete replaces cement paste as well as water with polymers to bind aggregates and fines. As such, aggregates and fillers occupy more than 75–80% of volume in polymer concrete and the remaining 20-25% is packed with polymer binders that can vary between unsaturated polyester, methyl methacrylate, epoxy, polyurethane, and urea formaldehyde resins [217]. The concrete mix is often heated (or exposed to UV light) to melt the polymer and bind the aggregates and fillers.

[17] A thorough review on history as well as properties, characteristics, and processing of polymer concrete can be found in [216,221].

The physical and mechanical properties of polymer concrete are governed by the amount and type of epoxy resin, mixing, and curing protocol and specifically by the degree of adhesion developed through polymerization between binders and aggregates. Polymer concrete achieves 70–75% of its strength after one day of curing at room temperature, as compared to 10-20% in ordinary concrete. Figure 16 shows a typical sample of polymer concrete with 6 and 16% polymer [218]. Through analysis via SEM micrographs, Elalaoui et al. [218] showed that increasing polymer content led to better filling of voids between the aggregates and the matrix and as such, improved durability and strength properties of this concrete.

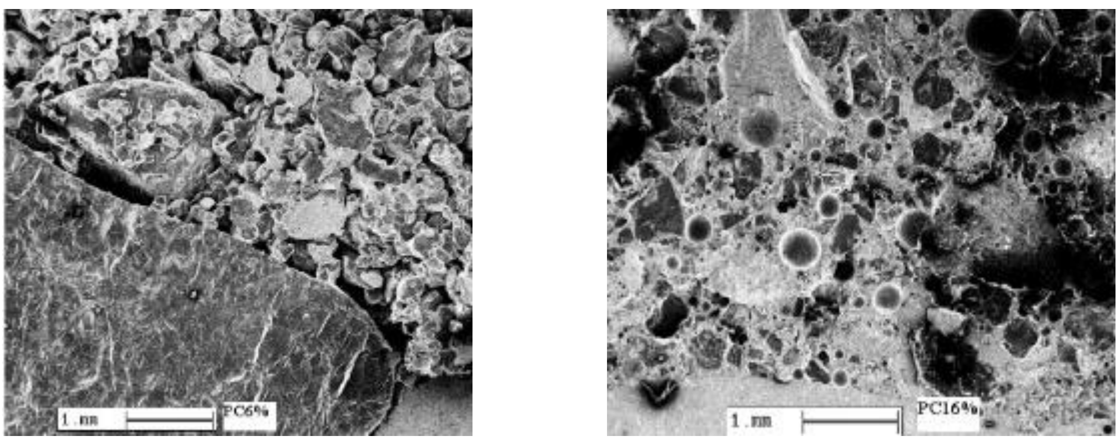

(a) 6% polymer (b) 16% polymer

Fig. 16 SEM observations of two polymer concretes with varying polymer content [218]

Bedi et al. [219] showed that further increase of polymer content does not usually improve mechanical properties. In fact, compressive strength could even reduce in epoxy-based polymer concrete when resin content increases beyond 15%. As such, they identified the optimum polymer content to be in the range between 14 and 16% by weight. When properly designed and cast, the compressive strength of polymer concrete is reported to vary between 17-129 MPa as listed in Table 14. This table also shows that unreinforced polymer concrete seems to have a relatively higher tensile strength than that of ordinary concrete.

Table 14 Comparison of mechanical properties of various types of extraterrestrial concrete.

Property	**Polyester concrete** [217]	**Carbon fiber-reinforced polymer concrete** [220,221]	**Glass fiber-reinforced polymer concrete** [218]	**Epoxy concrete** [217]
Compressive strength (MPa)	54	30-69.2	64.8	17-129
Modulus of elasticity (GPa)	11	11.5	10.8	15
Tensile strength (MPa)	11.6	-	-	9.3-16.3
Flexural strength (MPa)	15.1	42.6	24-37.6	21.3
Thermal expansion (°C^{-1})	-	-	-	-
Strain at failure (%)	-	0.1-0.2	0.17	1-11

In one study, Mani et al. [217] compared the response of two polymer concretes; made of unsaturated polyester resin binder and epoxy resin binder, against ordinary concrete. The binder to aggregates ratio in these tests was 12%. The mechanical performance of both polymer concretes was notably better than ordinary concrete. Mani et al. [217] reported the compressive and tensile strength at 54 and 84 MPa, and 11 and 15 MPa, for polyester and epoxy concrete, respectively. When compared to ordinary concrete, polymer concretes achieved improved performance by about 2-4 times (in compressive strength) and 3-6 times (in tensile strength). Similar to Mani et al. [217], other studies also examined the behavior of polymer concrete for terrestrial applications but only a few carried out efforts to investigate this type of concrete for lunar and Martian environments [221–223].

One such effort was carried out by Lee et al. [222] who developed a polymeric concrete consisting from 90% of a lunar simulant; similar to that collected by Apollo program i.e. lunar soil no. 14163, and 10% of polyethylene (a thermoplastic polymer). In order to simulate lunar environment, the cast polymer concrete was placed under vacuum conditions (<0.1 torr) and subjected to temperature variation between 20 and 123°C. Upon testing cubes made of this concrete, these cubes achieved an average compressive strength of 12.75 MPa. The pore structure of this concrete was also examined by mercury intrusion porosimetry and was reported to vary between 0.018-0.136 ml/g. Lee et al. [222] noted the development of large pores (10×10^3 - 100×10^3 nm) in areas with poor reaction to polymer. This poor reaction was attributed to the lower heat transfer which caused incomplete liquefying of the polymer. In cases where the polymer adequately liquefied, the porosity of the polymer concrete was shown to be equivalent to that of ordinary concrete[18].

Another set of experiments was carried out by Garnock and Bernold [224]. In these tests, water-free polymer concrete made of 90-95% of Australian Lunar Soil Simulant (ALRS-1); which is equivalent to JSC-1A. This simulant was mixed with 5-10% of thermoplastic polypropylene powder. This polymer had a low density (900 kg/m^3) and melting temperature (~160ºC) which makes it ideal for use in lunar and Martian construction. Unfortunately, Garnock and Bernold [224] reported that samples containing 5% polymer were not strong enough to be tested mechanically. On the positive side, concrete samples of 10% polymer were tested and achieved compressive and tensile strengths of 4 and 1.4 MPa, respectively.

With the hope of improving the performance of polymeric concretes, Reis and Ferreira [225] investigated supplementing polymer concrete with natural and synthetic reinforcements such as sugar cane, carbon and glass fiber. These researchers noted an increase in fracture toughness of 13-29% for polymer concrete samples reinforced with glass and carbon fibers, respectively. Other researchers, such as Brockenbrough [226] noted that incorporating steel fibers can increase both strength and ductility properties of polymer concrete. The properties of some of these concretes are listed in Table 14.

---

[18] Well-hardened concrete contains pores with a diameter in the range of <100–1000 nm.

Lee et al. [227] investigated manufacturing polyethylene concrete under simulated lunar environment with the main objective of reducing processing time and energy consumption as well as improving concrete solidification. In this study, a mixture comprising of 90% Korea-Hanyang Lunar Simulant-1 (KOHLS-1) and 10% polyethylene was selected for analysis. This mixture had a density of 1500 kg/m^3 and was mixed at 200°C in a specially designed thermal chamber capable of simulating a vacuum of 5.0×10^{-2} torr. The polymer concrete was mixed and heated for a duration varying from 1-5 hours in a mold measuring at 50×50×100 mm inside of this chamber. Lee at al. [227] noted that during curing, polyethylene bonded to surrounding minerals by developing thread-like structures in the process to solidify into polymer concrete. Cured concrete was then tested and achieved a compressive strength of 5.7 MPa which is suitable for constructing a lunar settlement. Lee et al. [227] reported that heating polymer concrete from the bottom-up in vacuum setting to better facilitate heating of polymer, as opposed to the conventional way of heating polymer concrete from top-to-bottom improved solidification by up to two times than that observed in using the traditional heating approach. Other findings indicate that the optimal curing time of this polymer concrete is in the range of 3–4 hours with reduced thermal energy to a temperature of 200°C as opposed to 230°C.

Similar to other construction materials, polymer concrete also suffers from number of limitations. Perhaps one of its major limitations is the sensitivity of polymers to creep effects and to temperature rise, especially near their glass temperature [228][19]. This is more so in epoxy concretes which seem to be more sensitive to rise in temperature than polyester mortars [229]. Other issues include de-attaching (debonding) between aggregates and binders (polymers), as well

[19] Note that the strength of polymer concrete seems to improve with decrease in temperature (lower than -20°C).

as high cost of specifically designed polymers and need for specialized processing which seem to limit the use of polymer concretes in lunar and Martian constructions [230].

Sulfur Concrete

The use of molten sulfur as a water replacement to bind aggregates and cement to produce *sulfur concrete* has been investigated for terrestrial applications over the past few decades [231]. When exploration missions on the Moon and Mars confirmed the availability of sulfur as well as cementitious-based resources, proposals were called to produce lunar (or Martian) water-free sulfur concrete [60,65]. Sulfur is present on the Moon and Mars in a few tens of parts per million (ppm) in ferroan anorthosites to over 2000 ppm as observed in samples returned from Apollo 11 and 17 [232]. The fundamental concept in manufacturing sulfur concrete is to liquefy sulfur at 120-150°C. The molten sulfur is then mixed with indigenous cementitious materials. Once the sulfur cools down, it solidifies and creates sulfur concrete. This type of concrete does not require hydration and gains most of its strength within few hours, unlike ordinary concrete which can take up to few days/weeks [233]. A typical sulfur concrete contains 80-90% aggregate, 10-20% sulfur, and about 5% of plasticizers added to improve concrete quality and properties as well as to mitigate cracking. Insights on to other properties and characteristics of sulfur concrete can be found in [234].

Omar and Issa [235,236] carried out a comprehensive test program that examined the mechanical properties of sulfur concrete and fiber-reinforced sulfur concrete and compared their behavior to ordinary concrete as well as epoxy concrete. The sulfur concrete mixture consisted of mixing sulfur of varying proportions between 25-70% with a lunar simulant (JSC-1). The fiber-reinforced sulfur concrete was of similar composition but supplemented with 2% of thin aluminum

This is a preprint draft. The published article can be found at: https://doi.org/10.1016/j.pmatsci.2019.100577

Please cite this article as:
Naser M.Z. (2019). "Extraterrestrial Construction Materials." *Progress in Materials Science*. Vol. 105, 100577. https://doi.org/10.1016/j.pmatsci.2019.100577.

fibers. In a few tests, Issa and Omar [235] reported that compacting concrete samples (with 40% sulfur content) under vacuum conditions and temperature of 150°C achieved a comparatively high compressive strength of 34.6 MPa, as compared to samples made of 40% of sulfur and epoxy (which were compacted at ambient conditions and achieved 22.3 and 28.6 MPa, respectively). Figure 17 presents the average compressive strength of various concretes tested by Omar and Issa's experiments. It can be seen from this figure that concrete samples utilizing a sulfur content of 35 and 40% seems to record the highest compressive strength. The addition of higher sulfur content (>50-60% of total mix) significantly reduced integrity and mechanical properties of sulfur concrete, possibly due to shrinkage of sulfur during cooling.

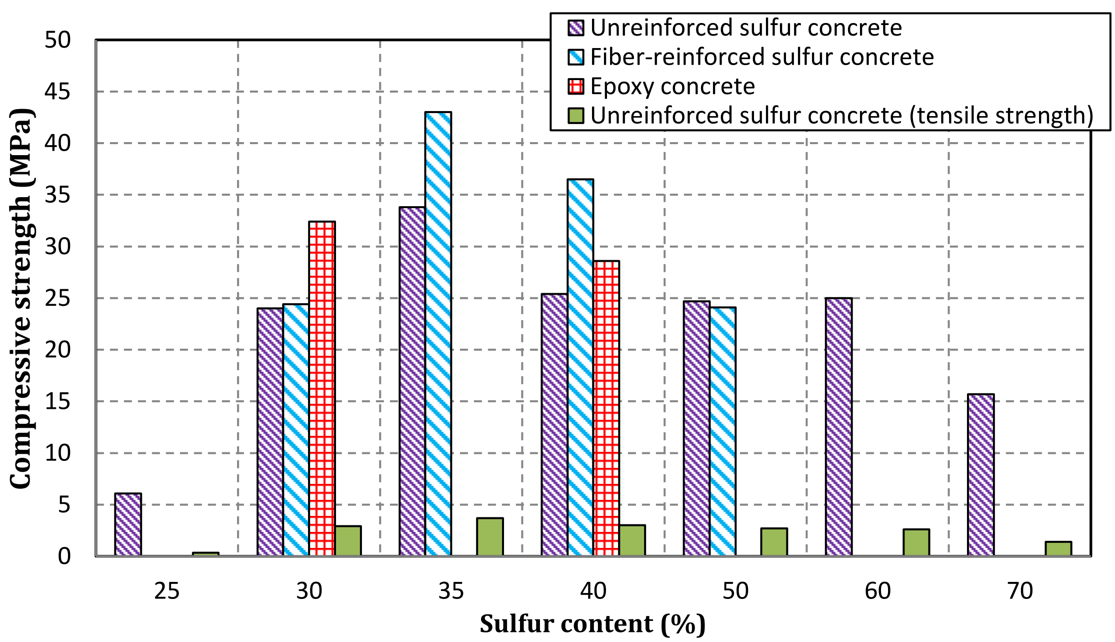

Fig. 17 Average compressive strength of various concretes tested in experiments by Omar and Issa [235,236]

In the early 2000's, the prominent works of Toutanji and Grugel led to number of successful investigations with regard to developing various types of sulfur concrete [233,237–239]. Toutanji and Grugel showed that sulfur concrete not only can achieve a compressive strength exceeding 30 MPa, but also showed that the addition of glass fibers can significantly improve the strength of sulfur concrete by up to 45%. When sulfur concrete was used in beams, the same researchers showed how glass fibers increased beams' flexural strength by about 40% (see Table 15). Toutanji et al. [240] also investigated the radiation shielding properties of sulfur concrete according to the recommendation of the International Commission on Radiological Protection (ICRP). Their analysis showed that the minimum required effective concrete thickness for short term shielding to radiation exposure is 67 mm. While Toutanji et al. [240] did not consider long term exposure, it is expected that a higher thickness would be required to limit total dose to that equivalent to 50 mSv, as specified by the U.S. nuclear regulatory commission.

Table 15 Mechanical properties of sulfur concrete

Property	**Sulfur concrete**	**Aluminum fiber-reinforced sulfur concrete** [236]	**Glass fiber-reinforced sulfur concrete** [241,242]
Compressive strength (MPa)	12-75	24-43	8-25
Tensile strength (MPa)	1.6-9.6	0.33-9.27	-
Modulus of elasticity (GPa)	20.7-32.4	-	-
Flexural strength (MPa)	~0.46-5.2	-	7-30
Strain at failure (%)	-	-	0.3-0.8

Grugel and Toutanji [233] also examined the effect of moderate exposure to vacuum (of about 60 days) on sulfur concretes made of JSC-1lunar simulant. The results of their research indicated that vacuum conditions induced substantial sublimation of sulfur, especially after 58 days of exposure, reaching about 30% of initial mass (see Fig. 18). Based on this observed behavior, these researchers estimated that it would take 1.63 hours to sublime a 10 mm layer made of sulfur at a lunar temperature of 120°C in contrast to 3.7 years on Earth (at a temperature of 15°C). It is interesting to note that Grugel and Toutanji [233] inferred that the rate of sublimation decreases, especially in sulfur concrete made with high aggregate contents, due to its higher density, and could reach a constant rate beyond the 60 day mark. Grugel [238] examined the performance of sulfur concrete subjected to temperatures and vacuum conditions analogs to that on the Moon. His tests showed that sulfur concrete can maintain its integrity under constant low temperature of -27°C. However, sulfur concrete was shown to severely degrade when exposed to thermal cycles between ambient and -191°C. This degradation was estimated at 5 times that observed in non-cycled samples.

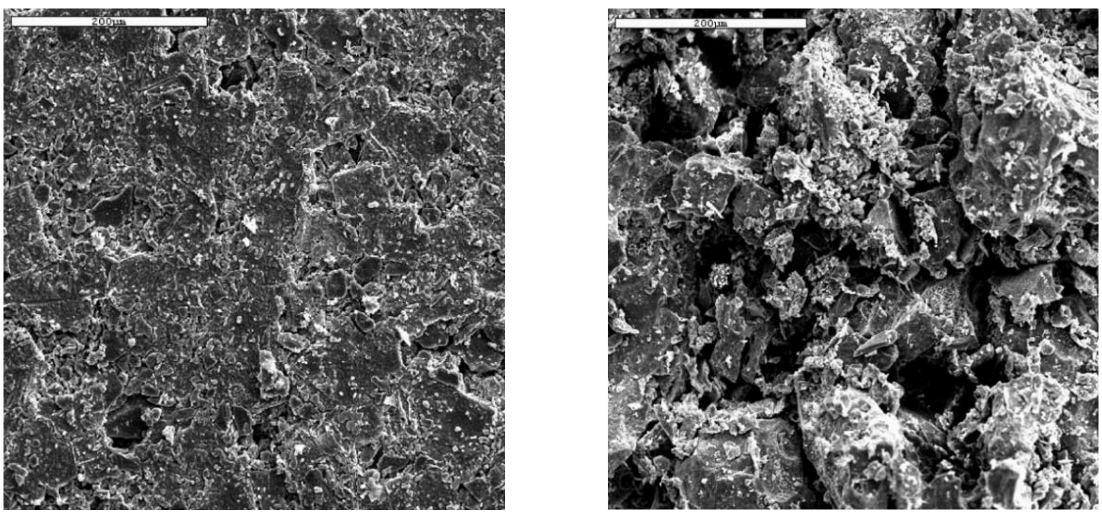

(a) As-cast sulfur (b) After 58 days in vacuum.

Fig. 18 Micrographs showing a comparison between sulfur concrete subjected to Earth-conditions (left) and vacuum (right) [238]

In a more recent study, Wan et al. [243] mixed varying contents of sulfur (40-60%) with a Martian simulant (Mars-1A) and reported that the best combination of sulfur-to-simulant, in terms of mechanical performance, was a 1:1 ratio (see Fig. 19a). In their work, Wan et al. [243] investigated the performance of two sulfur concretes intended for use on Mars. These researchers also compared the performance of this sulfur concrete with that made of 25% sulfur and 75% sand.

As part of this study, Wan et al. [243] investigated both microstructure as well as mechanical properties of these concrete. For a start, Figs. 19b and c show a comparison between microstructure of the two concretes. This figure shows how sulfur concrete made of Martian simulant is much denser (with smaller average particle size) than that of sulfur concrete made of sand. These images also show the lack of voids in Martian sulfur concrete, while the mixture of sand-based sulfur concrete shows dominance of distinguishably opaque orange to dark red spots associated with sand particles and voids. In the case of mechanical property testing, the compressive strength of sulfur concrete ranged between 20 to 63 MPa, while the concrete made of sand and sulfur achieved a strength varying between 24.5-28.3 MPa. Wan et al. [243] reported the findings of further tests carried out though X-ray photoelectron spectroscopy (XPS) which suggest that metal elements in Martian simulant show synergy and seem to better react with sulfur to form sulfates and polysulfates, which further enhances the strength of sulfur concrete. This kind of reaction was absent in the case of sand-based sulfur concrete as sand was shown not to react with sulfur during hot casting.

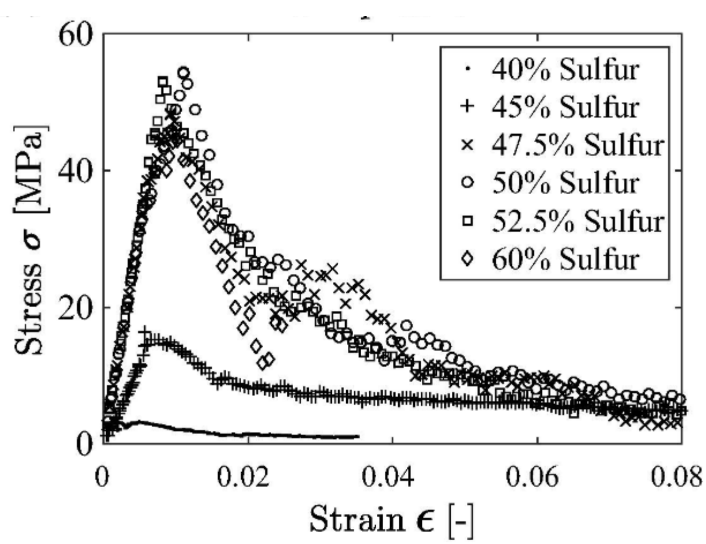

(a) Comparison of compressive stress-strain response for Martian concretes with various sulfur ratios

This is a preprint draft. The published article can be found at: https://doi.org/10.1016/j.pmatsci.2019.100577

Please cite this article as:
Naser M.Z. (2019). "Extraterrestrial Construction Materials." *Progress in Materials Science*. Vol. 105, 100577. https://doi.org/10.1016/j.pmatsci.2019.100577.

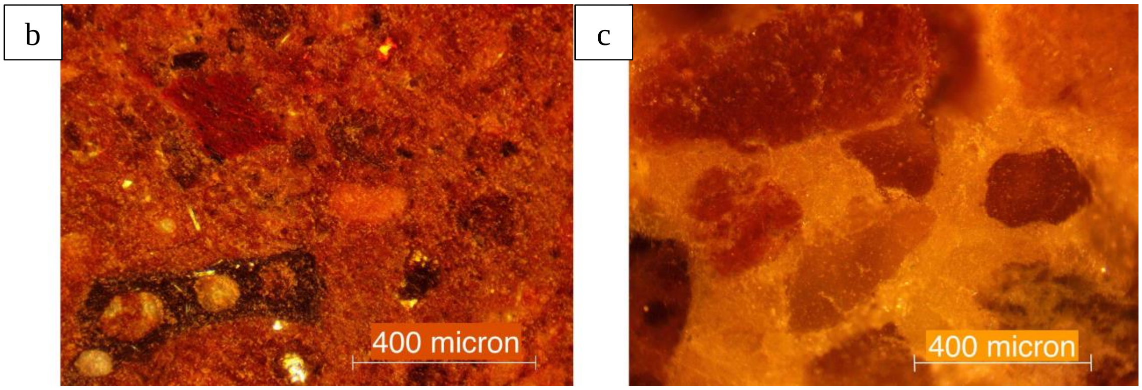

Fig. 19 Microscopic imagery of sulfur concrete with compositions of (b) 50% sulfur and 50% Martian soil simulant (c) 25% sulfur and 75% regular sand and a maximum particle size of 1 mm. [243]

In a number of instances, researchers reported that sulfur tends to shrink when cooled down and this might develop cracks in sulfur concrete and could cause debonding of hardened sulfur from aggregates. Significant shrinkage could also occur due to the large difference in thermal expansion between aggregate ($\sim 5.4 \times 10^{-7}$ $°C^{-1}$) and the sulfur (6.4×10^{-5} $°C^{-1}$). In one particular study, Osio-Norgaard and Ferraro [244] reported that sulfur concrete made of lunar simulant is more permeable than ordinary concrete as molten sulfur gets easily absorbed by regolith. Overall, curing of additive-free sulfur concrete is constrained between 130 and 140°C and it can only be used in an environment with temperature not exceeding 120°C unless thermal shielding is provided. As such, proper location of unprotected lunar and Martian structures made of sulfur concrete, if directly exposed to surface temperature, is only limited to higher latitudes or shaded locations with maximum temperatures less than 96°C and monthly variations not exceeding 114°C [245].

Geopolymer Concrete

Geopolymers are a class of amorphous, refractory, inorganic polymers that can be made from a powder-like aluminosilicate rich material such as fly ash or metakaolin, often mixed with amorphous silica dissolved in highly caustic alkaline solutions [246,247]. Concrete, when mixed with geopolymers, can turn into *geopolymer concrete*. Geopolymer concrete is a non-hydraulic concrete derivative that is highly dependent on the available silicon to aluminum (Si:Al) ratio in the concrete mix; where a ratio of ~2.0, or higher, yields smoother microstructure and improved mechanical properties (see Fig. 20) [248]. Geopolymer concrete consists of 20-30% of a geopolymer binder and 70-80% of coarse and fine aggregates. Despite its need for high shear mixing, geopolymer concrete has virtually near-zero water consumption, high resistance to thermal cycling and freezing-thawing as well as good vacuum stability [249,250]. This type of concrete also has twice and three times the compressive and flexural strength of traditional concrete, respectively. An interesting feature of geopolymer concrete is that it could designed with accelerated curing to achieve its full strength in only 1-2 days (as opposed to 28 days for ordinary concrete) [246,251][20].

Matta [252] found alkali metal elements on the Moon, and noted how these elements can be processed for alkali; an activator for geopolymers. In a parallel study, Wang et al. [253] speculated that since the composition of volcanic ash is similar to that of lunar regolith, then lunar soil could geopolymerize. Based on these two findings, geopolymer concrete comprising of more than 90% of regolith could be conveniently fabricated on the Moon and/or Mars.

[20] It is worth noting that a more in depth discussion on the composition, formulation, properties, and manufacturing of various geopolymer concretes at ambient working conditions can be found in the following notable studies [443–446].

This is a preprint draft. The published article can be found at: https://doi.org/10.1016/j.pmatsci.2019.100577

Please cite this article as:
Naser M.Z. (2019). "Extraterrestrial Construction Materials." *Progress in Materials Science*. Vol. 105, 100577. https://doi.org/10.1016/j.pmatsci.2019.100577.

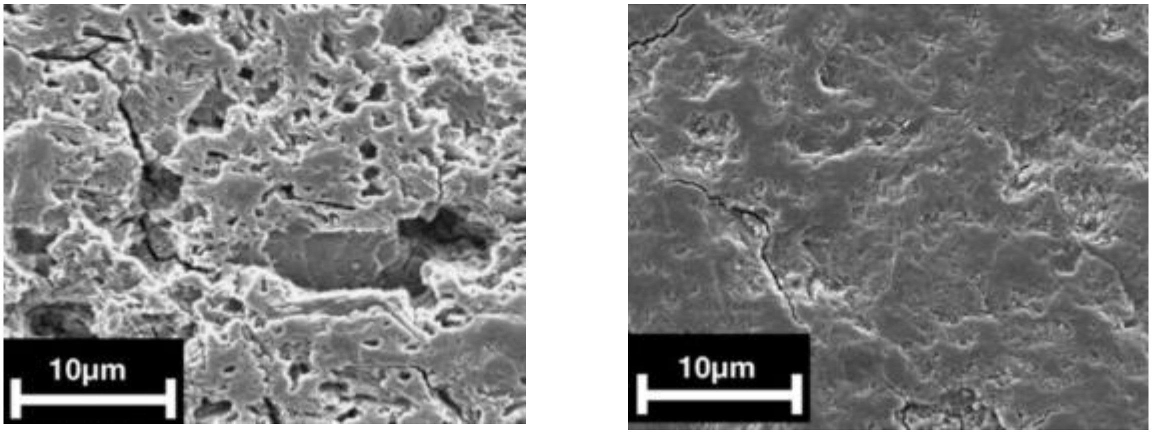

(a) Ratio of 1.45 (b) Ratio of 1.60

Fig. 20 SEM observations on the impact of the Si:Al ratio on microstructure of geopolymer concrete [248]

Geopolymer concrete is hypothesized to form in a three-step process (Dissolution-Polycondensation-Precipitation) [254,255]. This process starts in a high-pH alkaline solution with monomer polymerization in which alkali hydroxide or silicate bonds with alumina-silicate, alumina, or silica. This reaction forms, $Al(OH)_4$, and orthosilicic acid, $Si(OH)_4$. In the second stage, $Al(OH)^-_4$ and $Si(OH)_4$ turn into Al–O–Al and Si–O–Si bonds through catalyzing OH- ions. Finally, bonds formed in the second stage bind together and condense into amorphous structures [255].

In a similar trend to that of polymer and sulfur concrete, only few studies investigated the feasibility of utilizing geopolymer concrete in extraterrestrial construction [253,256]. In such one study, Wang et al. [253] developed geopolymer concrete made of lunar simulant, Va; with a composition similar to that of JSC-1A but made from volcanic ash and sodium hydroxide[21]. This geopolymer concrete was cast consuming 1.39% wt. of water and achieved a compressive strength of about 26-50 MPa once loaded in compression. The compressive strength of this geopolymer

[21] More specifically from augite and ferroan forsterite as oppose to olivine, pyroxene, ilmenite.

concrete was also studied after 24 hour exposure to moderate vacuum (of 1.5 torr) and reported to be 45 MPa. This developed concrete showed high resistance to freezing and thawing.

Using JSC-1 as a soil simulant, Montes et al. [256], developed another geopolymer concrete, named Lunamer, with good mechanical properties and high resistance to radiation. This concrete was studied under ambient conditions, hard vacuum (0.001 torr) and in combination of vacuum and elevated temperature of 106°C. As can be seen in Fig. 21, the compressive strength in samples cured under ambient conditions linearly increases with age (curing) of samples. This is unlike that observed in samples cured under the effects of vacuum and temperature which underwent a loss in compressive strength from 9.5 MPa to about 3 MPa after 28 days of exposure. Interestingly, the compressive strength in samples cured under vacuum conditions slightly increased (from 8.6 to 11.2 MPa) during the first 7 days of curing and then reduced to about 9 MPa after 28 days of exposure to vacuum (see Fig. 21a). A much more severe loss in strength was observed in the samples exposed to both vacuum and lunar temperatures. Montes et al. [256] did not specifically provide an explanation for this behavior other than reporting observations in which binder crumbles into smaller pieces with extended exposure time to vacuum and temperature (see SEM visuals in Fig. 21d and e). A companion study carried out by Montes et al. [256] showed how geopolymer binders, produced from regolith, can achieve a compressive strength in the range of 16.6 to 33.1 MPa. The same study also concluded that geopolymer concrete with a moderate density of 2290 kg/m^3 and thickness between 500-1000 mm can offer adequate protection from radiation such as that associated with lengthy lunar missions.

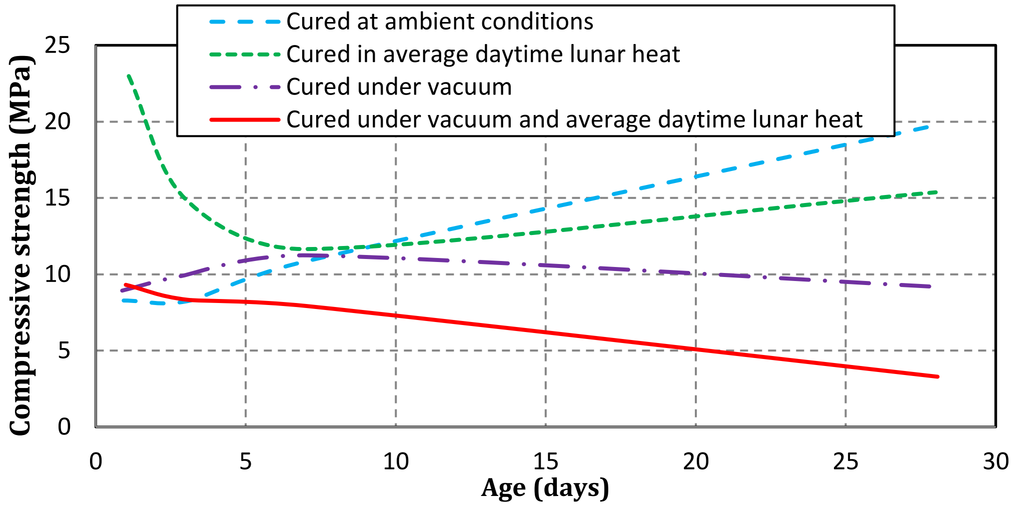

(a) Compressive strength of concrete under various curing conditions.

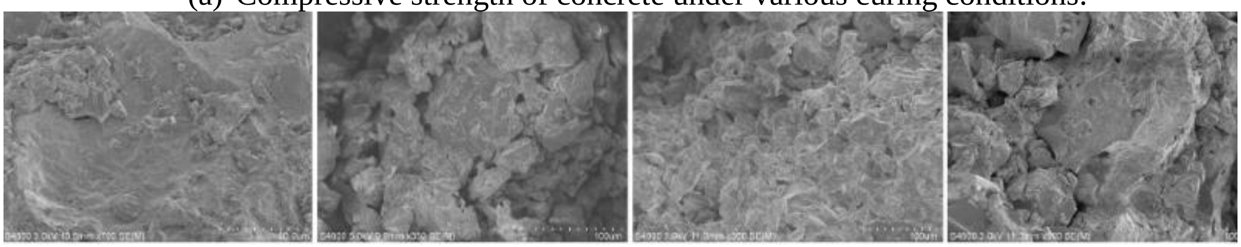

(b) Evolution of geopolymer cured in ambient conditions.

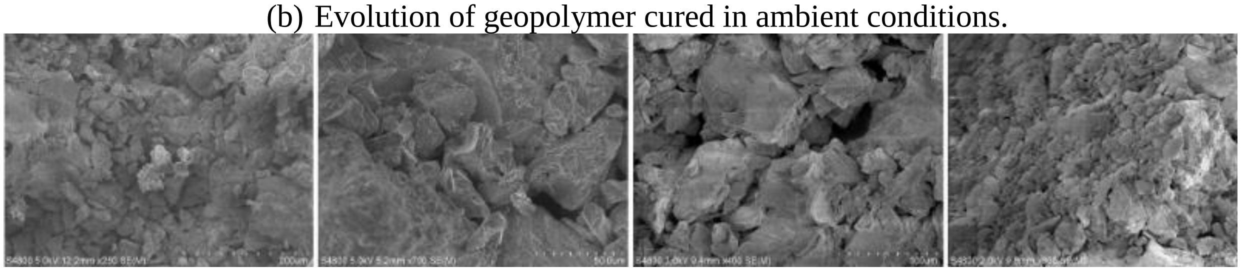

(c) Evolution of geopolymer cured in lunar average daytime heat.

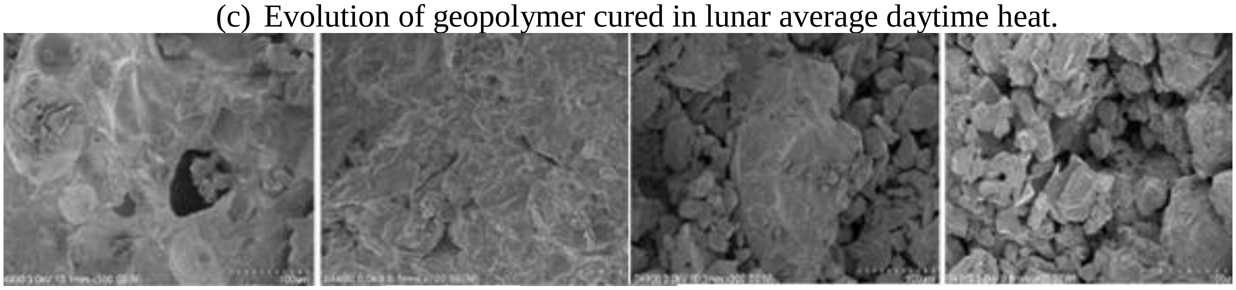

(d) Evolution of geopolymer cured in vacuum.

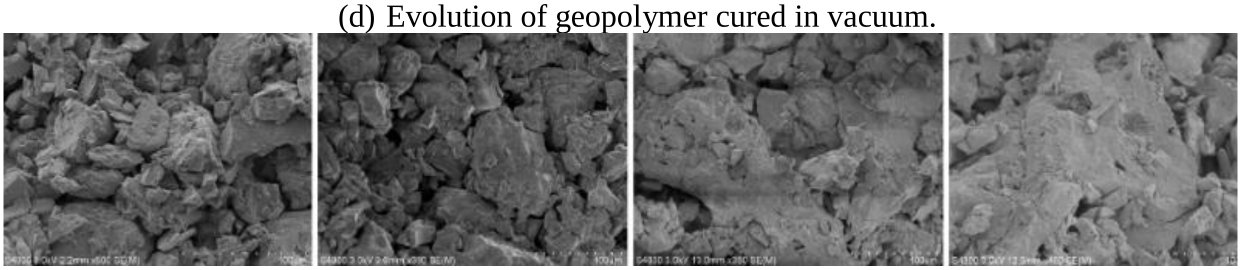

(e) Evolution of geopolymer cured in both heat and vacuum.

Fig. 21 SEM micrographs on various environmental conditions on geopolymer [256]

In another study, Alexiadis et al. [257] investigated the prospect of geopolymerizing lunar simulant JSC-1A and Martian simulant Mars-1A to produce in-situ geopolymer concrete. These researchers noted that geopolymerization of the lunar simulant was much faster and easier than that of the Martian simulant; possibly due to the pre-processing (milling to reduce particle sizes) required in the case of the later. Alexiadis et al. [257] carried out compression and flexural tests on lunar and Martian simulant geopolymer concrete samples. The outcome of these tests showed that lunar geopolymer concrete outperforms both Martian geopolymer as well as ordinary concretes. The lunar geopolymer achieved compressive and flexural strengths of 2-18.4 MPa and 13±3.7 MPa, respectively which were higher than in ordinary and Martian concrete (12.6±1.6 MPa and 4.8±0.9 MPa as well as 0.7-2.4 MPa and 3.6±1.3 MPa) (see Table 16). The distinctly low compressive strength of Martian geopolymer concrete was credited to the low reactivity of Mars-1A Martian simulants used in developing Martian polymer concrete.

Table 16 Comparison of mechanical properties of various types of geopolymer-based extraterrestrial concrete [257].

Property	Geopolymer lunar concrete	Geopolymer Martian concrete
Compressive strength (MPa)	2-37.6	0.7-2.5
Flexural strength (MPa)	13	3.6
Density (kg/m^3)	2600	1800

This is a preprint draft. The published article can be found at: https://doi.org/10.1016/j.pmatsci.2019.100577

Please cite this article as:
Naser M.Z. (2019). "Extraterrestrial Construction Materials." *Progress in Materials Science*. Vol. 105, 100577. https://doi.org/10.1016/j.pmatsci.2019.100577.

Multipurpose Concretes

The modern technological advancements and efforts of interdisciplinary research have led to developing new and functional concrete materials; often referred to as *multipurpose concretes* [258]. These concretes are specifically-designed and tailored to possess superior properties depending on their intended use and nature of application. Developing multipurpose concretes can be realized through articulated composition (mix) design, special mixing and processing procedures, integration of sensing technologies etc. with the aim to modify the microstructure of concrete in order to allow possession of new functionalities/capabilities.

One such concrete with high potential in additive printing of lunar and Martian habitats as well as structural components is that of high workability and flow properties. This concrete is referred to as *self-shaping concrete*. Self-shaping concrete is deposited through a layer-by-layer operation. This type of concrete has high viscosity, sufficient adhesion and rigidity. Due to the lack of formwork, self-shaping concrete is designed to cure and to have high strength immediately post printing. In one study, Gosselin et al. [259] reported the compressive and bending strength of ultra-high performance self-shaping concrete at 120 and 14 MPa, respectively. Cesaretti et al. [260] also developed a new additive printing technology, D-shape, that utilizes a self-shaping concrete of compressive strength of 20.35 MPa, porosity of 13%, density 1855 kg/m^3, and Young's modulus 2.35 GPa. Khoshnevis et al. [261] developed a different concrete printing technology that can accommodate sulfur to produce sulfur-based self-shaping concrete. This technology is referred to as Contour Crafting. Pilot studies on this concept show that it would be possible to print 232 m^2 habitat in about 20 hours. Xia and Sanjayan [262] also developed a geopolymer-based self-shaping concrete. The compressive strength of this concrete was low (0.9 MPa) but could be improved to

16 MPa via immersing printed concrete in saturated anhydrous sodium metasilicate solution at 60°C. At the moment, efforts are put in place to better this geopolymer-based self-shaping concrete to be effectively used for lunar and Martian construction.

Self-sensing concrete is a type of concrete designed with the ability to sense the changes within its structure, in addition to its surrounding environment, by incorporating functional fillers (i.e. carbon nanotubes, nickel powder) and/or sensing components (e.g.: piezoelectric materials) [263]. Electrical signals, such as electrical resistance or reactance, capacitance, and impedance tomography, can be used to characterize structural and environmental changes surrounding this concrete. This type of concrete can be used to identify crack development, damage or localized failure due to micrometeorites, and hence can be applied as layers on outer surfaces to structures. Another type of concrete that naturally complement self-sensing concrete is *self-healing concrete* which can independently restore damage (cracks). This type of concrete can be beneficial in scenarios where low maintenance and extended service life are required; both of which are desired on the lunar and Martian surface (see Fig. 22).

This is a preprint draft. The published article can be found at: https://doi.org/10.1016/j.pmatsci.2019.100577

Please cite this article as:
Naser M.Z. (2019). "Extraterrestrial Construction Materials." *Progress in Materials Science*. Vol. 105, 100577. https://doi.org/10.1016/j.pmatsci.2019.100577.

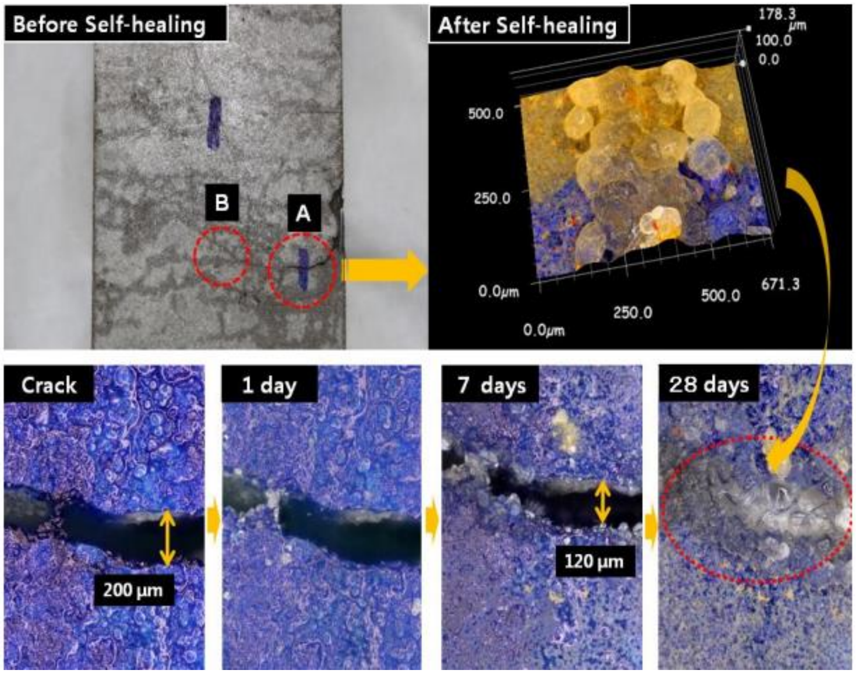

Fig. 22 Process of self-healing in concrete [264]

The self-healing process can be achieved through autogenous methods including hydration of cement, or carbonation of calcium hydroxide. More recently, concretes with autonomous healing abilities were also developed [263,265]. Depending on the type of binder/filler/healing technique, healing recovery rates can be in the range of 60-100% [263]. Yuan et al. [266] reported development of moderate strength hot-melt polyamide (HMP) concrete with healing abilities that can mitigate adverse effects of elevated temperature similar to that present on the Moon or Mars. Dade-Robertson et al. [267,268] proposed the use of bacteria to bioengineer self-healing concrete on Mars as it may hold preferable conditions for bacterial growth. Table 17 lists properties of some of multipurpose concretes.

Table 17 Mechanical properties of multipurpose concretes

Property	**Self-shaping concrete** [262,269]	**Self-sensing concrete** [262,270]	**Self-healing concrete** [266]
Compressive strength (MPa)	0.9-120	40-120	85-108
Modulus of elasticity (GPa)	2.35-5.67	-	-
Flexural strength (MPa)	7.1-14	~16	9-12
Strain at failure (%)	0.3	0.15	-
Density (kg/m^3)	1855	-	3100

Radiation shielding concrete is a dense type of concrete (3200-4000 kg/m^3) that comprises of heavy aggregates containing high content of crystalline water. This concrete is used to protect against various radiation sources including alpha, beta and gamma rays, as well as X-rays, and neutrons [271–274]. In the context of space construction, alpha and beta rays have low penetration capability and hence can be effectively absorbed through thin shields. On the contrary, gamma, X-rays and neutrons have high energy and penetration ability and can only be absorbed through dense metals or concretes. This type of concrete is to be preferably made of barium silicate cement or boron and iron containing phosphate cement as the later has high resistance to temperature changes. Some studies concluded that using ilmenite concrete (having a density of 3500 kg/m^3) could lead to 30% reduction in thickness for concrete shields against radiation, such as those to be use in lunar and Martian habitats [263]. Shams et al. [275] showed that heavy concretes made of barite and hematite aggregates can have a density close to 3000 kg/m^3, compressive strength of 50 MPa while maintaining high shielding capabilities against gamma rays. A concern arises on the attainability of lunar/Martian rocks or aggregates with similar features to terrestrial aggregates which would allow in-situ production of radiation shielding concrete.

Another type of concrete that could be of use in lunar and Martian habitats is that with *energy-harassing* capabilities. This type of concrete is impregnated with piezoelectric, thermoelectric, photovoltaic, or pyroelectric particles/fillers. There are two types of energy-harassing concretes. The first can store energy, and the second can convert energy generated by external sources (e.g., solar power, mechanical, and thermal forms) and turn it to a useable form of energy (i.e. electrical, thermal) to provide cost-effective and sustainable solutions for energy-constraint constructions. The mechanisms by which this concrete can harness or convert energy are as follows. Piezoelectrics generate a small voltage under mechanical pressure or deformations which can be directly used to generate electric power. In the case of energy-harassing concrete utilizing thermoelectrics or photovoltaics, electric voltage can be generated when a thermal gradient or, high radiation is developed [263]. Derivatives of this category of concretes include *light-transmitting concrete* and *light-emitting concrete* which, as their title suggest, can transmit light and trap solar energy during daylight to emit it at night. These concretes seem to best suit the environment on the Moon and Mars due to the poor atmosphere and abundance of solar energy.

At the time of this review, research efforts on the aforementioned concretes are still in early stages of development and as such, have been tailored towards terrestrial constructions. Actually, little is known about the behavior of multipurpose concretes in vacuum or low gravity conditions. It seems that most of the published works were heavily interested in reporting physical properties (i.e. electrical, thermal, radiation, and energy-related) and application efficiency (e.g. healing rate, energy production/conversion rate etc.) rather than mechanical properties of developed concretes. Still, a brief discussion on these novel concretes is presented here for comprehensiveness and also to highlight their possible use in extraterrestrial construction applications[22]. It is envisioned that

[22] Readers are encouraged to review the following references for in-depth details on the behavior of various smart and multipurpose concretes [263,447].

hybrid concretes with multi-functioning abilities and properties would better suit interplanetary construction than those of traditional nature.

Metals, Alloys and Metal Foams

In lieu of concrete and its derivatives, *metals* and *alloys* can also be used in extraterrestrial constructions. While metals and alloys are not readily available for use, unlike the case of regolith for concrete, lunar and Martian metallic ores can be mined and processed [276]. As discussed earlier, four metals (and their alloys) i.e. magnesium, aluminum, iron and titanium can be extracted from regolith and rocks. These metals, together with their alloys, have high prospective for use as construction materials, radiation shields and extra-vehicular components. Table 18 lists physical and construction/mechanical properties of these metals from a structural engineering prescriptive.

Table 18 Physical, mechanical and thermal properties of aluminum, magnesium, iron and titanium

Property	**Al**	**Mg**	**Fe**	**Ti**
Density (kg/m^3)	2700	1700	7900	4600
Yield Strength (MPa)	~170	90-195	280	434
Strength to weight ratio	62.9	114.7	35.0	94.3
Modulus of Elasticity (GPa)	70	45	196-207	107-119
Elongation (%)	5-25	14-45	12-45	18-30
Thermal Exp. Coefficient	2.31×10^{-5}	2.48×10^{-5}	1.18×10^{-5}	8.6×10^{-6}
Melting point (°C)	660	650	1538	1668
Mass Magnetic Susceptibility (m^3/Kg)	7.8×10^{-9}	6.9×10^{-9}	-	4.01×10^{-8}
Thermal conductivity (W/m.K)	235	160	79	22

According to Benaroya [277], *magnesium* has number of characteristics that makes it favorable for lunar in-situ refining and production, such as ease of casting and recycling. Considering it is the lightest of the above metals, magnesium also has high strength-to-weight ratio (~114.7) and could outperform structural steel in some applications. Magnesium is a relatively poor thermal conductor = 160 W/m.K (as compared to aluminum 235 W/m.K) and with small magnetic susceptibility of 6.9×10^{-9} m^3/Kg. Magnesium has electromagnetic and radiation shielding properties as well as adequate strength and low density as compared to other metals. Perhaps one of the most attractive traits of magnesium is that it has high vibration and damping properties, estimated at thirty times that of aluminum. If produced in large quantities, then magnesium can be beneficial when used for external shielding of lunar and Martian habitats against micrometeorite bombardment as well as to absorb seismic energy generated from Moon- and Mars-quakes [278]. Magnesium, when supplemented with other metals, turns to alloy with superior properties such as Mg-Zn-Cu alloy (ZCM). Magnesium alloys can generally be classified under two groups: aluminum-bearing and aluminum-free. Alloys of an aluminum-bearing nature are generally processed with ease due to the absence of zirconium [277].

The work of Mottaghi and Benaroya [278,279] investigated the thermal and structural (including seismic) response of a lunar habitat built of magnesium and covered with lunar regolith. Through complex numerical analysis, these researchers subjected a 226 ton igloo-shape habitat to effects of space weathering i.e. lunar diurnal temperature and moonquake. Predictions from this simulation showed the adequacy of magnesium construction under the harsh effect of lunar environment.

Magnesium can also be used to produce cementitious materials. Brichni et al. [280] investigated the use of magnesium oxychloride cement (Sorel cement) in concrete. This cement is formed by mixing a concentrated solution of magnesium chloride hexahydrate ($MgCl_2.6H_2O$) with magnesium oxide (MgO) powder. This magnesium-based cement, when compared to Portland cement, was shown to have high compressive strength reaching 75 MPa, rapid hardening rate, good cohesiveness and resistance to abrasion [280]. To allow its integration into additively printed structural components, Werkheiser et al. [281] developed improved Sorel cement by using magnesium di-chloride ($MgCl_2$).

Aluminum is also suitable for extraterrestrial construction due to its advantageous properties such as high strength, high fracture energy, low density and melting points (see Table 19). Another unique feature of aluminum (and its alloys) is that not only does their strength increases under low temperatures (a condition similar to that at poles in the Moon and Mars) but also does their ductility. A key advantage for aluminum alloys is that they do not tend to sublime (lose mass), unlike magnesium alloys which can lose up to 0.01 cm/year (at high temperature and vacuum) [282].

The use of aluminum as a construction material in space construction varies between fabricating shell (thin) modules to full-size scale structural members (i.e. columns and beams) as well as load bearing components in solar panels, and communication/transportation systems. In fact, at one point in time, the Apollo program utilized aluminum into a rigid space module [283]. In a more recent study, Gionet [284] examined the positive attributes of aluminum and the merit of extracting this metal from in-situ resources. In his study, Gionet also developed aluminum frame modules made of 2014-T6 aluminum alloy as a basis for a lunar habitat. Mazzolani historically details a number of space-like structures developed over the past years using various aluminum alloys [285]. More specifically, the Al 6351 series T6 were used in bars and columns, where Al 99.5 were utilized as raw for trapezoidal sheeting and galvanized steel bolts for connections in space structures. Lee et al. [222] showed how aluminum can also be thermally liquefied to bind regolith to produce waterless concrete as well as to form fibers that can be added to concrete mixtures as a reinforcement.

This is a preprint draft. The published article can be found at: https://doi.org/10.1016/j.pmatsci.2019.100577

Please cite this article as:
Naser M.Z. (2019). "Extraterrestrial Construction Materials." *Progress in Materials Science*. Vol. 105, 100577. https://doi.org/10.1016/j.pmatsci.2019.100577.

Table 19 Properties of various metal alloys.

Property	**2014-T6 Al** [286,287]	**Al 6351** [286,288]	**Al 99.5** [277]	**Al 2219** [277]	**Al-Li 8090-T8771** [289]	**ZCM 711** [289]	**Ti-6Al-4V** [290]	**Beryllium Alloys** [291]	**Steel metal foam** [292]
Ultimate Strength (MPa)	-	250	75-146	455	441.3	275	900-950	290-324	190-330
Yield Strength (MPa)	410	150	-	315	344.8	185	800-920	207-241	0.89-200
Elongation (%)	-	20	25	-	0.5-2.0	12	5-18	2-3	-
Modulus of Elasticity (GPa)	72.5	70-80	45	73.1	80.67	45	104-113	-	0.08-12
Density (kg/m^3)	2800	2650	2700	2795	2519	1795	4420	-	-
Thermal Exp. Coefficient	-	23×10^{-6}	24×10^{-6}	-	23×10^{-6}	27×10^{-6}	9.2×10^{-6}	-	-
Outgassing rate (torr.L/sec.cm^2)	2.5×10^{-9}	9.2×10^{-14}	-	-	-	-	-	-	-

Initial design of a 16 m metal spherical habitat was carried out by Yin [289] at NASA. This habitat was proposed to be made of high-strength structural aluminum, Al 2219. In a later study, Yin [289] refined his design and suggested the use of aluminum lithium (Al-Li/8090-T8771) and magnesium alloy (ZCM 711) to fabricate spherical and cylindrical framings for this lunar habitat. Yin [289] detailed how magnesium alloy can be used in compression supports and recommended using aluminum lithium alloy in resisting tensile load actions as well as in interior framing. This is due to the fact that the ZCM 711 loses ductility under low temperatures and hence is not well suited for resisting tensile actions. Further, the relatively low combustion temperature of ZCM 711, as well as poor resistance to corrosion, limited its use to exterior structural components where oxygen and moisture are not present. It should be noted that Yin [289] also designed a 600 m long lunar communication tower made of the same aluminum and magnesium alloys described above.

Another metal that may also be used as a construction material in space is *iron* (and steel). Iron is one of the most widely used construction materials on Earth. In fact, iron has been extensively used in wide variety of structural applications ranging from traditional (i.e. buildings) to those of an extreme nature (i.e. bridges) [293]. Perhaps one of the best attributes of iron is its strength, ductility, moldability and our knowledge of its behavior under extreme conditions. Since metal NEOs can contain >2% cobalt, >7% nickel, among other metals such as manganese, iron can be supplemented with these metals to improve its strength and ductility [294]. Lunar steel is expected to be of low carbon content, while Martian and NEO-based steel could consist of relatively high carbon content due to the high carbon content in the Martian atmosphere.

Steel can be grouped under three major classes: carbon steel, alloy steel, and stainless steel. An advantage of steel over other metals, such as aluminum, is that the energy required to produce iron is relatively low (i.e. 17% of that required to produce aluminum [295]). Still, steel is heavy with a strength to weight ratio of about 35, as opposed to 62.9 and 114.7 for aluminum and magnesium, respectively. As such, steel could be best suited for use in critical components including connections (bolts, welds etc.), reinforcing fibers/meshes and radiation shields.

Titanium, on the other hand has a relatively high strength to weight ratio of 94.3. This metal is 40% lighter than steel and about 2-3 times stronger than aluminum and magnesium. Titanium, and its alloys, are preferred in scenarios where aluminum, magnesium and steel alloys do not meet design requirements in terms of strength or working temperature. For example, Ti-6Al-4V is a titanium alloy that often replaces aluminum alloys as a result of its high mechanical properties, and low thermal expansion [296]. It is worth noting that pure titanium may not be appropriate for use in interior structural components as it tends to freely react with oxygen (as well as nitrogen and hydrogen) [297]. Structural cables made of pure titanium could be used as bracing and tensile load carrying members, especially in exterior and support structural systems.

While this review focused on aluminum, magnesium, steel and titanium as main construction materials, other metals and alloys could also be used in space construction. For instance, Szilard proposed the use of *beryllium* alloys, with an average yield strength of 220 MPa and superior radiation and temperature resistant, in the design of prefabricated sphere-shaped habitats [298]. However, the use of beryllium alloys was deemed inadequate as some studies reported a brittle behavior associated with beryllium alloys under impact and shock loading. Sen et al. [299] developed a framework that enables fabricating high-purity metallic alloys using elemental extraction and zone refining of lunar simulants (JSC-1) mixed with 20 wt.% graphite powder in an inert argon-filled atmosphere and held at 1500°C for one hour. This process has led

This is a preprint draft. The published article can be found at: https://doi.org/10.1016/j.pmatsci.2019.100577

Please cite this article as:
Naser M.Z. (2019). "Extraterrestrial Construction Materials." *Progress in Materials Science*. Vol. 105, 100577. https://doi.org/10.1016/j.pmatsci.2019.100577.

to forming an iron rich *Fe–Si–P* alloy with a composition of 87.5, 9.63 and 2.87 wt.% iron, silicon and phosphorus, respectively (Fig. 23 shows Fe-rich phases and precipitates containing graphite flakes). Lui et al. [300] carried out similar efforts and reported that it is possible to produce *aluminum-silicon (Al-Si)* alloy from Northeastern University lunar simulant 1 (NEU-1). The produced alloy had a composition of aluminum and silicon with a composition comprising mainly of aluminum and silicon (56.70 wt.% Al, 40.80 wt.% Si, 2.25 wt.% Fe, and 0.25 wt.% Ti). The aforementioned two studies did not report mechanical properties of the alloys produced.

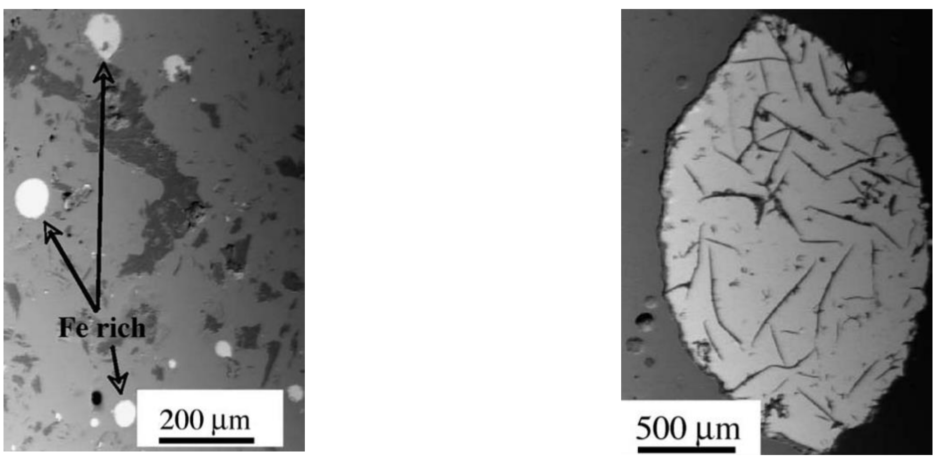

(a) Distribution of Fe-rich phases reduced JSC-1 matrix

(b) Fe-rich precipitate containing graphite flakes

Fig. 23 Microstructures of iron rich Fe–Si–P alloys [300]

Metal foams can be made of a base metal, i.e. aluminum, or titanium, and could also be formed from alloys. Metallic foams are mixtures of a molten metal/alloy and gas bubbles [301]. These foams can be formed by injecting melts with gas through direct injection, blowing agents, or solid-gas eutectic methods [302]. The foaming process introduces voids to the microstructure of the foam and forms a cellular-like structure [303] (see Fig. 24). The porosity of metal foams ranges between 70-95% which decreases its density, increases bending stiffness, energy dissipation, as well as vibration capabilities. Furthermore, the high porosity of foams reduces heat, radiation, and acoustic transfer as oppose to solid materials [292]. Metal foams are often grouped under two classes, open-cell (porous foam) and closed cell (foamed metal). In a recent study, Gaffey and McCord [304] laid out a plan for mining irony NEOs to extract iron and nickel and then process these metals to form metal foam of light density close to 500 kg/m^3 in an orbital mining facility.

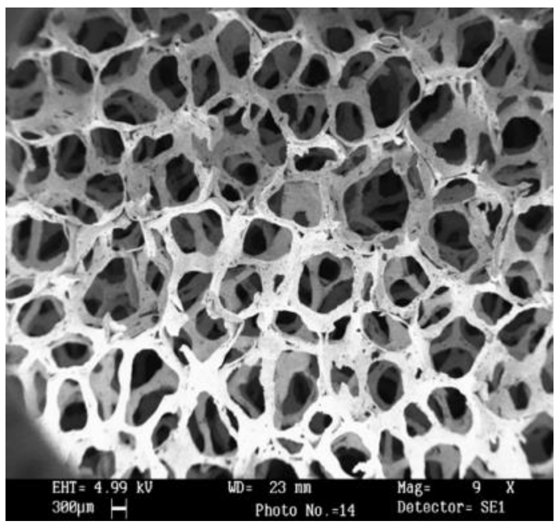

Fig. 24 SEM image of typical metal foam [305]

Stöbener and Rausch [306] developed aluminum foam elements by adhesive bonding to deliver a composite foam with approximately 80–95 wt.% aluminum foam and 5–20 wt.% adhesive. This foam had a compressive strength of 24 MPa and fracture strain of 60%. Hanan et al. [307] explored the merit of integrating bulk metallic glass (BMG) foams into structural components in lunar habitats. Some of the advantageous of BMGs include, low density and high strength-to-weight ratios and being easily processable at in-situ conditions. Veazey [308] reported that the mechanical properties of BMGs were highly dependent on their porosity. A compressive strength and modulus of elasticity of 200 and 600 MPa as well as 14 and 32 GPa was reported for porosity levels of 0.64 and 0.36, respectively [308]. BMGs are very versatile and can be used for construction as well as in repair applications. Metal foams have been applied in prosthetics, automotive and energy application, and while their application in civil construction is relatively immature, the potential of using metal foams in extraterrestrial construction seems promising, especially as exterior walls and shielding domes.

Composites

Composites are the result of joining two (or more) constituent materials with different physical attributes and chemical properties that when combined together produce a new material with unique characteristics [309]. Composite materials comprise of fiber/matrix combinations made of polymers, ceramics and/or metals [310–312]. The matrix (or binder) controls the physical features of the composite, while the fiber type influences the mechanical properties of the composite. The matrix is often selected with regard to its weight, cost and ease of manufacturing. Common fibers (reinforcement) can be of organic (i.e. polyethylene) or inorganic (ex: carbon, glass etc.) origin. Composite materials were designed to outperform metals and alloys in aerospace and military applications. In recent years, composites are also being employed in a variety of industries including new constructions or in strengthening of damaged or aging structures [313]. Some of the characteristics of composites include very high strength-to-weight ratio, dimensional stability, limited vacuum outgassing, and low tendency to expansion (see Table 20). The use of composites as extraterrestrial and construction materials have been duly noted in the open literature [314][23].

[23] Please refer to [448,449] for an in-depth review on properties of composites at working (ambient) conditions.

This is a preprint draft. The published article can be found at: https://doi.org/10.1016/j.pmatsci.2019.100577

Please cite this article as:
Naser M.Z. (2019). "Extraterrestrial Construction Materials." *Progress in Materials Science*. Vol. 105, 100577. https://doi.org/10.1016/j.pmatsci.2019.100577.

Table 20 Physical properties of composites suitable for space construction applications [315–317]

Material Property	**Gr/E (P75/1962)**	**Gr/TP (P75/PEEK)**	**SiC/Al (SiCp/2124 Al)**	**Gr/Al (P100/6061 Al)**	**Gr/Mg (P100/AZ91C Mg)**	**C/Gl (HMU/7070)**	**C/C (P100/C)**	**IOH**
Density (kg/m^3)	1730	1740	2880	2490	1890	1970	1660	-
Ply thickness (mm)	0.12	0.13	1.52	0.55	0.32	1.32	0.43	-
Tensile strength x-dire. (MPa)	307.5	240.7	582.6	905.3	422.0	282.0	304.1	3.5-25
Tensile strength y-dire. (MPa)	345.4	297.9	534.3	25.0	25.4	-	199.9	-
Comp. strength x-dire. (MPa)	182.7	147.2	557.1	321.4	200.6	597.8	47.9	40-110
Comp. strength y-dire. (MPa)	190.3	191.3	522.6	104.9	-	540.5	64.8	-
Strain x-dire.	0.261	0.263	1.26	0.262	0.21	0.405	0.17	-
Strain y-dire.	0.301	0.286	1.18	0.0707	-	-	0.15	-
Modulus of elasticity x-dire. (GPa)	104.8	91.7	114.7	342.8	175.4	80.7	223.4	-
Modulus of elasticity y-dire. (GPa)	104.8	96.5	117.2	35.4	28.3	-	140.0	-
Specific heat (J/kg-K)	808.1	849.9	830.7	812.2	916.9	753.6	707.6	-
Thermal conductivity x-dire. (W/m-K)	43.6	46.3	119.2	317.3	-	17.2	141.9	-
Thermal conductivity y-dire. (W/m-K)	43.6	48.6	116.6	69.2	-	17.2	67.5	-

What makes composites an attractive material for extraterrestrial construction is the possibility of mass production through processing lunar and Martian regolith [310,318]. Sen et al. [319] showed how it is possible to produce methane (CH_4) through reaction with Martian regolith. The produced methane is then converted into ethylene C_2H_4 ($H_2C{=}CH_2$) via catalytic oxidation and polymerized to produce polyethylene (see Eqs. 23-25).

$$CO_2 + 2H_2O \rightarrow CH_4 + 2O_2 \qquad \textit{Eqs. 23}$$

$$2CH_4 + O_2 \rightarrow H_2C = CH_2 + 2H_2O \qquad \textit{Eqs. 24}$$

$$(N+1)C_2H_4 \rightarrow H_3C(CH_2)nCH_3 \qquad \textit{Eqs. 25}$$

Sen and colleagues [319] also showed how this synthesized polyethylene (PE), when mixed with simulated Martian regolith (Mars-1), can produce an organic composite. Using this approach, samples of 38.1×38.1×25.4 mm were cast, and their mechanical properties were measured. The compressive strength and modulus of elasticity of these samples averaged at 41.1 MPa and 1 GPa, respectively. A significant improvement over those cast without PE (compressive strength = 4.9 MPa). Finally, Sen et al. [319] subjected these samples to impact loading equivalent to that to occur from micrometeorites (7 km/s). It was noted that the addition PE of 20 and 40 wt.% resulted in minor damage in the shape of a crater diameter of 3 mm and 1 mm, respectively.

Kaplicky and Nixon [98] proposed the use of *organic composites* in tube-like load bearing components (i.e. columns, beams and braces) for a deployable lunar habitat. This habitat was envisioned to have 56 columns, 70 beams and 143 lateral braces all to be made of graphite/epoxy (Gr/E) composite material. In their design, Kaplicky and Nixon [98] showed how composite columns would have a clear span of 5 m and axial capacity of 55 kN. In another study, Gosau [158] optimized a urethane resin capable of functioning in extreme weathers. This resin was developed as a water-free, two-part system and designed to stabilize lunar regolith into structural blocks (of 20:1 regolith to binder ratio). This system triggers polycondensation reactions with multifunctional reagents and generates polymer foam like structural materials. In his tests, Gosau mixed JSC-1A lunar simulant with polyurethane resin system. First a polyol component was mixed with the simulant, followed by addition of liquid isocyanate. Observations from these tests show that a homogenous solid material was formed within a short time. Cylinders made of this composite were tested under compressive loading and were reported to have a strength of 6.9 MPa. This material is currently being developed for use in an autonomous brickmaker that can fabricate building blocks on the Moon.

In order to investigate the performance of other composites under space conditions, Milkovich et al. [320] investigated T300/934 graphite-epoxy composite by subjecting it to low temperature (-156°C) or high temperature (121°C) in combination with a 1.0 MeV electron radiation at a rate of 5.0×10^{7} rads/hour for a total dose of 1.0×10^{10} rads (which is equivalent to a 30 years exposure in space). These researchers reported that radiation effects generated low molecular weight materials as a result of chain scissioning and crosslink breakage in the epoxy resin matrix. This breakage degraded the epoxy and caused embrittlement and softness at low and high temperatures, respectively (see Fig. 25). Overall, the adverse effects of radiation seem to affect tested composites in the transverse direction (rather than in the longitudinal direction) implying its adversity on the matrix. In a separate study, Kumar et al. reported a 29% degradation in IM7/997 carbon fiber-reinforced epoxy after 1000 hours of cyclic exposure to ultraviolet radiation.

This is a preprint draft. The published article can be found at: https://doi.org/10.1016/j.pmatsci.2019.100577

Please cite this article as:
Naser M.Z. (2019). "Extraterrestrial Construction Materials." *Progress in Materials Science*. Vol. 105, 100577. https://doi.org/10.1016/j.pmatsci.2019.100577.

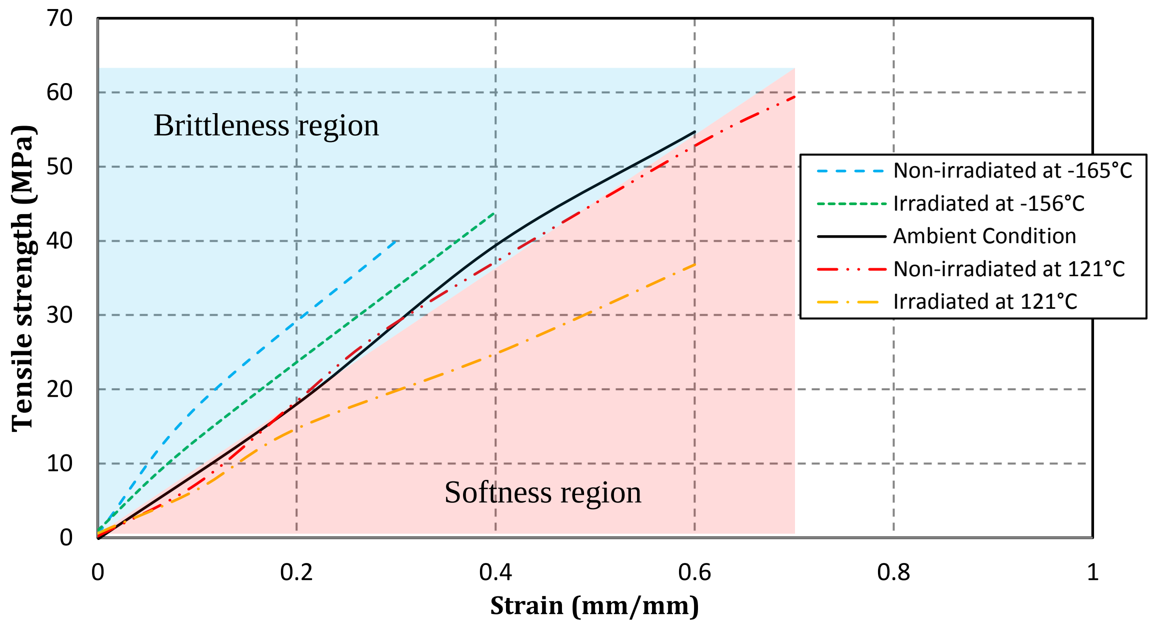

Fig. 25 Effect of radiation and temperature on tensile behavior of T300/934 graphite-epoxy composite [320]

The second type of composites are those made of metal matrix. Due to the metal component, these *metal composites* are the heaviest in the composite family but still lighter than most metals/alloys (see Table 20). Metal composites are used to replace metals where low weight and high creep resistance is required [321,322]. Williamson [318] showed the merit of metal matrix composites in multi-functional applications (i.e. structural, or thermal-control) for space habitats. More specifically, Williamson studied the behavior of silicon carbide/whisker reinforced aluminum composites (SiC/AI) and graphite reinforced aluminum metal composites (Gr/AI). He noted that the later had superior physical properties and how SiC/AI composites could be used in lieu of Gr/AI due to their lower cost. Johnson and Leonard [323] compared metal matrix composites and aluminum alloys and reported that metal matrix composites are superior to aluminum alloys since they can be tailored to have low thermal expansion and strength comparable to aluminum alloys. From a construction point of view, Bowles and Tenney [324] described successful attempts to manufacture circular truss elements (diameter = 50 mm and length = 1800 mm) made from metal matrix composites. The manufactured truss members were then used to construct a 3 m long, 3-bay truss system [315].

Alternatively, *ceramic matrix composites*, are non-brittle refractory materials designed to endure severe thermal and mechanical environments. Although ceramics, brittle materials, constitute the main component of ceramic composites, these composites tend to be relatively ductile with low creep response. These composites are impregnated with thin ceramic fiber reinforcement (with small diameter up to 10^{-3} mm) and as such have very high strength properties. Tóth and Desai [325] showed how ceramic composites can be readily made of lunar regolith. In their tests, these researchers thermally liquified two types of lunar simulants; Arizona Lunar Simulant (ALS) and Minnesota Lunar Simulant (MLS). These simulants were first heated to 1200°C to liquefy before they were left to cool down to room temperature in plates of 25×175×200 mm dimensions. Tensile tests were then carried out in order to investigate the tensile response of these composites. The modulus of elasticity, tensile strength, and strain at failure were reported at 33.7 GPa, 3.4 MPa, and 0.0007, respectively. In a companion study from the same research lab, Desai and Girdner [326] studied bending strength of similar composites and reported that the compressive strength could improve from 123 MPa to 201 MPa and 177 MPa when the composites are reinforced with aluminum and stainless fibers at 7.5 and 15%, respectively. These fibers can be produced from in-situ resources or can be imported from Earth during the early stages of habitation. In a similar work, Corrias et al. [159] reported on the development of complex composite ceramic–metal materials, consisting of mixed oxides, such as $MgAl_2O_4$, and $Ca(Al,Fe)_{12}O_{19}$ through the addition of higher percentage of ilmenite to lunar simulant, JSC.

Please cite this article as:
Naser M.Z. (2019). “Extraterrestrial Construction Materials.” *Progress in Materials Science*. Vol. 105, 100577. https://doi.org/10.1016/j.pmatsci.2019.100577.

Carbon/carbon (C/C) composites comprise of carbon fibers integrated into a carbon matrix. C/C composites are often produced by pre-forms of carbon fiber densified with carbon through chemical vapor deposition or infiltration. Moreover, carbon composites can be thermoformed (at low processing temperatures ~150°C) but require higher temperature to carbonize (~540°C) [327]. C/C composites can withstand thermal shock and extreme temperatures (above 2800°C). As a result, C/C composites were primarily used in the construction of space shuttles, and extra-vehicular. According to Noever et al. [328], lunar regolith can serve as a cheap, expendable mandrel for molding shaped composites. While little research has been carried out on these composites as construction materials, Noever et al. [328] proposed to re-use of C/C composites in space shuttles and structural components in lunar and Martian habitats. These materials could potentially be used as covers for habitats, and internal and/or external load bearing structural systems.

Other than organic polymers, inorganic polymers are defined as those materials composed of long chain molecules not containing carbon in their chain but may have carbon in pendant groups or inside chains. Some of inorganic polymers include glass and geopolymers. Lee [329] have shown how *inorganic composites* including glassy and cold-molded materials can be produced from lunar resources due to the high amount of silicates, especially in pyroxenes. Cotterill [330] reported the production of a metallic glass with 50% strain capacity and with a tensile fracture strength about 3 times that of stainless steel. Agosto [118] also showed that glass/glass composites can be formed from reinforcing fibers drawn from lunar basalt at high temperature (1000-1200°C) which can then be integrated into a low melting glass matrix.

More recently, Chen et al. [317] developed an inorganic-organic hybrid (IOH) composite comprised of ~92-96 wt.% JSC-1A lunar simulant and ~2-8 wt.% polymer binder (Epon-828 epoxy resin and m-Xylylenediamine hardener). When this binder is mixed with the lunar simulant, the binder forms a series of polymer micro-agglomerations (PMA) that bridge the filler grains together (see Fig. 26). This fills the microstructure of the IOH and significantly improves the mechanical properties of this composite. At the microscopic scale, the IOH consists of close-packed simulant grains and continuous nano-interphase. The nano-interphase can be viewed as polymeric membranes (with micrometer thickness) that bond simulant grains. This material is reported to be stronger than fiber-reinforced concrete and to be more durable under space environments. IOH has a compressive strength that varies between 40-110 MPa, flexural strength of 7-50 MPa, and maintains its properties at temperature ranging from -160 to 150°C, which is suitable for both Martian and lunar environments. This material may lose up to 5% of its weight at temperatures, exceeding 400°C. Recent outcome from the same research groups suggests that the flexural strength seems to increase linearly with the binder content and tends to saturate at binder content of 10 wt.% (and maintain satisfactory at temperature is below 130°C) [331]. It is envisioned that the binder will be produced on the Earth, and the fillers can be harvested locally on the Moon.

This is a preprint draft. The published article can be found at: https://doi.org/10.1016/j.pmatsci.2019.100577

Please cite this article as:
Naser M.Z. (2019). "Extraterrestrial Construction Materials." *Progress in Materials Science*. Vol. 105, 100577. https://doi.org/10.1016/j.pmatsci.2019.100577.

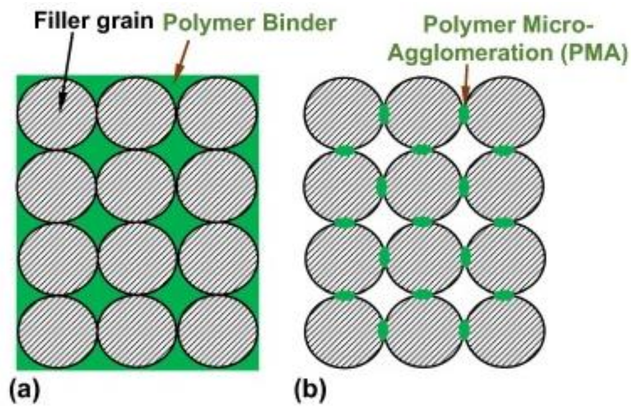

Fig. 26 Illustration of (a) close-packed grains filled by ~8.6 wt.% binder; and (b) polymer micro-agglomerations (PMA) that only bridges filler grains [317]

Advanced and Non-traditional Materials

Due to the extreme environmental conditions on the lunar and Martian surface, and the fact that common construction materials may not satisfy some of structural/construction requirements with respect to durability, and safety, have led to increasing research efforts aimed at developing specifically designed materials for use in space construction. These materials have unique features and characteristics that may not be present in traditional construction materials (i.e. concrete, metals) and as such are referred to herein as *advanced* and *non-traditional materials*. For the sake of this review, these materials are bundled under those with memory shape effect, of biological origin, made from single layer (2D) materials, ice, glass and those cultured in laboratory settings.

Shape memory materials (SMMs) are those that dynamically respond to external stimulus induced by mechanical stress, thermal, electrical or magnetic effects [332,333]. SMMs are often grouped under shape memory-alloys (SMAs), -polymers (SMPs), or -ceramics (SMCs). The product of mixing two (or more) types of SMMs can lead to developing a shape memory hybrid (SMH). The main feature of SMMs is their ability to recover their original shape once subjected to a particular stimulus despite undergoing plastic deformation. This shape memory effect is triggered via martensitic phase transformation (i.e. super-elasticity in alloys, or visco-elasticity in polymers etc.). Shape memory materials have been utilized in number of space exploration missions over the last few years [334]. For example, Schetky [335] reported that NASA integrated shape memory effects in SMAs to join structural members in the form of composite tubes through electric current that generates heat. Kalra et al. [336] also showed the merit of incorporating SMAs to achieve self-deploying mechanisms in adaptive space structural framing systems. Ellery [337] proposed the use of nitinol, a shape memory alloy of content close to 50% nickel and titanium, as the main material for structural applications on the Moon and Mars, including those for fabrication of rovers.

Shape memory polymers/foams are of much lower strength, in the range of 2-5% of SMAs (see Table 21). Nonetheless, these materials have a high compaction ratio, increased design flexibility, and reduced complexity [332]. Hence, SMPs can be used as low density (of about 15% of SMAs), and cheap solutions for self-deployable structures (habitats). Liang et al. [338] succeeded in employing reinforcing fibers to improve mechanical properties of SMPs so as to allow their use in structural components. Darooka et al. [339] also built an inflatable truss frame made of SMPs with analogous performance to that in Earth-based frames. Liu et al. [340] reported the outcome of a collaboration between ILC Dover Company and NASA to develop a self-deployable inflatable/expandable lunar habitat using SMP and SMC.

This is a preprint draft. The published article can be found at: https://doi.org/10.1016/j.pmatsci.2019.100577

Please cite this article as:
Naser M.Z. (2019). "Extraterrestrial Construction Materials." *Progress in Materials Science*. Vol. 105, 100577. https://doi.org/10.1016/j.pmatsci.2019.100577.

Table 21 Mechanical and thermal properties of advanced and non-traditional materials suitable for space construction applications

Material Property	**Shape memory alloy (Nitinol) (P75/1962)**[341]	**Shape memory polymer (P75/PEEK)** [342,343]	**Shape polymer foam** [344]	**Regolith bio-composite** [345]	**Spider silk (MA)** [346]
Density (kg/m^3)	6000-8000	900-1200	32	-	1300
Tensile Strength (MPa)	754-960	6-20	0.2	-	450-1100
Comp. Strength (MPa)	-	-	0.09–0.102	6.3-12.5	-
Ultimate Strain (%)	-	-	-	2-3	27
Young's Modulus (GPa)	75	1.0	0.2-11.4×10^{-3}	16.5	-
Specific Heat (J/kg.K)	-	-	1320	-	-
Thermal Conductivity (W/m.K)	100	-	0.027	-	-
Extent of deformation (%)	<8	up to 800	-	-	-

As part of the same work, Lin et al. [347] developed SMPs with customizable transition temperatures (T_g) ranging from 0-120°C as well as SMPs with dual transition temperatures (i.e. with an initial low T_g that can be triggered by heat, radiation or chemical exposure to a higher T_g). Once an SMP-based inflatable habitat is packed, it is cooled to approximately 15°C which locks the SMP and keeps it constrained until it is heated above the transition temperature (20°C above T_g). Upon deployment and when the SMP-based inflatable is heated, internal strain energy naturally (unassisted) returns the habitat to 90~98% of the initial cured shape and then turns rigid upon exposure to an external stimulus i.e. heat, radiation or vacuum. In the case of SMCs, Lai et al. [348] explained that the implementation of SMCs is still limited by cracking of ceramics at low strains (of about ~2%).

The second type of advanced materials highlighted herein is that of bio-origin. Rothschild [349] proposed a novel concept that enables biological utilization/processing of in-situ resources. In this concept, *bio-based construction materials* such as spider silk can be produced through genetically engineered organisms (i.e. microbes and bacteria such as Ralstonia eutropha H16). According to Rothschild [349], spider silk has low stiffness and density (~16.7% of steel), but also has very high tensile strength of ~2 GPa (approximately 4-6 times greater than steel). This concept was further explored by Roedel et al. [345,350] who integrated globular unfractionated blood proteins into regolith simulants to produce Regolith Bio-Composite (RBC) material. In this study, lunar Mare regolith simulant, JSC-1A, was prepared and mixed with Bovine Serum Albumin (BSA), a protein binder, through a vacuum assisted resin infusion method (VARIM). Roedel et al. [345] prepared and examined the response of 52 specimens under compression loading. These specimens varied in BSA levels from 6.6 to 7.6% of volume. The mean compressive strength of tested specimens was reported at 6.28, 8.42, 12.5, and 9.3 MPa for specimens with 6.6%, 7.1%, 7.5%, and 7.6% BSA, respectively. The stiffness moduli of the same samples were also reported at 0.85, 1.05, 1.18, and 1.3 GPa, respectively, indicating both properties to be dependent on the amount of protein binder present in the material. Upon further examination, failure of the protein phase was shown to govern the mechanical response of RBC, as the measured modulus of stiffness was closer to that of protein than JSC-1A lunar simulant.

Graphite has been shown to be present on the lunar surface as well as in fallen meteorites as tested by Zinner et al. [351]. Graphene-based materials present a unique opportunity for space construction. Qin et al. [352] were able to investigate physical properties of porous, additively printed, graphene samples. These tests indicated that graphene has very low density (about 5% of steel) with an exceptional high tensile strength of 2.7 GPa. Lepore et al. [346] investigated infusing graphene and nano-carbon tubes into spider silk and reported enhanced fracture strength and toughness modulus; ~5.4 GPa and ~1570 $J.g^{-1}$ (as opposed to values of uninfused silk (of strength ~1.5GPa) and (toughness ~150 $J.g^{-1}$)).

From the analysis of remote sensing missions carried out by *Odyssey's* gamma ray spectrometer, it is now clear that there are large ice pockets in the subsurface (within 0.2-1 m) of the higher and lower latitudes of Mars. In these locations, temperatures remain below the freezing point (between −10°C to −20°C) throughout the Martian year. Since water has unique ability to absorb high-energy short-wavelength radiation, while being transparent and allowing light to pass through its medium, a new concept of utilizing *ice-like* construction material has been proposed recently [353]. This concept employs a translucent hydrophobic aerogel layer with light transmittance of 66% to be installed between the inner ice shell and the inhabited spaces, in order to ensure thermal comfort. Since ice can have a compressive and tensile strength in the ranges of 5-25 MPa and 0.34-3.1 MPa, respectively thus, with proper design, load bearing walls made of ice can be fabricated. These walls can also shield against most radiation effects.

Glass is commonly manufactured on Earth. However, due to its brittle nature and weak mechanical properties, glass is not used in load-bearing structural application but rather in transparent components (windows, façades). The weak properties of glass arise as a result of stress corrosion effects, known as hydraulic weakening, caused by water vapor on Earth [354]. Blacic [119] expressed that glass formed in anhydrous environment (such as that present on the Moon) can possess superior mechanical properties and can be used in load bearing cables and pipes. Glass can be produced from molten lunar regolith that is cooled at relatively achievable rates between 2-89°C.s^{-1} (when compared to that of metals 10^5-10^6°C.s^{-1}) [355]. The properties of various lunar glass materials are listed in Table 9.

Interest in material behavior under low gravity conditions began in late 1950s, most notably with regard to the design of propellant management systems as well as procedures for brazing or welding in space when repairing or assembling metallic structures [37,356]. The outcome of these preliminary studies also noted that such materials tend to grow bigger crystals with fewer imperfections, and this led to the formation of high quality materials as compared to those manufactured on Earth (see Fig. 27). Under low (or micro) gravity, buoyancy driven forces are absent and the capillary forces become dominant, surface tension forces improve, and this significantly changes (and enhances) the solidification process [357]. As properties of construction materials are determined by their crystalline structure, tailoring microstructure during material formation can be crucial for quality control. Culturing crystals in laboratory settings enables

This is a preprint draft. The published article can be found at: https://doi.org/10.1016/j.pmatsci.2019.100577

Please cite this article as:
Naser M.Z. (2019). "Extraterrestrial Construction Materials." *Progress in Materials Science*. Vol. 105, 100577. https://doi.org/10.1016/j.pmatsci.2019.100577.

synthesizing organic or metal-organic crystal structures with desired characteristics (i.e. higher strength-to-weight ratio) over their Earth-based alternatives.

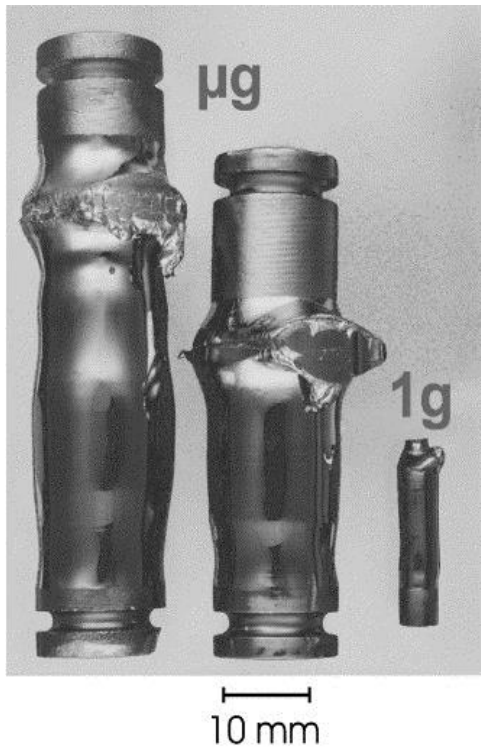

Fig. 27 Crystals grown is space under microgravity (µg) (left and center) and on Earth under normal gravity (1g) (right) [358]

Construction materials can be fabricated through *crystal growth* culturing. Crystals could be cultured using a variety of methods including, Czochralski technique, directional solidification, or zonal melting etc. Crystals can also be cultured from vapor, solutions, and melts. Doremus [359] reported how various types of pure and silicate/oxide-infused glasses, including those resistant to heat and shock, could be processed through containerless processing methods so as to avoid contamination and nucleation of crystals at container walls. Another potential material that can be cultured is spider silk which has high strength (about five times that of steel fibers), and elasticity (up to 27%) and can be utilized in construction/reinforcement of various structural components/elements [360].

It is envisioned that fragments of bio-like materials could be lunched in an inactive state during space flight, and once landed at the Moon or Mars, would start to grow into construction materials or even pre-engineered habitats [361]. Despite the attractiveness of this concept into developing extraterrestrial construction materials, it seems that much of the research on culturing materials in laboratory settings and under microgravity conditions has been directed towards aerospace-related and semiconducting materials, due to their high industrial application potential. At the time of this review, very limited work has been carried out on crystal growth of construction materials.

While this section was intended to highlight merit and characteristics of a few advanced and traditional materials from an extraterrestrial, structural and construction points of view, one should note that the behavior of such materials under low gravity and vacuum conditions is still not fully examined.

Processing of Extraterrestrial Construction Materials

Extraterrestrial processing is an operation that transforms ingredients (i.e. regolith/mined ores), acquired via mining operations, into building materials and products suitable for lunar and Martian constructions. This section overviews main processing methods associated with space construction materials; with special attention to melting/sintering, combustion, dry-mix/steam injection, and cold pressing.

Melting and Sintering

Two basic processing methods have evolved over the past years to form construction materials (with adequate strength) from lunar and Martian in-situ resources. One process involves *melting* regolith or mineral ore and then casting melt into molds to produce structural components [362]. Processing through melting results in a phase transition of the material from a solid to a liquid, to a new solid upon cooling. This method has been successfully applied in terrestrial applications, especially to producing near net-shape basaltic, metallic and glass materials. The second method, referred to as *sintering*, involves consolidating (compacting) regolith into the desired shape of a structural component. This compaction results in lesser voids, limits shrinkage and hence reduces energy (and duration) required for sintering. The compacted regolith is then heated under pressure until a dense medium is produced [363]. For lunar and Martian construction applications, where energy generating equipment and resources can be limited, sintering would be more efficient at producing construction materials than melting, as sintering is often achieved at temperatures well-below (~50-70%) of the material melting point. The efficiency of sintering can also be enhanced through supplementation with additives or binding agents.

In order for sintering to occur, mechanisms for material transport must be present. The two main mechanisms that commonly occur are viscous flow and diffusion. As a result, Pletka [363] classified sintering as liquid phase (viscous) or solid-state (diffusion). In the first mechanism, sintering occurs when a viscous liquid silicate is formed as a result of high glass content in regolith or due to thermochemical reactions between minerals in regolith. On the other hand, solid-state sintering is achieved by heating regolith to initiate mass transport as bridges (or necks) between

This is a preprint draft. The published article can be found at: https://doi.org/10.1016/j.pmatsci.2019.100577

Please cite this article as:
Naser M.Z. (2019). “Extraterrestrial Construction Materials.” *Progress in Materials Science*. Vol. 105, 100577. https://doi.org/10.1016/j.pmatsci.2019.100577.

compacted powder particles grow. In both cases, the application of pressure gives rise to driving forces that favor densification though increasing vacancy transport [363].

Through sintering, particles bond with a concurrent reduction in degree of porosity, forming a solid [364]. In general, the rise in temperature causes spherical grains to grow closer and finally form a ceramic (see Fig. 28). Frenkel [365] showed that the process of sintering can be approximated through the following expression:

$$X/R = \sqrt{\frac{3\pi t}{2\gamma n R}} \qquad \textit{Eq. 26}$$

where, X is the radius of the neck between coalescing grains, R is the grain radius, γ is the surface tension of soil, t is the time in seconds, n is the viscosity in poise.

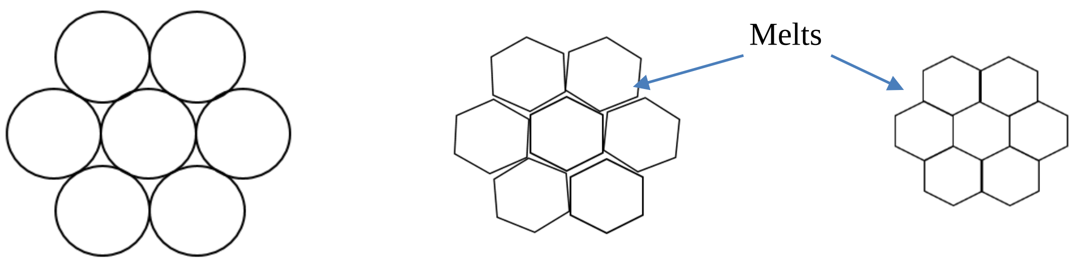

(a) initial heating (b) introduction of liquid and solid state diffusion (c) complete sintering

Fig. 28 Illustration of sintering process

Sintering can be applied to fabricate structural components in dry settings through subjecting a source of energy; such as amplified (concentrated) sunlight, microwave, or laser, to lunar (or Marian) regolith. Bonanno and Bernold [366] reported that the mean solar irradiance reaching the Earth’s atmosphere is 1370 W/m^2, but only 48% of this irradiance reaches the surface of the Earth as the atmosphere reflects and absorbs 29% and 23% of total solar energy, respectively. It is worth noting that solar irradiance on the Moon and Mars is estimated at 1425 and 590 W/m^2, respectively [367]. Due to the poor atmosphere which allows direct sunlight to reach the lunar and Martian surface, one can infer that solar sintering can be thought of as a dominant processing method on the Moon (and possibly Mars).

To amplify the amount of solar energy that can be harvested, Sun rays can be collected and concentrated using solar collectors/concentrators/furnace. Solar concentrators were shown to generate temperatures exceeding that needed to melt lunar regolith and simulants (1250-1500°C) and reaching 1800-2000°C [149]. In one study, Hintze et al. [149] showed how using a solar concentrator on Earth can generate a temperature of 1350°C, which is higher than that needed to melt lunar regolith and simulants. Hintze et al. [149] also showed how the use of this concentrator can sinter a 100 m^2 area, to a depth of 25 mm, in 24-36 days depending on its efficiency (100 vs. 65%, respectively).

In another study, Meurisse et al. [368,369], were able to produce bricks having dimensions of 200×100×30 mm, within five hours, through solar sintering at 1000°C. Later on, Meurisse et al. [143] utilized low-titanium lunar simulants in tests to simulate how sintering can be applied to lunar regolith similar to that of Mare soil. In this study, lunar simulants were first pressed at 255 MPa and then sintered under two conditions; in air or under vacuum. Then, heat was applied at a rate of 400°C/hr, until reaching temperatures in the range of 1070 and 1125°C, over a three hour period. The outcome of this study showed that the high content of anorthite ($CaAl_2Si_2O_8$) in regolith and simulants improves the sintering process. Taylor et al. [161] integrated solar sintering into an additive printer to sinter small structural components (trusses) at 1100°C. These trusses were made by mixing three components, poly (lactic-coglycolic acid) copolymer, a 15:2:1 mixture of dichloromethane (DCM), ethylene glycol butyl ether (EGBE), and dibutylphthalate (DBP), as

Please cite this article as:
Naser M.Z. (2019). “Extraterrestrial Construction Materials.” *Progress in Materials Science*. Vol. 105, 100577. https://doi.org/10.1016/j.pmatsci.2019.100577.

well as JSC-1A simulant. The compressive strength of these trusses measured between 1-19 MPa and was shown to be sensitive to sintering duration and density of sintered material.

A more recent study was sponsored by JAXA in which Hoshino et al. [370] tried to optimize the sintering process by examining various sintering temperatures and holding/heating durations. In this study, a lunar simulant (FJS-1) was selected for analysis and was sintered in a vacuum furnace. Sintering temperatures selected as a function of melting point of the simulant and the duration of sintering was also varied between 10-60 minutes. The results of various sintering regimes are shown in Fig. 29a and b. This study shows that buildings blocks comparable to those of typical concrete blocks used in terrestrial construction and possessing sufficient strength for extraterrestrial construction, could be manufactured (see Fig. 29c). These researchers noted that temperature required for sintering under vacuum was approximately 100 K lower than that for sintering under atmospheric pressure. The measured compressive and bending strengths were reported at 33.3-37.8 and 7.2-8.2 MPa, respectively. The measured modulus of elasticity was also reported at 6.1-13.8 GPa. The optimum regime for sintering seems to be at temperatures relatively high (close to melting point) for a duration of 30 minutes.

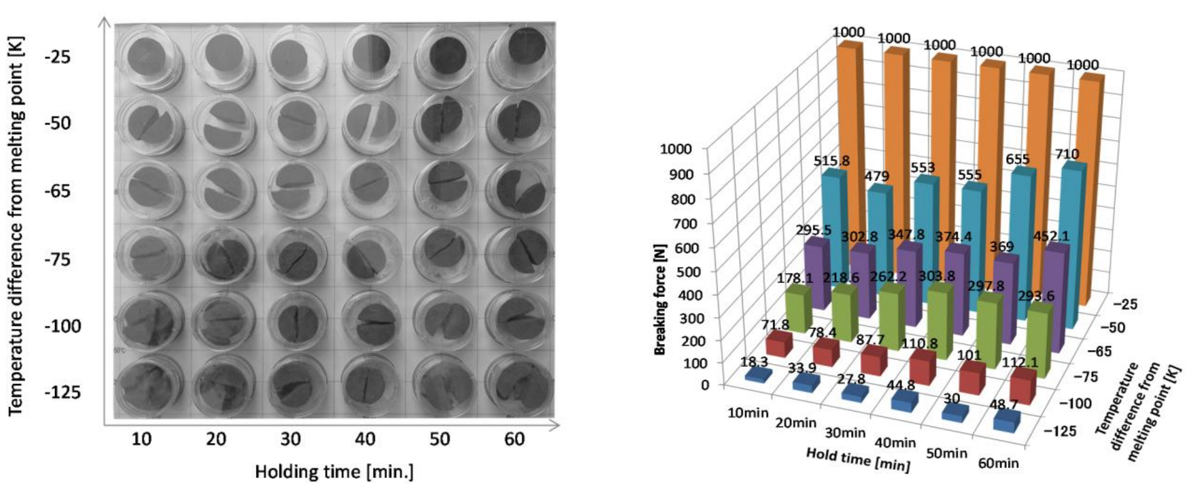

This is a preprint draft. The published article can be found at: https://doi.org/10.1016/j.pmatsci.2019.100577

Please cite this article as:
Naser M.Z. (2019). "Extraterrestrial Construction Materials." *Progress in Materials Science*. Vol. 105, 100577. https://doi.org/10.1016/j.pmatsci.2019.100577.

(a) Test pieces prepared under various sintering conditions

(b) Comparison of breaking forces

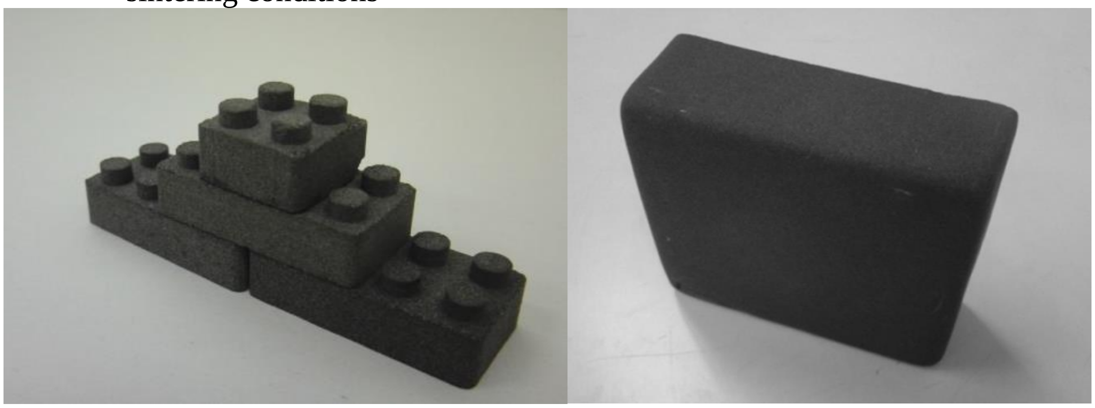

(c) Sample of sintered blocks

Fig. 29 Summary of tests carried out by Hoshino et al. [370] tests

Another approach to sintering is through microwaving [371]. Microwaves are in the range of 0.3 to 300 GHz and as such they lie between radiowave and infrared frequencies. Microwaves can interact with materials through either polarization, which involves short-range displacement of charge, or through long-range transport of charge (i.e. conduction). Microwaves can also be reflected, absorbed and/or transmitted by regolith materials. While reflection and absorption require direct interaction between microwaves and the regolith, transmission on the other hand occurs in a result of partial reflection and incomplete absorption. In any type of these interactions, heat energy is generated primarily through an absorption mechanism.

Taylor and Meek [107] showed how microwave energy not only could be used to sinter lunar regolith but also has the promise for producing oxygen, metals, and ceramics as by-products. Microwave processing can be carried out in two ways: firstly, through ultra-high frequency (e.g., 2.45 GHz) heating, or accordingly through extra high frequency microwaves (between 100 and 300 GHz). Using microwave energy of about 2.45 GHz, lunar simulants were found to sinter within minutes. This sintering technique could potentially outperform solar sintering as shown by Hintze and Quintana [149] and Taylor and Meek [107]. Allen [153] investigated the use of hybrid sintering via a combination of microwave and radiant heating and reported an optimum heating duration of 85 minutes. In lieu of solar and microwave sintering, laser sintering with laser beam(s) of 50-200 W and energy density of $5.89e^{-7}$ kW.h directed at simulants (with uniform particles in the range 10-150 μm) can cause their complete melting and then solidification [140]. Goulas et al. [372] fabricated specimens from lunar simulant JSC-1A using laser sintering with laser of energy density of 0.9 J/mm^2. Those specimens exhibited a porosity of 44–49% and had densities ranging from 1760 to 2300 kg/mm^3. The maximum compressive strength of these samples was 4.2 MPa and elastic modulus was of 287.3 MPa, which is comparable to masonry clay bricks (3.5 MPa).

Sintering, regardless if achieved through any of the aforementioned methods, been shown to suffer on number of fronts. For example, solar sintering equipment (i.e. concentrators or furnaces) requires shielding and continuous maintenance to clean mirrors and lenses from lunar/Martian dust and micrometeorites. When it comes to microwave sintering, selecting an appropriate microwave frequency is essential for adequate sintering. Also, the efficiency to convert electric energy to microwave energy was reported to be 60% of which 50% was absorbed by the regolith (due to the low conductivity of regolith [373]). In fact, only 16% of absorbed energy is expected to melt regolith and as such, the total efficiency of this system comes down to 5% [374]. With this efficiency rate, 70 GJ of total electric energy is required to sinter one cubic meter. It is clear that this sintering (as well as melting) could be energy extensive. The readers should be aware that Lim et al. [373] estimated that the amount of laser energy required to enable sintering of a practical habitat would necessitate a nuclear power source as laser absorption is directly proportional to electrical resistivity of regolith i.e. due to its poor conductance, regolith can absorbs

This is a preprint draft. The published article can be found at: https://doi.org/10.1016/j.pmatsci.2019.100577

Please cite this article as:
Naser M.Z. (2019). "Extraterrestrial Construction Materials." *Progress in Materials Science*. Vol. 105, 100577. https://doi.org/10.1016/j.pmatsci.2019.100577.

large amounts of laser energy prior to sintering [375]. Further, extended calcination of lunar regolith can generate large particle agglomerates which increases porosity and reduces the degree of microstructural homogeneity. Both of these effects have been shown to lower material mechanical properties [376]. Logistics, cost-effectiveness, and assurance of quality control are other areas with pressing challenges.

Combustion Synthesis

Another processing technique, that can overcome some of the associated limitations with sintering is, *combustion synthesis*. Combustion synthesis (also known as self-propagating high-temperature synthesis (SHS)) exploits the ability of highly exothermic reactions to be self-sustaining and, is therefore, energy efficient. This reaction initiates at an ignition temperature (T_{ig}) and generates heat which is manifested in a maximum combustion temperature (T_{comb} > that can exceed 2700°C (see Fig. 30). This high combustion temperature is capable of melting (or volatilizing) reactants. The sum of heat, $H(R)$, required to raise the temperature of the reactants from ambient temperature, T_{amb}, to ignite the exothermic reaction in the propagating mode can be approximated per Moore et al. [377–379]:

$$H(R) = \int_{T_{amb}}^{T_{ig}} \sum n_i C_p(R_i)\, dT + \sum_{T_{amb} \sim T_{ig}} n_i L(R_i) \qquad \textit{Eq. 27}$$

where, n_i, $C_p(R_i)$, and $L(R_i)$ are the reaction stoichiometry coefficients, heat capacities, and the phase transformation enthalpies (if the reactant[s] undergo a phase change, such as melting), of reactant R_j, respectively.

The amount of heat available to be absorbed by the products under adiabatic conditions, $H(P)$, raises the temperature from T_{ig} to adiabatic temperature, T_{ad} (T_o), such that:

$$\Delta H\left(T_{ig}\right) = -[H(R) + H(P)] \quad \textit{Eq. 28}$$

and,

$$H(P) = \int_{T_{ig}}^{T_{ad}(T_o)} \sum n_j C_p\left(P_j\right) dT + \sum_{ig\sim T_{ad}(T_o)} n_j L\left(P_j\right) \quad \textit{Eq. 29}$$

where, n_i, $C_p(P_j)$, and $L(P_j)$ are the reaction stoichiometry coefficients, heat capacities, and the phase transformation enthalpies (if the product[s] go through a phase change) of reactant P_i, respectively [377–379].

The reaction is ignited under the simultaneous combustion mode. The heat of reaction at ignition, $H(T_{ig})$, can be calculated as:

$$\Delta H\left(T_{ig}\right) = \Delta H(298) + \int_{298}^{T_{ig}} \left[\sum n_j C_p\left(P_j\right) - \sum n_i C_p(R_i)\right] dT + \left[\sum_{298\sim T_{ig}} n_j L\left(P_j\right) - n_i L(R_i)\right] \quad \textit{Eq. 30}$$

where, $\Delta H(298)$ is the reaction enthalpy at 298 K [377–379].

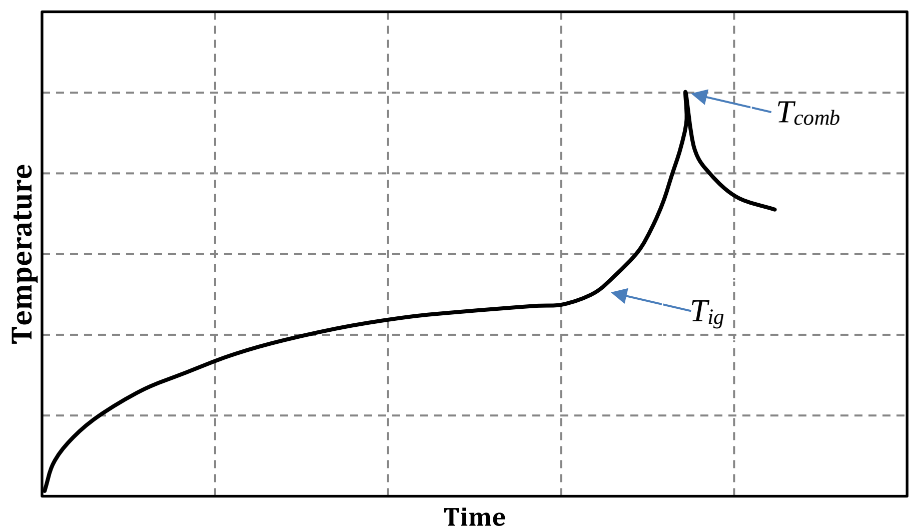

Fig. 30 Typical temperature-time history of combustion process

Please cite this article as:
Naser M.Z. (2019). "Extraterrestrial Construction Materials." *Progress in Materials Science*. Vol. 105, 100577. https://doi.org/10.1016/j.pmatsci.2019.100577.

In the case of space construction, processing through combustion synthesis initiates as a result of an oxidation-reduction reaction that can be triggered through combining regolith with aluminum or magnesium powdered minerals together with the addition of a relatively small thermal energy [379]. In this context, combustion synthesis occurs as:

$$FeTiO_3 + 7Al + 3C \rightarrow 3Al_2O_3 + TiC + Fe_3Al \quad \text{Eq. 31}$$

$$FeTiO_3 + 3Mg \rightarrow 3MgO + TiFe \quad \text{Eq. 32}$$

Combustion synthesis often produces a ceramic-composite solid-like material that is structurally stable and takes the form of the original unreacted mixture. Not only combustion allows fabricating of new structural members/components but can also be used to join (weld/bond) new structural members and repair damaged components.

This processing method envisions the use of a refinery plant for producing aluminum (or magnesium) or reusing these metals from spacecraft or landing equipment. Pilot studies were conducted by Faierson and Logan [380] where they processed lunar simulant (JSC-1A) and aluminum powder under vacuum conditions. The final products from this process achieved a mean compressive strength of 18 ± 3.7 MPa. Ferguson et al. [381] also examined the feasibility of joining regolith tiles using a nickel/aluminum mixture through combustion synthesis to fabricate launch and landing pads to be used on the Moon and Mars. Hobosyan and Marturosyan [160] investigated thermitic-base combustion reaction using JSC-1A lunar simulant mixed with aluminum (12% of total weight) and Teflon (1.5% wt.) tested under vacuum of magnitude 10^{-3} torr. The resulting solid from this reaction had a porosity varying between 40% and 60%. Hobosyan and Marturosyan [160] reported few observations; 1) occurrence of a very rapid temperature rise of 226.8°C/sec reaching a maximum combustion temperature of 1400°C; 2) using higher Teflon concentrations led to higher porosity in produced material; 3) due to bonding of particles and formation of a solid, the developed material had a thermal conductivity of 2-4 W/m.K, much higher than that of actual regolith or lunar simulant.

White et al. [382] proposed the use of magnesium instead of aluminum as a reacting metal as it is easily ignited and with relatively low boiling point. Carrying on with White's recommendation, Delgado and Shafirovich [383] fabricated structural bricks through a magnesium-attained combustion process. These bricks achieved a compressive strength and ultimate strain of 10 MPa and 15%, respectively. In order to optimize this combustion process, Delgado and Shafirovich [383] reported that heating lunar simulant to 100°C can reduce the required amount of magnesium needed from the combustion reaction from 13 to 10 wt.%.

Haagen et al. [384] showed that combustion synthesis can produce high quality titanium silicide intermetallics (compounds of Ti with Si). In this work, Haagen et al. [384] performed twenty experiments on metallic titanium and silicon powders made of TiSi, $TiSi_2$, and Ti_5Si_3 under microgravity conditions. These powders were then compressed into pellets and subjected to combustion processing under varying gravity conditions simulated on board flights of NASA's KC-135 microgravity aircraft. Observations from these tests showed that the pore size of the samples tested under microgravity were smaller and more consistent than those tested under normal gravity (see Fig. 31). Samples tested under normal gravity also had thicker walls between pores and contained increased amounts of silicon at nodes and in grain boundaries. Haagen et al. [384] noted that silicides formed in micro-gravity attained near-net shape formation, when compared to the porosity and structure of silicides formed in Earth gravity. Both combustion synthesis and micro-gravity conditions provided favorable conditions to developing a microstructure of superior homogeneity.

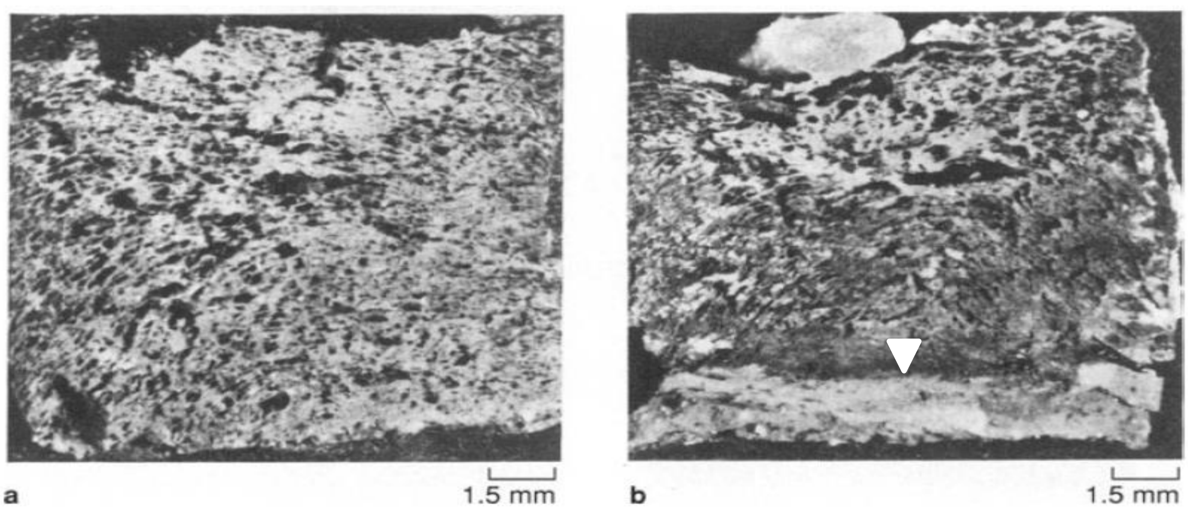

Fig. 31 Microstructures of products reacted (a) under microgravity conditions and (b) under normal gravity conditions (Downward arrow shows increase in aluminum segregation) [384]

It should be noted that Corrias et al. [159], carried out tests in which metallo-thermic reduction of lunar regolith enriched in iron-titanate reaction was proven to be self-propagating. The material obtained from these tests consisted of a complex mixture of a number of metals (i.e. Al-, Ti-, Mg-, and Ca-oxides) along with metallic and intermetallic phases. This product showed good compressive strength properties (25.8–27.2 MPa) which made it promising as a construction material. The same study also noted the high volatility of the magnesium, due to generation of gas expulsion, which tend to make the combustion process hard to control and may disintegrated samples.

Dry-Mix/Steam-Injection (DMSI)

As discussed earlier, the American Concrete Institute (ACI) sponsored efforts to promote the use of concrete and concrete-like materials for extra-territorial construction. The crown achievement of these efforts was the development of a new processing technique, referred to as *Dry-Mix/Steam-Injection (DMSI)*, primarily engineered by Lin and his colleagues [385]. This procedure was developed to overcome rapid outgassing of water under vacuum as well as issues related to mixing concrete under low gravity conditions. In this method, cement and aggregate are dry-mixed and placed in a steam boiler (or autoclave). The dry mix is then exposed to water steam. Steaming occurs at temperatures varying from 100-180°C and lasting from a few minutes to up to 30 hours so as to induce hydration of concrete [385]. Once cement is exposed to hot steam, heat is transferred from steam to cement, and a portion of this steam is forced (injected) into micropores of cement particles, causing the steam to partially condense and form a thin coating of moisture. Energy accumulated from activation and condensation effects enhances the efficiency of hydration and curing progression. DMSI significantly reduces the amount of cement and water needed to hydrate and cure concrete (by more than half) and eliminates the conglomerate grouping of cement matrix wetting that often occurs in the traditional casting method of concrete (wet method) – see Fig. 32.

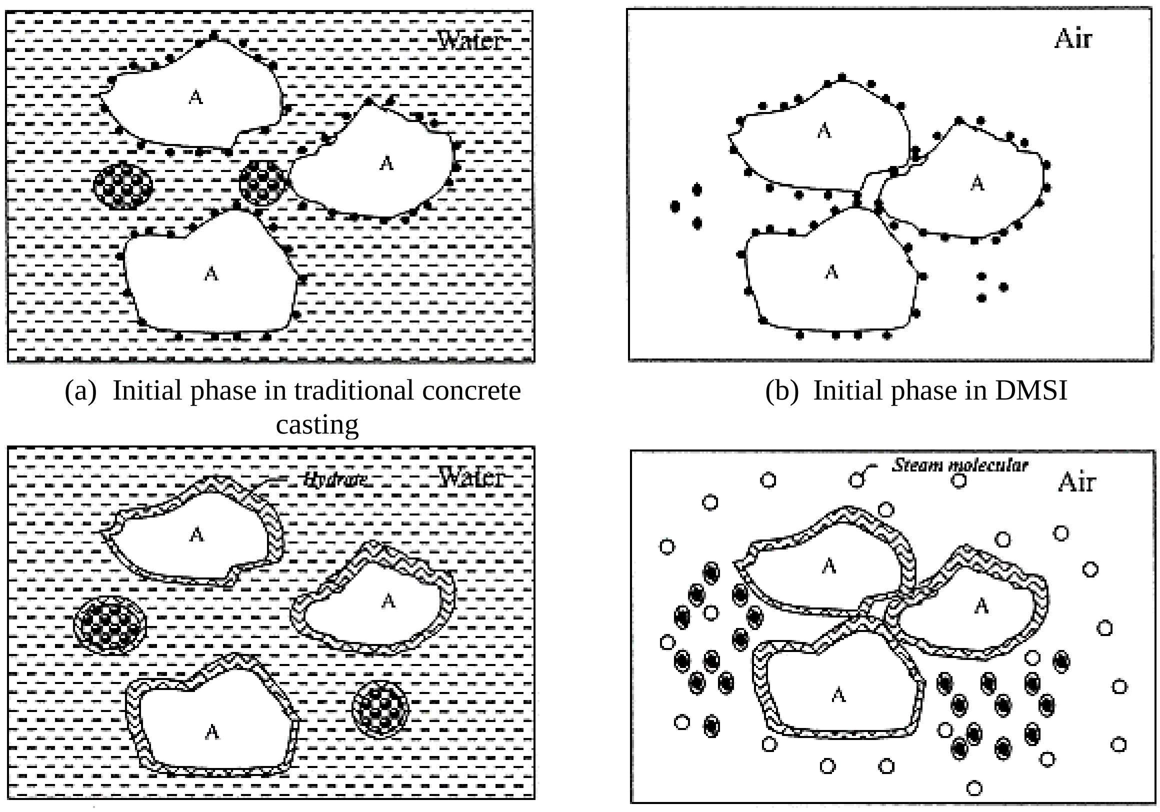

(a) Initial phase in traditional concrete casting

(b) Initial phase in DMSI

(c) After hydration

(d) After hydration

Fig. 32 Schematic of hydrates for traditional and DMSI process [386]

In their early tests, Lin and colleagues [387] examined the effects of steaming temperatures, atmospheric (pressure) magnitude, as well as curing duration on compressive strength of concrete. In these experiments, steaming temperature, applied pressure and curing duration were varied between 100-180°C, 0.14-0.69 MPa, and 6-57 hours, respectively. Figure 33 demonstrates that steaming temperature of 180°C and curing duration of 30 hours are optimum conditions and yield the highest strength. To further research efforts on this method of processing, Su and Peng [386] studied the effects of concrete mixture proportion, steaming duration, and sample dimensions on the compressive strength of DMSI-processed concrete. The outcome of these tests showed that the optimal steaming temperature for DMSI concrete was in the narrow range of 180–200°C (which agrees with findings from Lin et al.). Other findings include, a noticeable increase in compressive strength (of 236%) by increasing steaming duration from 6 to 30 hours and steaming temperature from 105 to 200°C, respectively. In a later study, Pakulski and Knox [388] investigated short duration of steaming on the compressive strength of concrete. In this study, concrete specimens were steamed at low pressure (0.2 MPa) and at 129°C and reported maximum measured strengths of 16.7, 18.2, and 33 MPa for specimens steamed for 5, 15 and 25 minutes, respectively. Figure 33 summaries findings of tests carried out by Lin and Su [387] as well as Pakulski and Knox [388][24]. It can be seen that concrete specimens steamed for 25 minutes in tests carried out by Pakulski and Knox [388] achieved a compressive strength exceeding that of specimens tested by Lin and Su [387] which were steamed in 24 hours. This interesting observation is attributed to the different steaming set-up, concrete mix as well as vibration methods used in these two studies.

[24] Results from Pakulski and Knox [388] are the average of both rodded and vibrated samples without curing.

This is a preprint draft. The published article can be found at: https://doi.org/10.1016/j.pmatsci.2019.100577

Please cite this article as:
Naser M.Z. (2019). "Extraterrestrial Construction Materials." *Progress in Materials Science*. Vol. 105, 100577. https://doi.org/10.1016/j.pmatsci.2019.100577.

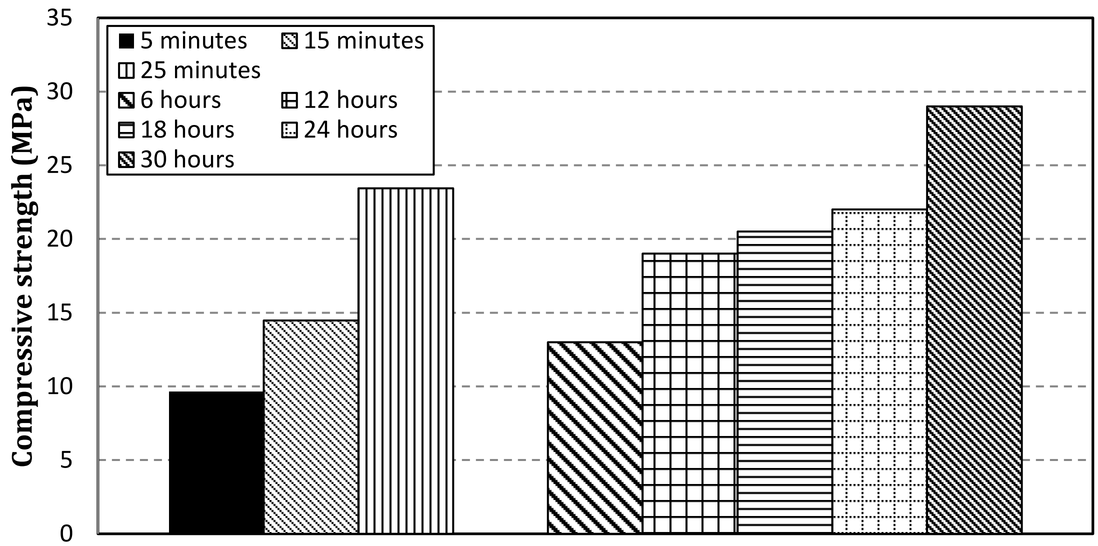

(a) Summary of tests carried out by Lin and Su [387] (steamed at 100-125°C; shown in the left) as well as Pakulski and Knox [388] (steamed at 129°C; shown in the right)

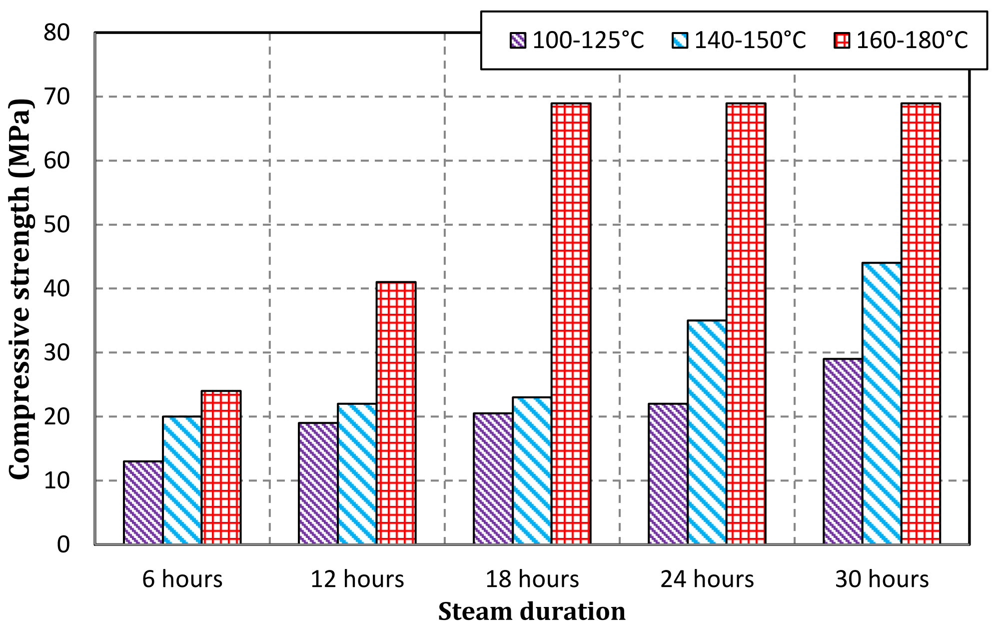

(b) Lin et al. [387,389]

Fig. 33 Summary of studies utilizing DMSI processing for extraterrestrial concrete

Research efforts were also carried out at NASA's Johnson Space Center in which the DMSI method was applied to lunar simulant JSC-1. As a result of these tests, concrete with a compressive strength of 11.6 MPa was achieved. This concrete had a density of 2000 kg/m^3 and maintained a high water-cement ratio of 0.73 after 72 hours of curing [390]. In another study, Hatanaka and Ishida [391] investigated the potential of using quick setting cement as a binder to accelerate hydration and reduce moisture loss under vacuum. Results from Hatanaka and Ishida [391] experiments showed that the rapid setting of this cement causes steamed concrete to achieve high compressive strength as well as led to avoiding excessive water evaporation. The amount of water loss at 28 days of casting in these specimens was found to be 12 and 30% as opposed to 75% using the ordinary curing method.

Other than the obvious need for water to hydrate and concrete [392], the need for complex processing facilities, specifically steaming and curing chambers as well as vibration equipment, seem to limit the integration of DMSI in producing concrete for extraterrestrial construction.

Cold-pressing

In the event where access to processing equipment is limited, a more convenient method of processing lunar and Martian in-situ resources is through *cold-pressing*. By definition, cold-pressing utilizes adhesive forces of regolith particles, especially smectite-like clay mineral and water moisture [393]. Smectite-like clay has high amounts of montmorillonite mineral. This mineral, made of silicate-aluminum-silicate layers with a large cation exchange capacity, has the ability to absorb a tremendous amount of water within soil/regolith layers. As a result, when regolith is pressed, the viscosity of montmorillonite turns into a binding force between the particles, transforming the pressed material into a solid.

Please cite this article as:
Naser M.Z. (2019). "Extraterrestrial Construction Materials." *Progress in Materials Science*. Vol. 105, 100577. https://doi.org/10.1016/j.pmatsci.2019.100577.

Ishikawa et al. [374] tested cold-pressed duricretes and reported that the compressive strength of Martian simulant mixture made with 20% water achieved higher strength than did that of the 30% water content. The same study also investigated the effects of curing method as well as clay type (in simulant). The outcome of these tests showed that specimens cured in a dry environment, demonstrated higher strength than non-dried samples. In a similar manner, specimens made of clay rich in bentonite achieved higher strength, reaching 7.39 MPa (see Table 22) [394]. In a companion study, Boyd et al. [395] used two types of mixtures to simulate Martian soil. These mixtures were made of the same composition 85% clay, 12% magnesium sulfate ($MgSO_4$), 2% ferric oxide (Fe_2O_3), and 1% sodium chloride (NaCl), but varied the clay origin, i.e. bentonite and Pennsylvania nontronite. While cold-pressing these two mixtures, Boyd et al. [395] reported cracking and warping of specimens and thus proposed to reinforce the mixture with nylon mesh, Kevlar fiber, or glass wool. When these reinforcement were embedded into a cold-pressed specimen, a 95% improvement in tensile strength was achieved. These researchers also investigated the prospect of integrating sulfur as a binding agent. The sulfur was heated to 150°C to polymerize and then upon cooling, polymerized material was pressed yielding *sulfur cemented duricretes.* Figure 34 shows a sample of a Martian brick made by cold pressing and Table 22 lists the findings of Ishikawa [374] as well as Boyd [395].

This is a preprint draft. The published article can be found at: https://doi.org/10.1016/j.pmatsci.2019.100577

Please cite this article as:
Naser M.Z. (2019). "Extraterrestrial Construction Materials." *Progress in Materials Science*. Vol. 105, 100577. https://doi.org/10.1016/j.pmatsci.2019.100577.

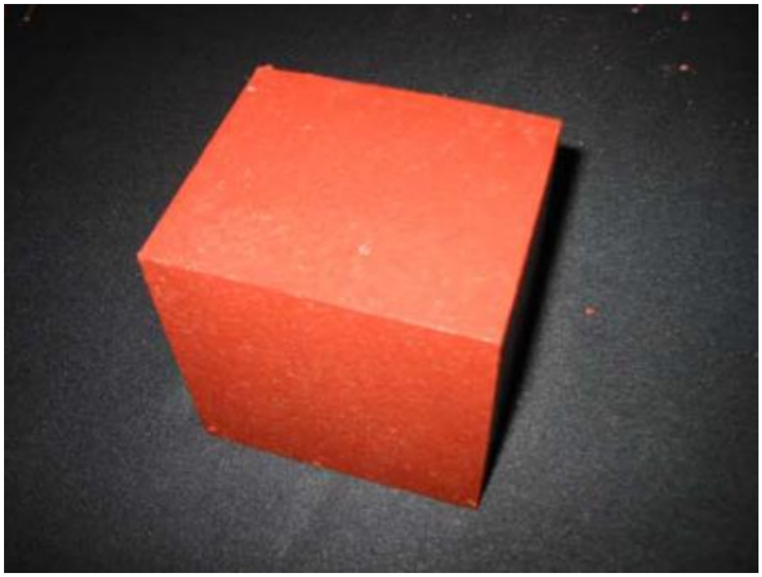

Fig. 34 Martian brick made by cold pressing [394] (Note: each side = 100 mm)

Table 22 Tests on duricretes through cold-pressing

Test	**Curing condition**	**Bentonite content**	**Sand content**	**Strength (MPa)**	**Density (kg/m^3)**
Ishikawa et al. [394]	Dry	70	30	7.39	1963
	Not Dry			2.00	1992
	Dry	30	70	1.33	1784
	Not Dry			0.87	1810
	Curing method	**Matrix material**		**Strength (MPa)**	
Boyd et al. [395]	Air dry	4-ply nylon mesh		1.8	
	Compressed, air dry	1% Kevlar fiber		3.95	
		2% Glass wool		3.97	
	Baked, compressed	45% Sulfur		2.19	

Chow et al. [396] capitalized on the idea that Martian regolith is formed by basaltic fines containing iron, with substantial nano-particulate iron oxides and oxyhydroxides, to develop a new construction material. In their work, Chow et al. [396] pressed a Martian simulant, Mars-1A, under mechanical pressure of 340 MPa. The external application of compressive force developed very high specific areas in which nano-particulate iron oxide bonded. Upon a high-pressure compression, Martian regolith formed strong cubes. The measured flexural strength of pressed cubes was in the range of 10-17 MPa; similar to that of typical ordinary concrete as well as that of some in-situ based construction materials formed through complex processing methods and addition of binders. This material has been shown to be sensitive to grain size distribution, applied compressive loading and compaction procedure.

The properties of cold-pressed regolith can significantly be improved by heating (firing) [397]. In one example, Effinger and Tucker [397] showed how ceramics can be fabricated from lunar regolith by cold-pressing. In this study, MLS-1 lunar simulant, with a similar composition to that of Apollo sample no. 10084, was selected for analysis. The lunar regolith was first mixed with 2-4 wt.% beewax binder and then was pressed at different pressures of 276, 345, or 414 MPa. The cold-pressed specimens were initially heated to 110°C and held for two hours to remove any moisture. The temperature was then raised to 600°C and maintained for four hours to remove the wax. Finally, the temperature of specimens was raised to 1100°C for 12, 18, or 24 hours. Results of tests conducted by Effinger and Tucker [397] indicate that lunar ceramic cold-pressed at 276 MPa and fired at 1100°C for 24 hours yielded the greatest compressive strength of 247 MPa. It is worth noting that the compressive strength achieved through this modified cold-pressing is greater than that obtained via microwave sintering at the same processing temperatures.

Similar observations were also noted by Altemir [398]. In this work, Altemir examined the effect of varying pressing pressure and firing temperature on the compressive strength of cold-pressed and fired MLS-1 lunar simulant. The pressing pressure and firing temperature were varied between 200-375 MPa and 800-1000°C, respectively. Figure 35 shows that cold-pressed lunar simulants can achieve a compressive strength greater than 14 MPa after being pressed at pressures above 253 MPa and subsequently heated above 1000°C for 30 minutes. This compressive strength is much lower than that obtained by Effinger and Tucker [397] due to the lack of binder and short firing duration.

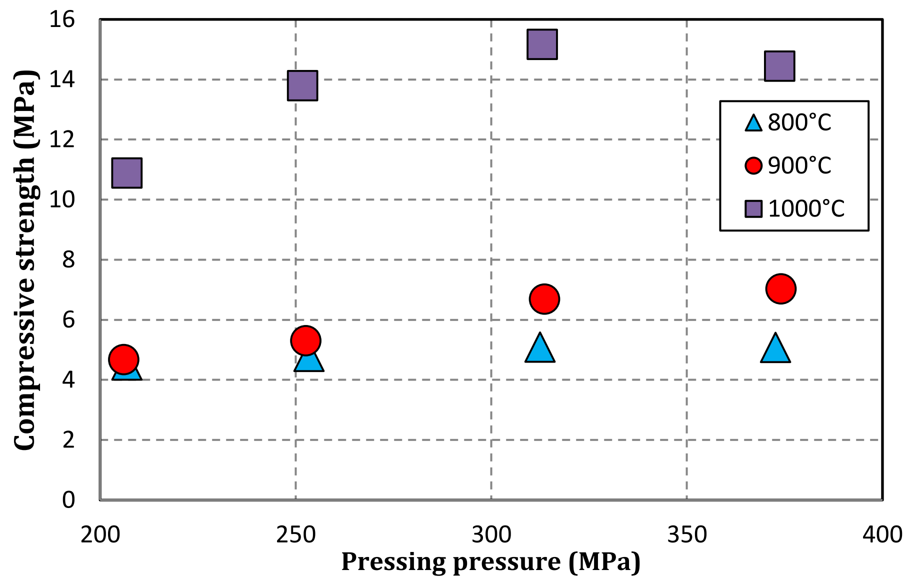

Fig. 35 Compressive strength of simulated lunar soil under varying conditions [398]

Ishikawa et al. [374,394] has shown that due to the lack of water and clay-like material on the lunar surface, cold-pressing could be more suited for the Martian environment. However, due to the recent discovery of iced-water pockets on the lunar poles, cold-pressing of lunar soil could perhaps be carried out, near the poles.

Other Processing Methods/Techniques

Besides the processing methods discussed above, the open literature also contains other techniques that can be applied to process numerous in-situ (or mined) materials. Some of these processing and elemental extraction methods have been summarized in Table 23 and a more complete review, together with, history of space mining, manufacturing, and processing can be found elsewhere [39,399,400].

This is a preprint draft. The published article can be found at: https://doi.org/10.1016/j.pmatsci.2019.100577

Please cite this article as:
Naser M.Z. (2019). "Extraterrestrial Construction Materials." *Progress in Materials Science*. Vol. 105, 100577. https://doi.org/10.1016/j.pmatsci.2019.100577.

Table 23 Methods for space processing of materials and elemental extraction methods

Processing method	**Definition/Suitability**	**Refs.**
Glass fiber processing	Infusing lunar and Martian simulants with 8% wt. boria yielded a glass material which could be spun continuously into fibers. In this method, a regolith simulant is first heated at 1200°C in a platinum boat in a tube furnace. Then, fiber glass was made by firing the simulant to 1450°C for 24 hours, then pouring the melt on an aluminum quench block.	[202]
Thermal liquefaction	Thermal liquefaction is defined as the creation of a composite material from regolith (with or without additions of fibers or admixtures) at a given temperature in the range of 15-500°C or though thermal cycling under which the regolith (or additives) may melt or not at all, resulting in a composite that is held together by binding regolith (or fibers) particles.	[326]
Thermal binding	Similar to thermal liquefaction but utilizes binding materials such as sulfur or iron (or their combinations) to provide improved binding effects.	[401]
Electrostatic	Separates mineral grains in lunar regolith through charges of static electricity. As different minerals possess different propensity to electrostatic attractions, charged minerals/grains can be separated by passing through an electric field.	[402]
Electrophoresis	Due to variation in molecular nature of minerals, each mineral type can accumulate a different net electric charge and migrate to a certain position in a charged tank filled with fluid. Respective minerals are the collected from different depths across the tank.	[403]
Electrolysis	Melted oxides can be put into electrodes through high voltage current (i.e. negative electrode attracts metals and positive electrode attracts oxygen)	[404]

Smelting	Often used to separate silicon and oxygen. In this process, minerals can be heated to very high temperatures, and then melted to liquid form.	[405,406]
Solar Oven Distillation	Solar distillation boils off materials under low gravity. Once an element boils, temperature can be raised to boils the next element.	[407,408]
Chemical processing	Collected regolith can be chemically processed to extract elements. This method emphasizes the usage of chemical agents with high recyclability.	[409–411]

This is a preprint draft. The published article can be found at: https://doi.org/10.1016/j.pmatsci.2019.100577

Please cite this article as:
Naser M.Z. (2019). "Extraterrestrial Construction Materials." *Progress in Materials Science*. Vol. 105, 100577. https://doi.org/10.1016/j.pmatsci.2019.100577.

Research Needs and Future Directions

The success of future space exploration programs, especially those planned for launch in the next two decades, depends on our ability to engineer Earth-independent lunar and Martian outposts. These habitats not only are expected to utilize indigenous resources, but also to be resilient to the alien environments present on the Moon and Mars. While the above discussion has compiled the main findings of classic and recent research efforts, this review has also pointed out that current expertise to manufacture extraterrestrial construction materials is lacking and is indeed one of the main challenges that continues to limit the extent of long-stay manned missions.

This section highlights some of the main research needs and future directions that have the merit of accelerating academic and industrial efforts into enabling development of resilient, space-native, and cost-effective structural and construction materials.

Earth-independency through Full Utilization of In-Situ Resources

Similar to early voyagers, those who went to explore the unknowns on Earth, space explorers will also need to use the best of in-situ resources in their destinations (whether it is the Moon, Mars, or those beyond that). A true and successful space exploration requires establishing lunar and Martian habitats that are feasible and self-sustaining. Establishing such habitats has been the ultimate goal in many of the past space exploration missions and manned landings and continues to be in those scheduled for launch in the near future. The discussion on utilizing in-situ resources does not only cover extraction of oxygen, water, fuel etc. but rather, as emphasized in the context of this review, goes beyond that to include construction materials. This perception has been a focal point of research in the last few decades and is expected to further evolve as a function of our technological advancements. In fact, a number of researchers and NASA officials have stated that all the resources needed to support long-term human stays are available in some form on the surfaces of the Moon and Mars [412,413]. What seems to be missing is the enabling technologies that allow direct and full utilization of lunar and Martian in-situ resources. An honest look into those challenges reveal that they remained unresolved for the past few decades.

The fact of the matter is, it would be costly, and perhaps impractical, to transport functioning habitats to the Moon and Mars. This emphasis is prompted by the current price tag of $5,000-20,000 to transport one kilo-gram of materials to the Moon; a cost that could exponentially scale in the case of Mars [414,415]. Given that this rate might reduce as a result of technological development and competition between rising private space industries, the monetary costs associated with such a mission (or even for staged missions) as well as risks are still unjustifiable and remain very risky. Perhaps the latest governmental and societal support for space exploration can aid in these venues by allocating funds and striking interest in young students and researchers.

Property Characterization of Extraterrestrial Construction Materials

A closer look into the references listed at the end of this review clearly, and unfortunately, shows that much of our knowledge with regard to property characterization of lunar and Martian in-situ resources is based on findings collected during the golden era of the space age (1960-1980s). Furthermore, out of the 450 works cited herein, only two studies reported testing actual lunar regolith for possible use as a construction material [151,196]. Not only does there seem to be a lack of fundamental understanding on in-situ resources with regard to construction and structural applications, but key aspects such as materials formation and processing under lunar and Martian environmental conditions is also deficient. The absence of such understanding can be attributed to the limited accessibility to research facilities (such as *ISS* etc.), lack of testing equipment (i.e. apparatus that can simulate vacuum conditions, low gravity, as well as sensors etc.), shortage of expertise and trained personnel required to design and carry out sophisticated experiments, and most of all, limited sizes of returned samples collected from previous space missions. While returned lunar samples and Martian remote sensing operations have provided the scientific community with unprecedented insights into the lunar and Martian geologic composition, physical aspects, and chemical contents etc., the reality is that these efforts only present a very restricted geological view on property characteristics of in-situ lunar and Martian resources[25].

In order to improve our understanding of extraterrestrial construction materials, research efforts should thoroughly examine formation and behavior of materials in their native environments. These efforts may re-evaluate physical and chemical characterization of returned samples using current state-of-the-art equipment and technology. This re-evaluation also needs to prioritize properties associated with space-based structural engineering (i.e. load bearing, durability, resilience, adhesion etc.). Future exploration missions are encouraged to plan on conducting extensive in-situ tests and analysis of regolith and to return additional samples to Earth. The outcome of such research can lead to improving the current knowledge base as well as to derive appropriate constitutive material models for integrating lunar, Martian and NEO materials into structural and construction engineering. Such models have the merit of modernizing principles

[25] For example, all manned lunar landings took place on the Moon's near face. An examination of the maximum distances covered by unammed lunar and Martian rovers show that *Lunokhod 2* and *Opportunity* were able to drive 42 and 45 km on the Moon and Mars, respectively. *Lunokhod 2* operated for about four months on the Moon (lost contact in 1973). Opportunity on the other hand, landed on Mars in 2004 and continued to officially operate till June of 2018.

of structural design as well as numerical modelling methods which can revolutionize structural engineering practice for space-like conditions [416]. The development of precise constitutive material models will also reduce dependency on obtaining/testing actual regolith as well as the need to carry out traditional destructive tests.

Integration of Artificial intelligence (AI)

The recent advances in computer science technology, especially with regard to artificial intelligence, opens a new opportunity for material scientists [417]. Artificial intelligence (AI) is a branch of computer science that develops machines and software that mimics human cognition computing abilities and intelligence. AI can identify critical parameters in a given phenomenon and is of particular interest to engineering problems where testing is not possible or limited. This technology is now being applied to evaluate complex physical problems (i.e. astronomy, human behavior) and could also be applied to understanding material formation and development, especially for structural engineering and construction of space habitats.

Artificial intelligence presents a new platform where virtually every single test and numerical simulation has been carried out so far can be integrated into a model that can comprehend relations between all input parameters (i.e. origin, composition, testing set-up etc.) to predict accurate behavior and response of extraterrestrial materials with various levels of complexity. The use of this technology can be simple, does not require complex processing, and most importantly AI-based models can evolve and self-learn from their past analyses in order to improve their prediction capability. It should be noted that the use of AI and advanced computing methods has been documented by a few researchers tackling construction and structural-based engineering problems as well as to derive constitutive material laws [418–422]. This technology, when combined with meta-data and cloud computing, can significantly improve the understanding of materials under space conditions.

Extraterrestrial Samples and High-fidelity Simulants

According to a report published by NASA, only 32 kg of returned lunar samples (out of 382 kg) were used in destructive tests [57]. In order to avoid using NASA's lunar sample inventory in destructive testing, and based on Martian sensing operations, a number of lunar and Martian simulants were formulated and developed (see Table 8). While analysis of extraterrestrial samples shows that regolith is very different than any naturally occurring material on Earth due to its unique formation processes, terrestrial simulants were developed to closely resemble the composition, particle size and distribution of lunar and Martian soils. Developing simulants relies on correlating the behavior of Earth-based materials to that of actual lunar/Martian regolith via material (small) scale testing as well as scaling principles [423].

While it is true that simulants share similar composition to those of regolith, terrestrial simulants are not formed under similar environmental exposures (i.e. low gravity, extreme vacuum, high radiation) or loading conditions (e.g. micrometeorite bombardment etc.) as that present on the Moon and Mars, nor contain specific compounds (such as glass, agglutinates[26] etc.). As such, simulants may not capture distinct aspects of lunar and Martian regolith, especially with regard to microstructural development, magnetic properties, the presence of radiative and rare elements etc. In fact, Gustafson et al. [424] and Heiken et al. [7] have reported that lunar soil has unusually higher shear strength than lunar simulants (i.e. JSC-1) due to interlocking and crushing

[26] Agglutinates are aggregates of smaller lunar soil particles (mineral grains, glasses, or older agglutinates) bonded together by vesicular, flow-banded glass.

of agglutinates. Taylor et al. [107] noted that the presence of the small metallic iron globules in the agglutinitic glass can affect the physical properties of regolith such as absorption of microwave energy, the magnetic susceptibility, and electrostatic properties. Since of most of the research carried out in the area of space construction and processing of extraterrestrial materials predominantly utilized lunar and Martian simulants, this begs the question as to the extent of applicability of findings of such studies if to be implemented using lunar and Martian regolith [424].

Thus, high-fidelity simulants should contain particles that mimic the unique properties of actual regolith. One approach of achieving high-fidelity simulants is to develop new processing techniques that allow production of lunar and Martian-like regolith by subjecting Earth simulants to similar conditions to those of the Moon and/or Mars. Another approach would be to mix actual regolith with terrestrial simulants to develop hybrid simulants. Incorporating high-fidelity simulants in developing extraterrestrial construction materials (as well as in evaluating newly proposed processing techniques) will ensure confidence in our expectation and accelerate our research progress. Once developed, these simulants would be manufactured in large quantities and shared with researchers to encourage research in this field.

Robo-scientists and Autonomous Processing (3D/4D Additive Printing)

Considering the harsh lunar and Martian conditions, it would be of utmost importance to develop robotic, autonomous processing and construction systems with the ability to survey, collect and process in-situ resources to extract/manufacture building materials. Integrating such systems can assure the safety of crew members, maximize construction speed, and uniformity. Autonomous systems can consist of two components, the first being a robotic surveyor/scientist that identifies useable in-situ resources and lays out plans for design and construction of habitats, and the second entailing a processing equipment that labors the processing of in-situ resources and construction of structural components (or in the case of continuous printing a complete habitat). Freitas Jr. et al. [425] proposed that such systems are preferable to enable a placement accuracy of 0.0254 mm with high-capacity arms and multi-arm coordination abilities.

One such autonomous processing and construction technique that has the potential for space application is additive printing. Additive printing is a robotic process that accumulates construction materials to produce quick and precise construction. This process is very attractive given that it could be tailored to include automation (robots), and the ability to independently perform in extreme atmospheres, self-exploiting in-situ resources, etc., all of which seem to fulfil the requirements of interplanetary construction on the Moon and Mars. Traditionally, additive printing involves fabricating structures with fixed geometry (and hence is formally referred to as three-dimensional (3D) printing). At the time of this review, only two methods were identified to successfully carry out 3D printing of space habitats i.e. D-Shape technology [260] and Contour Crafting [426]. It is worth noting that few "proof-of-concept" studies were carried out to explore 3D printing using regolith simulants as well as meteorite-based powders (obtained from *Campo del Cielo* meteorite) [146,427,428].

The potential of printing active structures i.e. those that can change their shape and/or property according to surrounding environment or with pre-defined time has been closely explored [429]. Four-dimensional (4D) additive (and autonomous) printing involves multi-material prints that integrates shape-memory polymer fibers into the process in order to enable manufacturing of a 3D object that, when heated or cooled to a specific temperature/radiation, can transform into a different 3D structure [429,430]. While the concept of 4D printing in space is expected to be integrated in large-scale printers in the near future, some of the research needs in this area may include developing robots and large-scale additive printers; able to conduct mineralogical examination, assessment of physical (e.g. radiation examination), mechanical (e.g., compression, tensile and bending strengths), thermal (e.g., specific heat, coefficient of thermal expansion, etc.) and deformational (i.e. creep) properties of additively printed construction materials in a vacuum or under low gravity conditions[27]. Development of multi-material printing, smart printing, Origami-based space-saving (compact) and new printable construction materials are other pressing issues. Efforts into developing printers capable of fabricating full structures, rather than structural components i.e. bricks or beams, are also required as issues related to joining/welding/sealing individual structural members may arise [431,432]. Additive printers that can utilize novel concretes (i.e. geopolymer-based [262,433]) as well as other multipurpose materials (with energy harvesting/conversion, self-healing and sensing abilities) and those for rapid repair, inspection and maintenance are also expected to be developed [434,435].

Summary and Conclusions

The next step to realize a true and modern space exploration program requires enabling long-stay manned missions on prospective planets and moons. This objective cannot be achieved without development of resilient habitats made of extraterrestrial construction materials; and those mined from in-situ resources or NEOs. This review aims at highlighting past and recent research

[27] NASA has recently performed 3D printing on the ISS where CubeSat were printed and deployed. This was shown to significantly reduce the resources needed for launch, and fuel. Leist and Zhou [450] reported that the frame of the CubeSat could be 3D printed in a flat shape and then activated with light to transform into a 3D shape.

efforts of non-terrestrial materials, together with their processing techniques and envisioned future research directions. The outcome of this review can be summarized in the following points:

- Space holds a multitude of environments (such as low gravity, absence of atmosphere, extreme radiation etc.) that are fundamentally different than those on Earth. These environments impose severe conditions on materials, especially for those to be used in construction of lunar and Martian habitats.
- The Moon and Mars contain an abundance of natural in-situ resources that could potentially be utilized to produce space-resilient extraterrestrial construction materials with minimum processing and human interaction.
- Regolith derivatives and concrete-like products have the highest potential for use in space construction due to their inherent resilience, durable characteristics, and possible efficient production.
- Processing of construction materials under the harsh environment of space can be complex and energy extensive. This could limit the size and type of materials that could possibly be fabricated in-situ.
- Realizing sustainable and functional lunar and Martian settlements may not be achieved without overcoming related to processing, manufacturing and utilization of extraterrestrial resources etc.

Acknowledgment

The author would like to acknowledge the support of Prof. Eduard Arzt and Prof. Philip John Withers as well as their help and understanding throughout the review process of this work.

This is a preprint draft. The published article can be found at: https://doi.org/10.1016/j.pmatsci.2019.100577

Please cite this article as:
Naser M.Z. (2019). "Extraterrestrial Construction Materials." *Progress in Materials Science*. Vol. 105, 100577. https://doi.org/10.1016/j.pmatsci.2019.100577.

The author would also like to acknowledge the tremendous role of the reviewers and their valuable comments and suggestions that helped shape this manuscript. A special thanks goes to my wife, Jasmine, as she continued to spark my interest in pursuing this review.

Dedication

"My battery is low and it's getting dark" – a poetic translation of *Opportunity's* last transmission.

References

[1] Johnson S, Leonard R. Evolution of concepts for lunar bases. Lunar bases Sp. Act. 21st century, 1985.

[2] Wilhelms DE. To a rocky moon - A geologist's history of lunar exploration. University of Arizona Press; 1993.

[3] Ezell E, Ezell L. On Mars: Exploration of the Red Planet, 1958-1978--The NASA History. 2013.

[4] Perminov V. The difficult road to Mars: a brief history of Mars exploration in the Soviet Union. 1999.

[5] Sagan C. Pale blue dot: A vision of the human future in space. 1997.

[6] Ganapathi G, Ferrall J, Seshan P. Lunar base habitat designs: Characterizing the environment, and selecting habitat designs for future trade-offs. 1993.

[7] Heiken G. Petrology of lunar soils. vol. 13. 1975. doi:10.1029/RG013i004p00567.

[8] Steinhoff E. The Use of Mars and Phobos to Advance Interplanetary Flight. Adv Sp Sci Technol 1966;8:347–83. doi:10.1016/B978-1-4831-9966-5.50010-2.

[9] Bodiford M, Ray J, Gilley S, Kennedy J, Howard R. Are We There Yet?....Developing In-situ Fabrication & Repair Technologies to Explore and Live on the Moon and Mars. 1st Sp. Explor. Conf. Contin. Voyag. Discov., Reston, Virigina: American Institute of Aeronautics and Astronautics; 2005. doi:10.2514/6.2005-2624.

[10] Benaroya H. An Overview of Lunar Base Structures: Past and Future. AIAA Sp Archit Symp 2002:1–20. doi:10.2514/6.2002-6113.

[11] Manzey D. Human missions to Mars: new psychological challenges and research issues. Acta Astronaut 2004;55:781–90. doi:10.1016/J.ACTAASTRO.2004.05.013.

[12] Paine T. A timeline for Martian pioneers. Case Mars II, 1984.

[13] DeLucas LJ. International space station. Acta Astronaut 1996;38:613–9. doi:10.1016/0094-5765(96)00056-2.

[14] Jianping Z. A Review of Tiangong-1/Shenzhou-8 Rendezvous and Docking Mission. Manned Spacefl 2012;1.

[15] Goswami JN, Annadurai M. Chandrayaan-1: India's first planetary science mission to the moon. Curr Sci n.d.;96:486–91. doi:10.2307/24105456.

[16] Seedhouse E. SpaceX: making commercial spaceflight a reality. 2013.

[17] Stern A. Commercial space flight is a game-changer. Nature 2012;484:417–417. doi:10.1038/484417a.

[18] Seedhouse E. Red Dragons, Ice Dragons, and the Mars Colonial Transporter. SpaceX's Dragon Am. Next Gener. Spacecr., Cham: Springer International Publishing; 2016, p. 145–62. doi:10.1007/978-3-319-21515-0_9.

[19] Jenkins JM, Twicken JD, Batalha NM, Caldwell DA, Cochran WD, Endl M, et al. Discovery and validation of Kepler-452b: A 1.6 R<inf>⨁</inf> super earth exoplanet in the habitable zone of a G2 star. Astron J 2015. doi:10.1088/0004-6256/150/2/56.

[20] Anglada-Escudé G, Amado P, Barnes J, Nature ZB-, 2016 undefined. A terrestrial planet candidate in a temperate orbit around Proxima Centauri. NatureCom n.d.

[21] Fogg MJJ. Terraforming Mars: A review of current research. vol. 22. Pergamon; 1998. doi:10.1016/S0273-1177(98)00166-5.

[22] McKay CP. On Terraforming Mars. Extrapolation 1982;23:309–14. doi:10.3828/extr.1982.23.4.309.

[23] Dunbar B. Moon to Mars Overview 2018. https://www.nasa.gov/topics/moon-to-mars/overview (accessed June 5, 2019).

[24] McKay DS, Heiken G, Basu A, Blanford G, Simon S, Reedy R, et al. The Lunar Sourcebook: A User's Guide to the Moon. 1991. doi:10.1006/icar.1999.6165.

[25] Good A. 'Marsquakes' Could Shake Up Planetary Science 2018.

[26] Oberst J, Nakamura Y. A seismic risk for the lunar base. Second Conf. Lunar Bases Sp. Act. 21st Century, 1992, p. 231–3.

[27] Frank LA, Sigwarth JB, Craven JD. Reply to Davis and Nakamura et al. Geophys Res Lett 1986;13:1186–9. doi:10.1029/GL013i011p01186.

[28] David D. Earth - Mars - Moon Comparison 2018. http://www.digipac.ca/chemical/mtom/contents/chapter1/marsfacts.htm (accessed June 5, 2019).

[29] McKay CP. The Case for Mars II : proceedings of the Second Case for Mars Conference held July 10-14, 1984, at the University of Colorado, Boulder, Colorado 80309. Published for the American Astronautical Society by Univelt; 1985.

[30] Owen T, Biemann K, Rushneck DR, Biller JE, Howarth DW, Lafleur AL. The composition of the atmosphere at the surface of Mars. J Geophys Res 1977. doi:10.1029/js082i028p04635.

[31] Johnston DH, Toksöz MN. Internal structure and properties of Mars. Icarus 1977. doi:10.1016/0019-1035(77)90050-1.

[32] Mars Facts - NASA Mars. NASA n.d. https://mars.nasa.gov/allaboutmars/facts/#?c=inspace&s=distance (accessed June 5, 2019).

[33] Cucinotta FA, Hu S, Schwadron NA, Kozarev K, Townsend LW, Kim MHY. Space radiation risk limits and Earth-Moon-Mars environmental models. Sp Weather 2010. doi:10.1029/2010SW000572.

[34] Zubrin R. The Mars direct plan. Sci Am 2000. doi:10.1038/scientificamerican0300-52.

[35] Benaroya H. Lunar settlements. 2010. doi:10.1201/9781420083330.

[36] Benaroya H. The lunar environment. Build. Habitats Moon, Cham: Springer International Publishing; 2018, p. 42–84. doi:10.1007/978-3-319-68244-0_3.

[37] Feuerbacher B, Hamacher H, Naumann R. Materials sciences in space: a contribution to the scientific basis of space processing. 1953.

[38] Madorsky SI, Hart VE, Straus S, Sedlak VA. Thermal degradation of tetrafluoroethylene and hydrofluoroethylene polymers in a vacuum. J Res Natl Bur Stand (1934) 2012. doi:10.6028/jres.051.036.

[39] Congress CM-65th IA, 2014 undefined. Technology development for NASA's asteroid redirect mission. n.d.

[40] Johnson S, Leonard R. Manned Mars missions and extraterrestrial resource engineering test and evaluation. case Mars III Strateg. Explor., 1989, p. 455–68.

[41] Williams R, Jadwick J. Handbook of lunar materials 1980.

[42] Taylor SR. Lunar Science: A Post - Apollo View: Scientific Results and Insights from The Lunar Samples. n.d.

[43] Keller LP, McKay DS. The nature and origin of rims on lunar soil grains. Geochim Cosmochim Acta 1997. doi:10.1016/S0016-7037(97)00085-9.

[44] Bibring J, Burlingame A, … JC-L and P, 1974 undefined. Simulation of lunar carbon chemistry. I-Solar wind contribution. InLunar Planet. Sci. Conf. Proc., 1974, p. 1747–62.

[45] Taylor LA, Pieters CM, Keller LP, Morris R V., McKay DS. Lunar mare soils: Space weathering and the major effects of surface-correlated nanophase Fe. J Geophys Res E Planets 2001. doi:10.1029/2000JE001402.

[46] McKay D, Heiken G, Basu A, Blanford G, Simon S, Reedy R, et al. The lunar regolith. Lunar Sourceb., 1991, p. 285–356.

[47] Colwell JE, Robertson SR, Horányi M, Wang X, Poppe A, Wheeler P. Lunar Dust Levitation. J Aerosp Eng 2008. doi:10.1061/(asce)0893-1321(2009)22:1(2).

[48] Pollack JB, Colburn DS, Flasar FM, Kahn R, Carlston CE, Pidek D. Properties and effects of dust particles suspended in the Martian atmosphere. J Geophys Res 1979. doi:10.1029/jb084ib06p02929.

[49] Colwell JE, Batiste S, Horányi M, Robertson S, Sture S. Lunar surface: Dust dynamics and regolith mechanics. Rev Geophys 2007;45:1–26. doi:10.1029/2005RG000184.

[50] Gilmore, S. M. Craters as an Indicator of Martian Regolith Thickness. Fifth Int. Conf. Mars, 1999.

[51] Ryder G, Norman M. Catalog of Apollo 16 Rocks. NASA Curatorial Branch Publication 52; 1980.

[52] Fruland R, Reimold J. Introduction to the Core Samples from the Apollo 16 Landing Site. NASA; 1981.

[53] Morris RRVR, Score R, Dardano C, Heiken GH. Handbook of Lunar Soils. Planetary. NASA; 1983.

[54] Banin A, Clark B, Mars HW. Surface chemistry and mineralogy. Mars, 1992.

[55] Glass P. Major element composition of glasses from Apollo 11, 16, and 17 soil samples. Lunar Planet. Sci. Conf. Proc., 1976, p. 679–93.

[56] Ridley WI, Reid AM, Warner JL, Brown RW. Apollo 15 green glasses. Phys Earth Planet Inter 1973. doi:10.1016/0031-9201(73)90002-2.

[57] Sibille L, Carpenter P, Schlagheck R, French RR a. Lunar Regolith Simulant Materials: Recommendations for Standardization, Production, and Usage. vol. 214605. 2006. doi:10.4028/www.scientific.net/AMM.419.67.

[58] Sobolev A, Dmitriev L, Barsukov V, Nevsorov V, Slutskii A. The formation conditions of the high-magnesium olivines from the monomineralic fraction of Luna 24 regolith. Lunar Planet. Sci. Conf. Proc., 1980, p. 105–16.

[59] Jakes P. Cast basalt, mineral wool and oxygen production: early industries for planetary (lunar) outposts. Using situ Resour. Constr. Planet. Outposts, 1998.

[60] Vaniman D, Pettit D, Heiken G. Uses of lunar sulfur. Lunar Bases Sp 1992:429–35.

[61] Weast R, Astle M, Beyer W. CRC handbook of chemistry and physics. 1988.

[62] Vroom AH. Sulfur Concrete Goes Global. Concr Int 1998.

[63] Gibson Jr E, Moore G. Carbon and sulfur distributions and abundances in lunar fines. Lunar Planet. Sci. Conf. Proc., 1973, p. 1577.

[64] Kuck D. Lunar sulfur. Resour. Near-Earth Sp., 1991.

[65] Binder A. Lunar resources-What is known and expected. Eng. Constr. Oper. Sp. , 1988, p. 48–54.

[66] Happel JJA. Indigenous Materials for Lunar Construction. Appl Mech Rev 1993;46:313. doi:10.1115/1.3120360.

[67] Fairén AG, Davila AF, Gago-Duport L, Amils R, McKay CP. Stability against freezing of aqueous solutions on early Mars. Nature 2009. doi:10.1038/nature07978.

[68] Papike JJ, Fowler GW, Shearer CK, Layne GD. Ion microprobe investigation of plagioclase and orthopyroxene from lunar Mg-suite norites: Implications for calculating parental melt REE concentrations and for assessing postcrystallization REE redistribution. Geochim Cosmochim Acta 1996. doi:10.1016/0016-7037(96)00212-8.

[69] McCallum IS, Domeneghetti MC, Schwartz JM, Mullen EK, Zema M, Cámara F, et al. Cooling history of lunar Mg-suite gabbronorite 76255, troctolite 76535 and Stillwater pyroxenite SC-936: The record in exsolution and ordering in pyroxenes. Geochim Cosmochim Acta 2006. doi:10.1016/j.gca.2006.08.009.

[70] Landis GA. Materials refining on the Moon. Acta Astronaut 2007;60:906–15. doi:10.1016/j.actaastro.2006.11.004.

[71] Goldsworthy W. Composites: Fibers and Matrices From Lunar Regolith 1985:165–71.

[72] Rao D, Choudary U, Erstfeld T, Williams R. Extraction processes for the production of aluminum, titanium, iron, magnesium, and oxygen and nonterrestrial sources. NASA; 1979.

[73] Duke MB. Development of the Moon. Rev Mineral Geochemistry 2006;60:597–655. doi:10.2138/rmg.2006.60.6.

[74] Schwandt C. Understanding the electro-deoxidation of titanium dioxide to titanium metal via the FFC-Cambridge process. Miner Process Extr Metall 2014. doi:10.1179/0371955313z.00000000071.

[75] Bottke WF, Cellino A, Paolicchi P, Binzel RP. An Overview of the Asteroids: The Asteroids III Perspective. Asteroids III 2002.

[76] Talbert T. Planetary Defense Frequently Asked Questions. NASA 2018. https://www.nasa.gov/planetarydefense/faq.

[77] Lewis J. Space Resources. John Wiley & Sons; 1987.

[78] O'Leary B. Mining the Apollo and Amor asteroids. Science (80-) 1977. doi:10.1126/science.197.4301.363-a.

[79] Brophy J, Oleson S. Spacecraft conceptual design for returning entire near-earth asteroids. 48th AIAA/ASME/SAE/ASEE Jt. Propuls. Conf. Exhib., 2012.

[80] Zacny K, Cohen MM, James WW, Hilscher B. Asteroid Mining. AIAA Sp 2013 Conf Expo 2013. doi:10.2514/6.2013-5304.

[81] Brophy J, Friedman L, Culick, F. Asteroid retrieval feasibility. Aerosp. Conf. IEEE 2012, n.d.

[82] Letters JL-E and PS, 1972 undefined. Metal/silicate fractionation in the solar system. Elsevier n.d.

[83] Korotev RL. Lunar geochemistry as told by lunar meteorites. Chemie Der Erde 2005;65:297–346. doi:10.1016/j.chemer.2005.07.001.

[84] Rubin AE, Ma C. Meteoritic minerals and their origins. Chemie Der Erde - Geochemistry 2017;77:325–85. doi:10.1016/j.chemer.2017.01.005.

[85] Pepin R, Carr M. Major issues and outstanding questions. Mars, 1992, p. 120–43.

[86] McSween Jr. HY. SNC meteorites: Clues to martian petrologic evolution? Rev Geophys 1985. doi:10.1029/RG024i001p00141.

[87] Laul JC, Smith MR, Wänke H, Jagoutz E, Dreibus G, Palme H, et al. Chemical systematics of the shergotty meteorite and the composition of its parent body (Mars). Geochim Cosmochim Acta 1986. doi:10.1016/0016-7037(86)90373-X.

[88] Axon HJ. The metallurgy of meteorites. Prog Mater Sci 2003. doi:10.1016/0079-6425(68)90021-2.

[89] Joy KH, Crawford IA, Anand M, Greenwood RC, Franchi IA, Russell SS. The petrology and geochemistry of Miller Range 05035: A new lunar gabbroic meteorite. Geochim

Cosmochim Acta 2008. doi:10.1016/j.gca.2008.04.032.

[90] NASA. Calcalong Creek n.d. https://curator.jsc.nasa.gov/antmet/pdffiles/m03_calcalongv3.pdf.

[91] Yamato n.d. https://curator.jsc.nasa.gov/antmet/pdffiles/b01_yamato-793169v3.pdf.

[92] Kieffer H. Mars. www.jstor.org/stable/j.ctt207g59v; 1992.

[93] Khoshnevis B, Carlson A, Thangavelu M. ISRU-based robotic construction technologies for lunar and Martian infrastructures. 2017.

[94] Mitchell J, Houston W, Scott R, Costes N, Carrier III W, Bromwell L. Mechanical properties of lunar soil: Density, porosity, cohesion and angle of internal friction. Lunar Planet. Sci. Conf. Proc., 1972, p. 3235.

[95] Carrier WD, Olhoeft GR, Mendell W. Physical properties of the lunar surface. Lunar Sourceb 1991:475–594.

[96] Gromov V. Physical and mechanical properties of lunar and planetary soils. Earth. Moon. Planets, 1998, p. 51–72.

[97] Nealy J, Wilson J, Townsend L. Preliminary Analyses of Space Radiation Protection for Luner Base Surface Systems 1989.

[98] Kaplicky J, Nixon D. A surface-assembled superstructure envelope system to support regolith mass-shielding for an initial-operational-capability lunar base. Lunar bases Sp. Act. 21st century, 1985, p. 375.

[99] Ortiz A, Rygalov V, León P. Radiation Protection Strategy Development for Mars Surface Exploration 2015.

[100] Langseth M, Keihm S, Peters K. Revised lunar heat-flow values. InLunar Planet. Sci. Conf. Proc., 1976, p. 3143–71.

[101] Jakosky BM. On the thermal properties of Martian fines. Icarus 1986. doi:10.1016/0019-1035(86)90011-4.

[102] Zent AP, Hecht MH, Cobos DR, Campbell GS, Campbell CS, Cardell G, et al. Thermal and Electrical Conductivity Probe (TECP) for phoenix. J Geophys Res E Planets 2009. doi:10.1029/2007JE003052.

[103] Colozza AJ. Analysis of lunar regolith thermal energy storage. Nasa Cr 1991:9p.

[104] Kieffer HH. Soil and surface temperatures at the Viking landing sites. Science (80-) 1976. doi:10.1126/science.194.4271.1344.

[105] Robie RA, Hemingway BS, Wilson WH. Specific heats of lunar surface materials from 90 to 350 degrees Kelvin. Science (80-) 1970. doi:10.1126/science.167.3918.749.

[106] Fujii N, Osako M. Thermal diffusivity of lunar rocks under atmospheric and vacuum conditions. Earth Planet Sci Lett 1973;18:65–71. doi:10.1016/0012-821X(73)90035-6.

[107] Taylor LA, Meek TT. Microwave Sintering of Lunar Soil: Properties, Theory, and Practice. J Aerosp Eng 2005;18:188–96. doi:10.1061/(ASCE)0893-1321(2005)18:3(188).

[108] Perkins S. Modeling of Regolith Structure Interaction in Extraterrestrial Constructed Facilities. University of Colorado, 1991.

[109] Badescu V. Mars: prospective energy and material resources. Springer Science & Business Media; 2009. doi:10.1007/978-3-642-03629-3.

[110] Brook N. The equivalent core diameter method of size and shape correction in point load testing. Int J Rock Mech Min Sci 1985. doi:10.1016/0148-9062(85)92328-9.

[111] Kieffer SW. From regolith to rock by shock. Moon 1975. doi:10.1007/BF00567522.

[112] Simonds C. Hot pressing of lunar soil and qualification for manned applications. Second Conf. Lunar Bases Sp. Act. 21st Century, 1988, p. 220.

[113] Taylor S. Planetary science: a lunar perspective. Lunar and Planetary Institute; 1982.

[114] Housley R, … RG-L and P, 1973 undefined. Origin and characteristics of excess Fe metal in lunar glass welded aggregates. AdsabsHarvardEdu n.d.

[115] Blair BRBR, Economics E. The role of Near-Earth asteroids in long-term platinum supply. Sp Resour Roundtable 2 2000:1–15. doi:10.3390/s150305032.

[116] Dalton C, Hohmann E. Conceptual design of a lunar colony. 1972.

[117] Binder A, Culp M, Toups L. Lunar derived construction materials: Cast basalt. Eng. Constr. Oper. Sp. II, 1990, p. 117–22.

[118] Agosto W, Wickman J, James E. Lunar cements/concretes for orbital structures. Eng. Constr. Oper. Sp., 1988, p. 157–68.

[119] Blacic J. Mechanical properties of lunar materials under anhydrous, hard vacuum conditions: Applications of lunar glass structural components 1984.

[120] Rogers W, Sture S. Indigenous lunar construction materials. 1991.

[121] Allen C, Hines J, McKay D, Morris R. Sintering of lunar glass and basalt. Eng. Constr. Oper. space-III Space'92, 1992, p. 1209–18.

[122] Carrier W, Bromwell L, & RM-J of SM, 1973 undefined. Behavior of returned lunar soil in vacuum. TridTrbOrg n.d.

[123] Aulesa V. Architecture of lunar habitats. Explor. Util. Moon, 2000, p. 289.

[124] Khoshnevis B, Carlson A, Leach N, Thangavelu M. Contour Crafting Simulation Plan for Lunar Settlement Infrastructure Buildup. Earth Sp. 2012, 2012. doi:10.1061/9780784412190.155.

[125] Kading B, Straub J. Utilizing in-situ resources and 3D printing structures for a manned Mars mission. Acta Astronaut 2015. doi:10.1016/j.actaastro.2014.11.036.

[126] Kopecký L, Voldán J. The cast basalt industry. Ann N Y Acad Sci 1965;123:1086–105. doi:10.1111/j.1749-6632.1965.tb20421.x.

[127] Kopecký L. Geologic Interpretation of the Study of Lunar Rocks. Symp. Astron., 1972.

[128] Capps S, Wise T. Lunar basalt construction materials. Eng. Constr. Oper. Sp. II, 1990.

[129] Taylor LA, Pieters CM, Britt D. Evaluations of lunar regolith simulants. Planet Space Sci 2016. doi:10.1016/j.pss.2016.04.005.

[130] Taylor L, Liu Y. Important considerations for lunar soil simulants. Earth Sp. 2010 Eng. Sci. Constr. Oper. Challenging Environ., 2010, p. 106–18.

[131] NASA. All simulant listing 2018. https://isru.msfc.nasa.gov/lib/Documents/Simulant-listing.pdf.

[132] NASA. [143] Planetary Simulant Database: Johnson Space Center JSC-1/1A/1AF/1AC/2A. 2018 n.d. http://sciences.ucf.edu/class/simulant_jsc1/.

[133] Beegle L, Peters G, … GM-L and P, 2007 undefined. Mojave Martian simulant: a new martian soil simulant. AdsabsHarvardEdu n.d.

[134] Ray CS, Reis ST, Sen S, O'Dell JS. JSC-1A lunar soil simulant: Characterization, glass formation, and selected glass properties. J. Non. Cryst. Solids, 2010. doi:10.1016/j.jnoncrysol.2010.04.049.

[135] McKay D, Carter J, Boles W, Allen C, Allton J. JSC-1: A new lunar soil simulant. Eng. Constr. Oper. Sp., 1994, p. 857–66.

[136] FJS-1/2/3 Fuji Japanese Simulant 2018. https://sciences.ucf.edu/class/simulant_fjs/.

[137] Bodiford M, Burks K, Perry M, Cooper R, Fiske M. Lunar in situ materials-based habitat technology development efforts at NASA/MSFC. Earth Sp. 2006 Eng. Constr. Oper. Challenging Environ., 2006, p. 1–8.

[138] Fabes B, Poisl W. Processing of glass-ceramics from lunar resources. 1991.

[139] Bell LS, Fahey MG, Wise TK, Spana PC. Indigenous Resource Utilization in Design of Advanced Lunar Facility. J Aerosp Eng 2007. doi:10.1061/(asce)0893-1321(1992)5:2(230).

[140] Balla VK, Roberson LB, O'Connor GW, Trigwell S, Bose S, Bandyopadhyay A. First demonstration on direct laser fabrication of lunar regolith parts. Rapid Prototyp J 2012. doi:10.1108/13552541211271992.

[141] Naser MZ, Chehab AI. Materials and design concepts for space-resilient structures. Prog Aerosp Sci 2018;98:74–90. doi:10.1016/j.paerosci.2018.03.004.

[142] Fateri M, Gebhardt A. Process parameters development of selective Laser Melting of lunar regolith for on-site manufacturing applications. Int J Appl Ceram Technol 2015. doi:10.1111/ijac.12326.

[143] Meurisse A, Beltzung JC, Kolbe M, Cowley A, Sperl M. Influence of Mineral Composition on Sintering Lunar Regolith. J Aerosp Eng 2017. doi:10.1061/(asce)as.1943-5525.0000721.

[144] Personal communication through email to Alexandre.Meurisse@dlr.de 2018.

[145] Song L, Xu J, Fan S, Tang H, Li X, Liu J, et al. Vacuum sintered lunar regolith simulant: Pore-forming and thermal conductivity. Ceram Int 2019. doi:10.1016/j.ceramint.2018.11.023.

[146] Liu M, Tang W, Duan W, Li S, Dou R, Wang G, et al. Digital light processing of lunar regolith structures with high mechanical properties. Ceram Int 2019. doi:10.1016/j.ceramint.2018.12.049.

[147] Indyk SJ, Benaroya H. A structural assessment of unrefined sintered lunar regolith simulant. Acta Astronaut 2017. doi:10.1016/j.actaastro.2017.09.018.

[148] Indyk S. Structural members produced from unrefined lunar regolith, a structural assessment. Rutgers University, 2015.

[149] Hintze PE, Quintana S. Building a Lunar or Martian Launch Pad with In Situ Materials: Recent Laboratory and Field Studies. J Aerosp Eng 2013. doi:10.1061/(asce)as.1943-5525.0000205.

[150] Gualtieri T, Bandyopadhyay A. Compressive deformation of porous lunar regolith. Mater Lett 2015;143:276–8. doi:10.1016/j.matlet.2014.11.153.

[151] Meek T, Fayerweather L, Godbole M, Vaniman D, Honnell R. Sintering lunar simulants using 2.45 GHz radiation. Eng. Constr. Oper. Sp., 1988, p. 102–10.

[152] Meek T, Vaniman D, Cocks F, Wright R. Microwave processing of lunar materials:

Potential applications. Lunar bases Sp. Act. 21st century, 1985, p. 479.

[153] Allen C, Graf J, McKay D. Sintering bricks on the Moon. Eng. Constr. Oper. Sp. IV, 1994.

[154] Allen C. Bricks and ceramics. Using situ Resour. Constr. Planet. Outposts, 1998.

[155] McLemore CA, Fikes JC, McCarley KS, Good JE, Kennedy JP, Gilley SD. From lunar regolith to fabricated parts: Technology developments and the utilization of moon dirt. Earth Sp Conf 2008 Proc 11th Aerosp Div Int Conf Eng Sci Constr Oper Challenging Environ 2008;323:1–11. doi:doi:10.1061/40988(323)132.

[156] McLemore C, Fikes J, Darby C, Good J, Gilley S. Fabrication capabilities utilizing in situ materials. 2008.

[157] Hintze P, Curran J, Back T. Lunar Surface Stabilization via Sintering or the Use of Heat Cured Polymers. 47th AIAA Aerosp Sci Meet Incl New Horizons Forum Aerosp Expo 2009. doi:10.2514/6.2009-1015.

[158] Gosau J-M. Regolith stabilization and building materials for the lunar surface. Earth Sp 2012:243. doi:10.1061/9780784412190.028.

[159] Corrias G, Licheri R, Orrù R, Cao G. Self-propagating high-temperature reactions for the fabrication of Lunar and Martian physical assets. Acta Astronaut 2012;70:69–76. doi:10.1016/j.actaastro.2011.07.022.

[160] Hobosyan M, Science KM-L and P, 2012 undefined. Sintering of regolith by activated thermites: A novel approach for lunar in-situ resource utilization. AdsabsHarvardEdu n.d.

[161] Taylor SL, Jakus AE, Koube KD, Ibeh AJ, Geisendorfer NR, Shah RN, et al. Sintering of micro-trusses created by extrusion-3D-printing of lunar regolith inks. Acta Astronaut 2018;143:1–8. doi:10.1016/j.actaastro.2017.11.005.

[162] Jakus AE, Koube KD, Geisendorfer NR, Shah RN. Robust and Elastic Lunar and Martian Structures from 3D-Printed Regolith Inks. Sci Rep 2017. doi:10.1038/srep44931.

[163] Flynn GJ, McKay DS. An assessment of the meteoritic contribution to the Martian soil. J Geophys Res 1990. doi:10.1029/jb095ib09p14497.

[164] Flynn GJ, Consolmagno GJ, Brown P, Macke RJ. Physical properties of the stone meteorites: Implications for the properties of their parent bodies. Chemie Der Erde - Geochemistry 2017. doi:10.1016/j.chemer.2017.04.002.

[165] Marvin UB. Ernst Florens Friedrich Chladni (1756-1827) and the origins of modern meteorite research. Meteorit Planet Sci 1996. doi:10.1111/j.1945-5100.1996.tb02031.x.

[166] Biot J. Relation d'un voyage fait dans le départment de l'Orne pour constater la réalité d'un Méteore observé a l'Aigle le 26 floréal an 11. Baudouin, Paris. An English translation of a

letter to Chaptal from Biot describing the report appeared in. Phil. Phil Mag(Tilloch's 1803;16:224–8.

[167] McKay M, McKay D, Duke M. Space Resources: Materials. National Aeronautics and Space Administration; 1992.

[168] Yomogida K, Matsui T. Physical Properties of Ordinary Chondrites. J Geophys Res 1983;88:9513–33.

[169] Opeil CP, Consolmagno GJ, Safarik DJ, Britt DT. Stony meteorite thermal properties and their relationship with meteorite chemical and physical states. Meteorit Planet Sci 2012. doi:10.1111/j.1945-5100.2012.01331.x.

[170] Anders E. Origin, age, and composition of meteorites. Space Sci Rev 1964. doi:10.1007/BF00177954.

[171] Mason B, Fleischer M. Cosmochemistry: Meteorites. 1979.

[172] Medvedev R, Gorbatsevich F, Meteoritika IZ-, 1985 undefined. Determination of the physical properties of stony meteorites with application to the study of processes of their destruction. AdsabsHarvardEdu n.d.

[173] Zotkin I, Medvedev P, Meteoritika FG-, 1987 undefined. Strength properties of the Tsarev meteorite. AdsabsHarvardEdu n.d.

[174] Petrovic JJ. Review: Mechanical properties of meteorites and their constituents. J Mater Sci 2001. doi:10.1023/A:1017546429094.

[175] Buddhue JD. The Compressive Strength of Meteorites. Contrib Soc Res Meteorites 1942;3:39–40. doi:10.1111/j.1945-5100.1942.tb00140.x.

[176] Popova O, Borovička J, Hartmann WK, Spurný P, Gnos E, Nemtchinov I, et al. Very low strengths of interplanetary meteoroids and small asteroids. Meteorit Planet Sci 2011;46:1525–50. doi:10.1111/j.1945-5100.2011.01247.x.

[177] Petrovic JJ. Mechanical properties of meteorites. J Mater Sci 2001;36:1579–83.

[178] Gordon RB. Mechanical properties of iron meteorites and the structure of their parent planets. J Geophys Res 1970;75:439–47. doi:10.1029/JB075i002p00439.

[179] Rudge W, Douglas W, udge M. On a Meteoric Iron from Winburg, Orange Free State. Proc R Soc London Ser A, Contain Pap a Math Phys Character 1914;90:19–25. doi:DOI: 10.1098/rspa.1914.0030.

[180] Lin T, Senseney JA, Arp LD, Lindbergh C. Concrete lunar base investigation. J Aerosp Eng 1989. doi:10.1061/(ASCE)0893-1321(1989)2:1(10).

[181] Meyers C, Engineering HT-J of A, 2007 undefined. Analysis of lunar-habitat structure using waterless concrete and tension glass fibers. AscelibraryOrg n.d.

[182] Hanus MJ, Harris AT. Nanotechnology innovations for the construction industry. Prog Mater Sci 2013. doi:10.1016/j.pmatsci.2013.04.001.

[183] Czernin W. Cement chemistry and physics for civil engineers. Lockwood: 1962.

[184] Talling B, Krivenko P. Blast furnace slag-the ultimate binder. Waste Mater. Used Concr. Manuf., 2008. doi:10.1016/b978-081551393-3.50008-9.

[185] Taylor SR. Lunar and terrestrial crusts: a constrast in origin and evolution. Phys Earth Planet Inter 1982;29:233–41. doi:10.1016/0031-9201(82)90014-0.

[186] Lin T, Bhattacharja S. Lunar and Martian resources utilization: cement. Sp. 1998, 1998.

[187] Boles W, Kirby K, Baird S. Concrete for Lunar and Mars Soils In Situ Resource Utilization. Sp. 2002 Robot. 2002, 2002, p. 143–7.

[188] Schindler AK, Folliard KJ. Heat of hydration models for cementitious materials. ACI Mater J 2005.

[189] Neville A. Properties of Concrete. 5th ed. Prentice Hall; 2012.

[190] Brandt AM. Cement-Based Composites. CRC Press; 2005. doi:10.1201/9781482265866.

[191] Koh SW, Yoo J, Bernold LE, Lee TS. Experimental Study of Waterless Concrete for Lunar Construction. Earth Sp (12th), March 14-17 2010;41096:7. doi:10.1061/41096(366)102.

[192] Ishikawa N, Kanamori H, Okada T. The possibility of concrete production on the Moon. Lunar Bases Sp. Act. 21st Century, 1992, p. 489.

[193] Lin T. Concrete for lunar base construction. Concr Int Des Constr 1987:48–53.

[194] Lin TD, Ahmed G, Hill G, Robinson S, Lindbergh C, Gallagher JO, et al. Stresses in Concrete Panels Exposed to the Sun on the Moon. ACI Spec Publ 1991:141–54.

[195] Lin T, Burns N. Design of prestressed concrete structures. Wiley New York; 1963.

[196] Lin TD, Love H, Stark D. Physical properties of concrete made with Apollo 16 lunar soil sample. 2nd Conf Lunar Bases Sp Act 1992;1:483–7.

[197] Swint D, Schmidt S. Optimizing lunar concrete. ACI Spec Publ 1991;125:41–56.

[198] Mishulovich A, Lin TD, Tresouthick SW, West PB. Lunar Cement Formulation. Spec Publ 1991;125. doi:10.14359/2450.

[199] Naser M. Behavior of RC Beams Strengthened with CFRP Laminates Under Fire-A Finite

Element Simulation. American University of Sharjah, 2011.

[200] Composites RZ-C and C, 1997 undefined. Fiber-reinforced concrete: an overview after 30 years of development. Elsevier n.d.

[201] Matsumoto S, Yoshida T, Kanamori H, Takagi K. Construction Engineering Approach for Lunar Base Development. J Aerosp Eng 1998;11:129–37. doi:10.1061/(ASCE)0893-1321(1998)11:4(129).

[202] Tucker D, Ethridge E, Toutanji H. Production of Glass Fibers for Reinforcement of Lunar Concrete. 44th AIAA Aerosp. Sci. Meet. Exhib., Reston, Virigina: American Institute of Aeronautics and Astronautics; 2006. doi:10.2514/6.2006-523.

[203] Tjiptobroto P, Hansen W. Tensile strain hardening and multiple cracking in high-performance cement-based composites containing discontinuous fibers. ACI Mater J 1993.

[204] Young J. Concrete and other cement-based composites for lunar base construction. Lunar bases Sp. Act. 21st century, 1985, p. 391.

[205] Horiguchi T, Saeki N, Yoneda T, Hoshi T, Lin TD. Behavior of Simulated Lunar Cement Mortar in Vacuum Environment. Sp. 98, 1998, p. 571–6. doi:10.1061/40339(206)65.

[206] Cullingford H, Keller MD, S.Cullingford H, Keller MD. Lunar concrete for construction. Second Conf. Lunar Bases Sp. Act. 21st Century, 1992. doi:19930004802.

[207] Kanamori H, Matsumoto S, Ishikawad N, Ishikawa N. Long-Term Properties of Mortar Exposed to a Vacuum. ACI Spec Publ 1991;125:57–69.

[208] Namba H, Ishikawa N, Kanamori H. Concrete production method for construction of lunar bases. Eng. Constr. Oper. Sp. , 1988, p. 169–77.

[209] McKay D, Allen C. Concrete—A Practical Construction Material for Mars. Eng. Constr. Oper. Sp. V, 1996, p. 566–70.

[210] Scheerbaum G. In-Situ Manufacture of Martian Construction Materials. Sp. 2000, Reston, VA: American Society of Civil Engineers; 2000, p. 934–40. doi:10.1061/40479(204)111.

[211] Young J, Berger R. Cement-based materials for planetary facilities. InEngineering, Constr. Oper. Sp. , 1988, p. 134–45.

[212] Birchall J, Howard A, Kendall K. Strong hydraulic cements. Br. Ceram. Soc., 1982, p. 25.

[213] Bache H. Dense cement ultrafine particle based material. Proc. 2nd Symp. Superplast. Concr., 1981.

[214] Anand M, Crawford IA, Balat-Pichelin M, Abanades S, Van Westrenen W, Péraudeau G, et al. A brief review of chemical and mineralogical resources on the Moon and likely initial

in situ resource utilization (ISRU) applications. Planet. Space Sci., 2012. doi:10.1016/j.pss.2012.08.012.

[215] Anand M, Tartèse R, Barnes JJ. Understanding the origin and evolution of water in the Moon through lunar sample studies. Philos Trans R Soc A Math Phys Eng Sci 2014. doi:10.1098/rsta.2013.0254.

[216] Fowler DW. Polymers in concrete: A vision for the 21st century. Cem Concr Compos 1999. doi:10.1016/S0958-9465(99)00032-3.

[217] Mani P, Gupta AK, Krishnamoorthy S. Comparative study of epoxy and polyester resin-based polymer concretes. Int J Adhes Adhes 1987;7:157–63. doi:10.1016/0143-7496(87)90071-6.

[218] Elalaoui O, Ghorbel E, Mignot V, Ben Ouezdou M. Mechanical and physical properties of epoxy polymer concrete after exposure to temperatures up to 250 °c. Constr Build Mater 2012;27:415–24. doi:10.1016/j.conbuildmat.2011.07.027.

[219] Bedi R, Chandra R, Singh SP. Mechanical Properties of Polymer Concrete. J Compos 2013;2013:1–12. doi:10.1155/2013/948745.

[220] Chen PW, Chung DDL. Carbon fiber reinforced concrete for smart structures capable of non-destructive flaw detection. Smart Mater Struct 1993. doi:10.1088/0964-1726/2/1/004.

[221] Wongpa J, Kiattikomol K, Jaturapitakkul C, Chindaprasirt P. Compressive strength, modulus of elasticity, and water permeability of inorganic polymer concrete. Mater Des 2010. doi:10.1016/j.matdes.2010.05.012.

[222] Sik Lee T, Lee J, Yong Ann K. Manufacture of polymeric concrete on the Moon. Acta Astronaut 2015;114:60–4. doi:10.1016/j.actaastro.2015.04.004.

[223] Rashid K, Wang Y, Ueda T. Influence of continuous and cyclic temperature durations on the performance of polymer cement mortar and its composite with concrete. Compos Struct 2019. doi:10.1016/j.compstruct.2019.02.057.

[224] Garnock B, Bernold L. Experimental Study of Hollow-Core Beams Made with Waterless Concrete. Earth Sp. 2012, Reston, VA: American Society of Civil Engineers; 2012, p. 119–27. doi:10.1061/9780784412190.014.

[225] Reis JML, Ferreira AJM. Assessment of fracture properties of epoxy polymer concrete reinforced with short carbon and glass fibers. Constr Build Mater 2004;18:523–8. doi:10.1016/j.conbuildmat.2004.04.010.

[226] Brockenbrough T, Proceedings DP-J, 1982 undefined. Fiber reinforced methacrylate polymer concrete. ConcreteOrg n.d.

[227] Lee J, Ann KY, Lee TS, Mitikie BB. Bottom-up heating method for producing polyethylene lunar concrete in lunar environment. Adv Sp Res 2018;62:164–73. doi:10.1016/j.asr.2018.03.039.

[228] Bisby LA LA, Green MMF, Kodur VVKR. Response to fire of concrete structures that incorporate FRP. Prog Struct Eng Mater 2005;7:136–49. doi:10.1002/pse.198.

[229] Ribeiro MCS, Nóvoa PR, Ferreira AJM, Marques AT. Flexural performance of polyester and epoxy polymer mortars under severe thermal conditions. Cem Concr Compos 2004;26:803–9. doi:10.1016/S0958-9465(03)00162-8.

[230] Tavares CML, Ribeiro MCS, Ferreira AJM, Guedes RM. Creep behaviour of FRP-reinforced polymer concrete. Compos Struct 2002. doi:10.1016/S0263-8223(02)00061-2.

[231] Leutner B, Dieh l L. Manufacture of sulfur concrete, 1977.

[232] Casanova I. Feasibility and applications of sulfur concrete for lunar base development: a preliminary study. Lunar Planet. Sci. Conf. , 1997, p. 209.

[233] Grugel RN, Toutanji H. Sulfur "concrete" for lunar applications - Sublimation concerns. Adv Sp Res 2008. doi:10.1016/j.asr.2007.08.018.

[234] Mohamed A, El-Gamal M. Sulfur concrete for the construction industry: a sustainable development approach. J. Ross Publishing; 2010.

[235] Issa M, Omar H. Feasibility of dual technology in manufacturing lunar concrete. InProceedings 4th Int. Conf. Eng. Constr. Oper. Sp., 1994.

[236] Omar H. Production of lunar concrete using molten sulfur. 1993.

[237] Toutanji H, Grugel R. Performance of "waterless concrete." Concr. Solut., 2009, p. 215.

[238] Grugel RN. Integrity of sulfur concrete subjected to simulated lunar temperature cycles. Adv Sp Res 2012. doi:10.1016/j.asr.2012.06.027.

[239] Toutanji H, Grugel R. Mechanical Properties and Durability Performance of waterless concrete. Earth Sp. 2008 Eng. Sci. Constr. Oper. Challenging Environ. , Reston, VA: American Society of Civil Engineers; 2008, p. 1–8. doi:10.1061/40988(323)46.

[240] Toutanji HA, Evans S, Grugel RN. Performance of lunar sulfur concrete in lunar environments. Constr Build Mater 2012. doi:10.1016/j.conbuildmat.2011.10.041.

[241] Jong B, McBee W, Rasmussen K, Sullivan T. Fiber Reinforcement of Sulfur Concrete to Enhance Flexural Properties. 1985.

[242] Ho JLK, Woodhams RT. Fracture Toughness of Fiber Reinforced Sulfur Concrete. J. Am. Concr. Inst., 1982.

[243] Wan L, Wendner R, Cusatis G. A novel material for in situ construction on Mars: experiments and numerical simulations. Constr Build Mater 2016. doi:10.1016/j.conbuildmat.2016.05.046.

[244] Osio-Norgaard JM, Ferraro CC. Permeability of Sulfur Based Lunar Concrete. Earth Sp. 2016 Eng. Extrem. Environ. - Proc. 15th Bienn. Int. Conf. Eng. Sci. Constr. Oper. Challenging Environ., 2016. doi:10.1061/9780784479971.085.

[245] Gracia V, Casanova I. Sulfur Concrete: A Viable Alternative for Lunar Construction. Sp 98 1998:585–91. doi:doi:10.1061/40339(206)67.

[246] Kriven WM. 5.9 Geopolymer-Based Composites. Compr. Compos. Mater. II, Elsevier; 2018, p. 269–80. doi:10.1016/B978-0-12-803581-8.09995-1.

[247] Provis JL, Van Deventer JSJ. Geopolymers: Structures, processing, properties and industrial applications. 2009. doi:10.1533/9781845696382.

[248] Davis G, Montes C, Eklund S. Preparation of lunar regolith based geopolymer cement under heat and vacuum. Adv Sp Res 2017;59:1872–85. doi:10.1016/j.asr.2017.01.024.

[249] Wang KT, Tang Q, Cui XM, He Y, Liu LP. Development of near-zero water consumption cement materials via the geopolymerization of tektites and its implication for lunar construction. Sci Rep 2016. doi:10.1038/srep29659.

[250] Davidovits J. Geopolymers - Inorganic polymeric new materials. J Therm Anal 1991. doi:10.1007/BF01912193.

[251] Sankar K, Stynoski P, Al-Chaar GK, Kriven WM. Sodium silicate activated slag-fly ash binders: Part I - Processing, microstructure, and mechanical properties. J Am Ceram Soc 2018;101:2228–44. doi:10.1111/jace.15391.

[252] Matta M, Smith S, Baumgardner J, Wilson J, Martinis C, Mendillo M. The sodium tail of the Moon. Icarus 2009. doi:10.1016/j.icarus.2009.06.017.

[253] Wang K tuo, Lemougna PN, Tang Q, Li W, Cui X min. Lunar regolith can allow the synthesis of cement materials with near-zero water consumption. Gondwana Res 2017;44:1–6. doi:10.1016/j.gr.2016.11.001.

[254] Fernández-Jiménez A, Palomo A. Nanostructure/microstructure of fly ash geopolymers. Geopolymers, Woodhead Publishing; 2009, p. 89–117. doi:10.1533/9781845696382.1.89.

[255] Liew YM, Heah CY, Mohd Mustafa AB, Kamarudin H. Structure and properties of clay-based geopolymer cements: A review. Prog Mater Sci 2016. doi:10.1016/j.pmatsci.2016.08.002.

[256] Montes C, Broussard K, Gongre M, Simicevic N, Mejia J, Tham J, et al. Evaluation of lunar

regolith geopolymer binder as a radioactive shielding material for space exploration applications. Adv Sp Res 2015;56:1212–21. doi:10.1016/j.asr.2015.05.044.

[257] Alexiadis A, Alberini F, Meyer ME. Geopolymers from lunar and Martian soil simulants. Adv Sp Res 2017;59:490–5. doi:10.1016/j.asr.2016.10.003.

[258] Han B, Zhang L, Ou J. Smart and multifunctional concrete toward sustainable infrastructures. Springer; 2017. doi:10.1007/978-981-10-4349-9.

[259] Gosselin C, Duballet R, Roux P, Gaudillière N, Dirrenberger J, Morel P. Large-scale 3D printing of ultra-high performance concrete - a new processing route for architects and builders. Mater Des 2016. doi:10.1016/j.matdes.2016.03.097.

[260] Cesaretti G, Dini E, De Kestelier X, Colla V, Pambaguian L. Building components for an outpost on the Lunar soil by means of a novel 3D printing technology. Acta Astronaut 2014. doi:10.1016/j.actaastro.2013.07.034.

[261] Khoshnevis B. Automated construction by contour crafting - Related robotics and information technologies. Autom. Constr., 2004. doi:10.1016/j.autcon.2003.08.012.

[262] Xia M, Sanjayan J. Method of formulating geopolymer for 3D printing for construction applications. Mater Des 2016. doi:10.1016/j.matdes.2016.07.136.

[263] Han B, Ding S, Yu X. Intrinsic self-sensing concrete and structures: A review. Meas J Int Meas Confed 2015. doi:10.1016/j.measurement.2014.09.048.

[264] Kim DJ, Kang SH, Ahn TH. Mechanical Characterization of High-Performance Steel-Fiber Reinforced Cement Composites with Self-Healing Effect. Materials (Basel) 2014. doi:10.3390/ma7010508.

[265] Awaja F, Zhang S, Tripathi M, Nikiforov A, Pugno N. Cracks, microcracks and fracture in polymer structures: Formation, detection, autonomic repair. Prog Mater Sci 2016. doi:10.1016/j.pmatsci.2016.07.007.

[266] Yuan X, Xu W, Sun W, Xing F, Wang W. Properties of cement mortar by use of hot-melt polyamides as substitute for fine aggregate. Materials (Basel) 2015. doi:10.3390/ma8063714.

[267] Dade-Robertson M, Ramirez-Figueroa C, Zhang M. Radical vernacular: Bacterial architecture on Mars. JBIS - J Br Interplanet Soc 2014.

[268] Dade-Robertson M. Building Science: Synthetic Biology and emerging technologies in architectural research. Archit Res Q 2016. doi:10.1017/s1359135516000142.

[269] Feng P, Meng X, Chen JF, Ye L. Mechanical properties of structures 3D printed with cementitious powders. Constr Build Mater 2015. doi:10.1016/j.conbuildmat.2015.05.132.

[270] You I, Yoo D, Kim S, Kim M, Zi G. Electrical and self-sensing properties of ultra-high-performance fiber-reinforced concrete with carbon nanotubes. Sensors 2017;17:2481.

[271] Makarious A, Kany A, Abdo A. Measurement of the transmitted and reflected capture gamma rays for heat resistant concrete shield. Acta Phys Hungarica 1986;60:213–20. doi:https://doi.org/10.1007/BF03156043.

[272] Creutz E, Downes K. Magnetite Concrete for Radiation Shielding. J Appl Phys 1949;20:1236–40. doi:10.1063/1.1698315.

[273] Horszczaruk E, Brzozowski P. Investigation of gamma ray shielding efficiency and physicomechanical performances of heavyweight concrete subjected to high temperature. Constr Build Mater 2019. doi:10.1016/j.conbuildmat.2018.09.113.

[274] Baltas H, Sirin M, Celik A, Ustabas, El-Khayatt AM. Radiation shielding properties of mortars with minerals and ores additives. Cem Concr Compos 2019. doi:10.1016/j.cemconcomp.2019.01.006.

[275] Shams T, Eftekhar M, Shirani A. Investigation of gamma radiation attenuation in heavy concrete shields containing hematite and barite aggregates in multi-layered and mixed forms. Constr Build Mater 2018. doi:10.1016/j.conbuildmat.2018.06.032.

[276] Johnson S, Wetzel J. Engineering, Construction, and Operations in Space II. ASCE; 1990.

[277] Benaroya H, Mottaghi S, Porter Z. Magnesium as an ISRU-Derived Resource for Lunar Structures. J Aerosp Eng 2013;26:152–9. doi:10.1061/(ASCE)AS.1943-5525.0000235.

[278] Mottaghi S, Benaroya H. Design of a Lunar Surface Structure. II: Seismic Structural Analysis. J Aerosp Eng 2015. doi:10.1061/(ASCE)AS.1943-5525.0000396.

[279] Mottaghi S, Benaroya H. Design of a Lunar Surface Structure. I: Design Configuration and Thermal Analysis. J Aerosp Eng 2015. doi:10.1061/(ASCE)AS.1943-5525.0000382.

[280] Brichni A, Hammi H, Aggoun SS, Mnif A. Optimization of magnesium oxychloride cement properties by silica glass. Adv Cem Res 2016;28:654–63. doi:10.1680/jadcr.16.00024.

[281] Werkheiser MMJ, Fiske MR, Edmunson JE, Khoshnevis B, Way P, Ray M Del. On the development of additive construction technologies for application to development of lunar/martian surface structures using in-situ materials. AIAA Sp. 2015 Conf. Expo., Reston, Virginia: American Institute of Aeronautics and Astronautics; 2015, p. 4451. doi:https://doi.org/10.2514/6.2015-4451.

[282] Detwiler M, Foong C, Stocklin C. Conceptual design of equipment to excavate and transport regolith from the lunar maria. 1990.

[283] Belvin W, Watson J, Singhal S. Structural Concepts and Materials for Lunar Exploration

Habitats. Sp. 2006, Reston, Virigina: American Institute of Aeronautics and Astronautics; 2006. doi:10.2514/6.2006-7338.

[284] Gionet T. The Structural Response of a Frame-Membrane Lunar Habitat Subjected to Impact and Thermal Loads. University of Connecticut, 2011.

[285] Mazzolani FM. Structural Applications of Aluminium in Civil Engineering. Struct Eng Int 2006;16:280–5. doi:10.2749/101686606778995128.

[286] Committee AH. ASM Handbook, Volume 2: Properties and Selection: Nonferrous Alloys and Special-Purpose Materials. n.d.

[287] Wong M. Review of papers regarding vacuum system and materials 2019. http://home.fnal.gov/~mlwong/outgas_rev.htm.

[288] GmbH VVK& M. Outgassing Rates of Aluminum compared to Stainless Steel n.d. https://www.vacom.de/en/downloads/white-paper?download=3024:outgassing-rates-of-aluminum-compared-to-stainless-steel.

[289] Yin P. Structural concept studies for a horizontal cylindrical lunar habitat and a lunar guyed tower. 1990.

[290] Chu P, Lu X. Low temperature plasma technology: methods and applications. CRC Press; 2013.

[291] Beryllium D and F. Materion Brush Beryllium & Composites 2018. https://materion.com/-/media/files/pdfs/beryllium/beryllium-materials/mb-001designingandfabricatingberyllium.pdf.

[292] Smith BH, Szyniszewski S, Hajjar JF, Schafer BW, Arwade SR. Steel foam for structures: A review of applications, manufacturing and material properties. J Constr Steel Res 2012. doi:10.1016/j.jcsr.2011.10.028.

[293] Naser M. Response of steel and composite beams subjected to combined shear and fire loading. Michigan State University, 2016.

[294] Cutler A. Power requirements for space resource utilization 1986.

[295] Zhuk AZ, Sheindlin AE, Kleymenov B V., Shkolnikov EI, Lopatin MY. Use of low-cost aluminum in electric energy production. J Power Sources 2006. doi:10.1016/j.jpowsour.2005.11.097.

[296] Peters M, Engineering CL-M science and, 2009 undefined. Aerospace and space materials. PdfsSemanticscholarOrg n.d.

[297] Ruess F, Schaenzlin J, Benaroya H. Structural Design of a Lunar Habitat. J Aerosp Eng 2006;19:133–57. doi:10.1061/(ASCE)0893-1321(2006)19:3(133).

[298] Szilard R. Structures for the Moon. Am Soc Civ Eng 1959.

[299] Sen S, Schofield E, O'Dell S, Ray C. A Viable Scheme For Elemental Extraction And Purification Using In-Situ Planetary Resources. 1st Sp. Explor. Conf. Contin. Voyag. Discov., Reston, Virigina: American Institute of Aeronautics and Astronautics; 2005. doi:10.2514/6.2005-2787.

[300] Liu A, Shi Z, Hu X, Gao B, Wang Z. Lunar Soil Simulant Electrolysis Using Inert Anode for Al-Si Alloy and Oxygen Production. J Electrochem Soc 2017. doi:10.1149/2.1381702jes.

[301] Ramamurty U, Paul A. Variability in mechanical properties of a metal foam. Acta Mater 2004. doi:10.1016/j.actamat.2003.10.021.

[302] Banhart J. Manufacturing routes for metallic foams. JOM 2000. doi:10.1007/s11837-000-0062-8.

[303] Banhart J. Manufacture, characterisation and application of cellular metals and metal foams. Prog Mater Sci 2001. doi:10.1016/S0079-6425(00)00002-5.

[304] Gaffey MJ, McCord TB. Asteroid surface materials - Mineralogical characterizations and cosmological implications. 8th Lunar Sci. Conf., 1977.

[305] Zhao CY, Lu TJ, Hodson HP. Natural convection in metal foams with open cells. Int J Heat Mass Transf 2005. doi:10.1016/j.ijheatmasstransfer.2005.01.002.

[306] Stöbener K, Rausch G. Aluminium foam-polymer composites: Processing and characteristics. J. Mater. Sci., vol. 44, 2009, p. 1506–11. doi:10.1007/s10853-008-2786-8.

[307] Hanan J, Johnson W, Peker A. Advanced Metal Foam Structures for Outer Space. 2005.

[308] Veazey C. Amorphous metallic foam: synthesis and mechanical properties. California Institute of Technology, 2007.

[309] González C, Vilatela JJ, Molina-Aldareguía JM, Lopes CS, LLorca J. Structural composites for multifunctional applications: Current challenges and future trends. Prog Mater Sci 2017. doi:10.1016/j.pmatsci.2017.04.005.

[310] Krenkel W, Berndt F. C/C-SiC composites for space applications and advanced friction systems. Mater Sci Eng A 2005. doi:10.1016/j.msea.2005.08.204.

[311] Pater RH, Curto PA. Advanced materials for space applications. Acta Astronaut 2007. doi:10.1016/j.actaastro.2007.06.002.

[312] Misra M. Engineered Materials for Space Applications. Astronaut Gr J 1990:14–23.

[313] Naser MZ, Hawileh RA, Rasheed HA. Performance of RC T-beams externally strengthened

with CFRP laminates under elevated temperatures. J Struct Fire Eng 2014;5:1–24. doi:10.1260/2040-2317.5.1.1.

[314] Rasheed HA. Strengthening design of reinforced concrete with FRP. CRC Press; 2014.

[315] Rawal S. Metal-matrix composites for space applications. JOM 2001. doi:10.1007/s11837-001-0139-z.

[316] Rawal S, Misra M. Measurement of mechanical and thermophysical properties of dimensionally stable materials for space applications. 1992.

[317] Chen T, Chow BJ, Wang M, Shi Y, Zhao C, Qiao Y. Inorganic–Organic Hybrid of Lunar Soil Simulant and Polyethylene. J Mater Civ Eng 2015. doi:10.1061/(asce)mt.1943-5533.0001450.

[318] Williamson JR. Advanced materials for space structures. Acta Astronaut 1991. doi:10.1016/0094-5765(91)90167-4.

[319] Sen S, Carranza S, Pillay S. Multifunctional Martian habitat composite material synthesized from in situ resources. Adv Sp Res 2010;46:582–92. doi:10.1016/j.asr.2010.04.009.

[320] Milkovich, Scott M. ; Herakovich, Carl T. ; Sykes, George F. J. Space Radiation Effects on Graphite-Epoxy Composite Materials. Cent Compos Mater Struct 1984.

[321] Cole GS, Sherman AM. Light weight materials for automotive applications. Mater Charact 1995. doi:10.1016/1044-5803(95)00063-1.

[322] LLorca J. Fatigue of particle-and whisker-reinforced metal-matrix composites. Prog Mater Sci 2002. doi:10.1016/S0079-6425(00)00006-2.

[323] Johnson SWS, Leonard RS. Design of lunar-based facilities: The challenge of a lunar observatory. Lunar Bases Sp. Act. 21st Century, 1985, p. 413.

[324] Bowles D, Tenney D. Composite tubes for the space station truss structure. 1986.

[325] Tóth J, Desai C. Development, testing and modeling of ceramic composites for lunar applications. Eng. Constr. Oper. Sp. IV, 1994, p. 358–67.

[326] Desai C, Girdner K. Structural materials from lunar simulants through thermal liquefaction. Eng. Constr. Oper. space-III, 1992, p. 528–36.

[327] Fitchmun D. Thermoplastic thermoformable composite material. 4,778,717, 1988.

[328] Noever D, Smith D, Sibille L, Brown S, Cronise R, Lehoczky S. High performance materials applications to Moon/Mars missions and bases. Sp. 98, 1998, p. 275–85.

[329] Lee S. Lunar Building Materials-Some Considerations on the Use of Inorganic Polymers.

Sp. Resour. Sp. Settlements, 1979, p. 233.

[330] Cotterill R. Glassy Metals: A new class of metallic materials offers challenges to the research scientist and may be useful in a variety of applications. Am Sci 1976:430–7.

[331] Chen T, Chow BJ, Zhong Y, Wang M, Kou R, Qiao Y. Formation of polymer micro-agglomerations in ultralow-binder-content composite based on lunar soil simulant. Adv Sp Res 2018. doi:10.1016/j.asr.2017.10.050.

[332] Leng J, Lan X, Liu Y, Du S. Shape-memory polymers and their composites: Stimulus methods and applications. Prog Mater Sci 2011. doi:10.1016/j.pmatsci.2011.03.001.

[333] Otsuka K, Ren X. Physical metallurgy of Ti-Ni-based shape memory alloys. Prog Mater Sci 2005. doi:10.1016/j.pmatsci.2004.10.001.

[334] Sun L, Huang WM, Ding Z, Zhao Y, Wang CC, Purnawali H, et al. Stimulus-responsive shape memory materials: A review. Mater Des 2012. doi:10.1016/j.matdes.2011.04.065.

[335] McDonald Schetky L. Shape memory alloy applications in space systems. Mater Des 1991. doi:10.1016/0261-3069(91)90089-M.

[336] Kalra S, Bhattacharya B, Munjal BS. Design of shape memory alloy actuated intelligent parabolic antenna for space applications. Smart Mater Struct 2017. doi:10.1088/1361-665X/aa7468.

[337] Ellery A. Environment-robot interaction - The basis for mobility in planetary micro-rovers. Rob. Auton. Syst., 2005. doi:10.1016/j.robot.2004.08.007.

[338] Liang C, Rogers CA, Malafeew E. Investigation of shape memory polymers and their hybrid composites. J Intell Mater Syst Struct 1997. doi:10.1177/1045389X9700800411.

[339] Darooka D, Scarborough S, Cadogan D. An evaluation of inflatable truss frame for space applications. Proc. 42nd AIAA/ASME/ASCE/AHS/ASC Struct. Struct. Dyn. Mater. Conf. Exhib., 2001. doi:https://doi.org/10.2514/6.2001-1614.

[340] Liu Y, Du H, Liu L, Leng J. Shape memory polymers and their composites in aerospace applications: A review. Smart Mater Struct 2014. doi:10.1088/0964-1726/23/2/023001.

[341] Company TNA. Introduction To Shape Memory Alloys 2003. http://www.tinialloy.com/pdf/introductiontosma.pdf.

[342] Gross K. Mechanical characterization of shape memory polymers to assess candidacy as morphing aircraft skin. University of Pittsburgh, 2009.

[343] Liu C, Qin H, Mather PT. Review of progress in shape-memory polymers. J Mater Chem 2007. doi:10.1039/b615954k.

[344] Sokolowski WM, Tan SC. Advanced Self-Deployable Structures for Space Applications. J Spacecr Rockets 2007;44:750–4. doi:10.2514/1.22854.

[345] Roedel H, Lepech MD, Loftus DJ. Protein-Regolith Composites for Space Construction. Earth Sp 2014 2014:291–300. doi:10.1061/9780784479179.033.

[346] Lepore E, Bosia F, Bonaccorso F, Bruna M, … ST-2D, 2017 U. Spider silk reinforced by graphene or carbon nanotubes. IopscienceIopOrg n.d. doi:https://doi.org/10.1088/2053-1583/aa7cd3.

[347] Lin J, Knoll C, Willey C. Shape Memory Rigidizable Inflatable (RI) Structures for Large Space Systems Applications, 2012. doi:10.2514/6.2006-1896.

[348] Lai A, Du Z, Gan CL, Schuh CA. Shape memory and superelastic ceramics at small scales. Science (80-) 2013. doi:10.1126/science.1239745.

[349] Rothschild LJ. Synthetic biology meets bioprinting: enabling technologies for humans on Mars (and Earth). Biochem Soc Trans 2016;44:1158–64. doi:10.1042/BST20160067.

[350] Roedel H, Plata IR, Lepech M, Loftus D. Sustainability assessment of protein-soil composite materials for limited resource environments. J Renew Mater 2015;3:183–94. doi:10.7569/jrm.2015.634107.

[351] Geim AK. Graphene: status and prospects. Science 2009;324:1530–4. doi:10.1126/science.1158877.

[352] Qin Z, Jung GS, Kang MJ, Buehler MJ. The mechanics and design of a lightweight three-dimensional graphene assembly. Sci Adv 2017;3:1–9. doi:10.1126/sciadv.1601536.

[353] NASA. NASA might build an ice house on Mars 2018. https://phys.org/news/2016-12-nasa-ice-house-mars.html.

[354] MICHALSKE TA, FREIMAN SW. A Molecular Mechanism for Stress Corrosion in Vitreous Silica. J Am Ceram Soc 1983. doi:10.1111/j.1151-2916.1983.tb15715.x.

[355] Uhlmann D, Onorato P, Scherer G. A simplified model for glass formation. Lunar Planet. Sci. Conf. Proc., 1979.

[356] Sani R, Koster J. Low-gravity fluid dynamics and transport phenomena. American Institute of Aeronautics and Astronautics; 1990.

[357] Li J, Tilbury CJ, Kim SH, Doherty MF. A design aid for crystal growth engineering. Prog Mater Sci 2016. doi:10.1016/j.pmatsci.2016.03.003.

[358] Cröll A, Kaiser T, Schweizer M, Danilewsky AN, Lauer S, Tegetmeier A, et al. Floating-zone and floating-solution-zone growth of GaSb under microgravity. J Cryst Growth 1998. doi:10.1016/S0022-0248(98)00215-2.

[359] Doremus R, Nordine P. Materials processing in the reduced gravity environment of space. MRS Symp. Proc., 1986.

[360] Hermanson KD, Huemmerich D, Scheibel T, Bausch AR. Engineered microcapsules fabricated from reconstituted spider silk. Adv Mater 2007. doi:10.1002/adma.200602709.

[361] Karana E, Giaccardi E, Nimkulrat N, Niedderer K. Alive. Active. Adaptive. Int. Conf. 2017 DRS Spec. Interes. Gr. Exp. Knowl., 2017.

[362] Crockett R, Fabes B, Nakamura T, Senior C. Construction of large lunar structures by fusion welding of sintered regolith. Eng. Constr. Oper. Sp. IV, 1994, p. 1116–27.

[363] Pletka BJ. Processing of Lunar Basalt Materials. Resour Near Earth Space, Univ Arizona Press 1993.

[364] Simonds C. Processing Lunar Soils. Eng. Constr. Oper. Sp., 1988, p. 90.

[365] Frenkel J. Viscous flow of crystalline bodies under the action of surface tension. J Phys 1945. doi:10.4319/lo.2013.58.2.0489.

[366] Bonanno A, Sproul A, Bernold LE. Thermal Energy Storage Capacity of Sintered Australian Lunar Soil Simulants, 2012. doi:10.1061/9780784412190.045.

[367] Appelbaum J, Flood DJ. Solar radiation on Mars. Sol Energy 1990;45:353–63. doi:10.1016/0038-092X(90)90156-7.

[368] Meurisse A, Cowley A, Cristoforetti S, Makaya A, Pambaguian L, Sperl M. solar 3D printing of lunar regolith. Eur. Lunar Symp., 2016.

[369] Meurisse A, Makaya A, Willsch C, Sperl M. Solar 3D printing of lunar regolith. Acta Astronaut 2018. doi:10.1016/j.actaastro.2018.06.063.

[370] Hoshino BT, Wakabayashi S, Yoshihara S, Hatanaka N. Key Technology Development for Future Lunar Utilization - Block production using lunar regolith - 2015;14:1–6.

[371] Clark DE, Sutton WH. Microwave Processing of Materials. Annu Rev Mater Sci 1996;26:299–331. doi:10.1146/annurev.ms.26.080196.001503.

[372] Goulas A, Binner JGP, Engstrøm DS, Harris RA, Friel RJ. Mechanical behaviour of additively manufactured lunar regolith simulant components. Proc Inst Mech Eng Part L J Mater Des Appl 2018. doi:10.1177/1464420718777932.

[373] Lim S, Prabhu VL, Anand M, Taylor LA. Extra-terrestrial construction processes – Advancements, opportunities and challenges. Adv Sp Res 2017;60:1413–29. doi:10.1016/j.asr.2017.06.038.

[374] Ishikawa Y, Sasaki T, Higasayama T. Simple and efficient methods to produce construction

materials for lunar and Mars bases. Eng. Constr. Oper. space-III, 1992, p. 1335–46.

[375] Goulas A, Friel RJ. Laser sintering of ceramic materials for aeronautical and astronautical applications. Laser Addit. Manuf., Woodhead Publishing; 2017, p. 373–98. doi:10.1016/B978-0-08-100433-3.00014-2.

[376] Martirosyan K, Luss D. Combustion synthesis of ceramic composites from Lunar soil simulant. 37th Annu. Lunar Planet. Sci. Conf., 2007.

[377] Moore JJ, Feng HJ. Combustion synthesis of advanced materials: Part I. Reaction parameters. Prog Mater Sci 1995. doi:10.1016/0079-6425(94)00011-5.

[378] Moore JJ, Feng HJ. Combustion synthesis of advanced materials: Part II. Classification, applications and modelling. Prog Mater Sci 1995. doi:10.1016/0079-6425(94)00012-3.

[379] Moore JJ, Readey DW, Feng HJ, Monroe K, Mishra B. The combustion synthesis of advanced materials. JOM 1994;46:72–8. doi:10.1007/BF03222640.

[380] Faierson E, Logan K. Geothermite reactions for in situ resource utilization on the moon and beyond. Earth Sp. 2010 Eng. Sci. Constr. Oper. Challenging Environ., 2010, p. 1152–61. doi:https://doi.org/10.1061/41096(366)106.

[381] Ferguson R, Shafirovich E, Mantovani J. Combustion Joining of Regolith Tiles for In-Situ Fabrication of Launch/Landing Pads on the Moon and Mars. 16th Bienn. Int. Conf. Eng. Sci. Constr. Oper. Challenging Environ., 2018.

[382] White C, Alvarez F, Shafirovich E. Combustible Mixtures of Lunar Regolith with Metals: Thermodynamic Analysis and Combustion Experiments. J Thermophys Heat Transf 2011;25:620–5. doi:10.2514/1.T3707.

[383] Delgado A, Shafirovich E. Towards better combustion of lunar regolith with magnesium. Combust Flame 2013;160:1876–82. doi:10.1016/j.combustflame.2013.03.021.

[384] Haagen C, Mink M, Chin E, Prisbrey W, Bhaduri SB, Bhaduri S, et al. Production of titanium silicide intermetallics in microgravity. Sp 2000, Proc 2000:431–7.

[385] Lin TD, Tseng L, Chou S. Lunar Concrete Made with the Dry-Mix/Steam-Injection Method, 2007. doi:10.1061/40177(207)82.

[386] Su N, Peng Y. The characteristics and engineering properties of dry-mix/steam-injection concrete. Cem Concr Res 2001;31:609–19. doi:https://doi.org/10.1016/S0008-8846(01)00460-4.

[387] Lin T, Su N. Lunar concrete update. Concr Int 1991:73–6.

[388] Pakulski DM, Knox KJ. Steam injection system for lunar concrete. Eng. Constr. Oper. Sp. III Sp. '92; Proc. 3rd Int. Conf. Denver, CO, May 31-June 4, 1992. Vol. 2 (A93-41976 17-

12), p. 1347-1358., vol. 2, 1992, p. 1347–58.

[389] Lin T, Tseng L, Chou S. Lunar concrete made with the dry-mix/steam-injection method. Eng. Constr. Oper. Sp. V, 1996, p. 592–9. doi:https://doi.org/10.1061/40177(207)82.

[390] Wilhelm S, Curbach M. Manufacturing of Lunar Concrete by Steam 2015:274–82. doi:10.1061/9780784479179.031.

[391] Hatanaka N, Ishida T. Hydration Reaction and Strength Development of Lunar Concrete Under Vacuum Condition. SAE Tech. Pap. Ser., 2010. doi:10.4271/2004-01-2270.

[392] Williamson RB. Solidification of Portland Cement. 1970.

[393] Ahrens T, Conference DC-L and PS, 1974 undefined. Shock compression and adiabatic release of lunar fines from Apollo 17. AdsabsHarvardEdu n.d.

[394] Ishikawa Y. Utilization of Regolith for Manufacturing Construction Material on Mars 19.1 Habitat on Mars 19.1.1 Requirement for Habitat. Mars, Springer; 2009, p. 543–50.

[395] Boyd R, Thompson P, Clark B. Duricrete and composites construction on Mars. case Mars III Strateg. Explor. Gen. Interes. Overv., 1989.

[396] Chow BJ, Chen T, Zhong Y, Qiao Y. Direct Formation of Structural Components Using a Martian Soil Simulant. Sci Rep 2017. doi:10.1038/s41598-017-01157-w.

[397] Effinger M, Tucker D. Statistical design study of lunar ceramic. 1994.

[398] Altemir DA, A. D. Cold press sintering of simulated lunar basalt. Lunar Planet Inst, Twenty-Fourth Lunar Planet Sci Conf Part 1 A-F p 23-24 (SEE N94-12015 01-91) 1993;24:23–4.

[399] Bochenek K, Basista M. Advances in processing of NiAl intermetallic alloys and composites for high temperature aerospace applications. Prog Aerosp Sci 2015. doi:10.1016/j.paerosci.2015.09.003.

[400] Sanders GB, Larson WE. Progress Made in Lunar In Situ Resource Utilization under NASA's Exploration Technology and Development Program. J Aerosp Eng 2013;26:5–17. doi:10.1061/(ASCE)AS.1943-5525.0000208.

[401] Girdner KK. Development and mechanical properties of structural materials from lunar simulants by thermal liquefaction. The University of Arizona., 1991.

[402] Afshar-Mohajer N, Wu CY, Sorloaica-Hickman N. Efficiency determination of an electrostatic lunar dust collector by discrete element method. J Appl Phys 2012. doi:10.1063/1.4739734.

[403] DUNNING J, SNYDER R. Electrophoretic separation of lunar soils in a space manufacturing facility. 4th Sp. Manuf. Proc. Fifth Conf., Reston, Virigina: American

Institute of Aeronautics and Astronautics; 1981. doi:10.2514/6.1981-3264.

[404] Lee PC-C, Clayton-Clyde P. Physical Properties and Processing of Asteroid Regoliths and Interiors. Thesis (PHD). CORNELL Univ. , Source DAI-B 58/05, p. 2470, Nov 1997, 285 pages., 1997.

[405] Walker D, Grove T. Ureilite smelting. Meteoritics 1993. doi:10.1111/j.1945-5100.1993.tb00633.x.

[406] Cutler A, Krag P. A carbothermal scheme for lunar oxygen production. Lunar Bases Sp. Act. 21st Century, 1985, p. 559.

[407] Sadoway DR. Recent Advances in Scale-up Development of Molten Regolith Electrolysis for Oxygen Production in support of a. AIAA Aerosp Sci Meet 2009. doi:10.2514/6.2009-659.

[408] Sibille L, Sadoway D, Tripathy P, Standish E. Performance Testing of Molten Regolith Electrolysis and Transfer of Molten Material for Oxygen and Metals Production on the Moon, 2013. doi:10.2514/6.2010-1550.

[409] Sviatoslavsky I. Processes and energy costs for mining lunar Helium-3. 1988.

[410] Kulcinski GL, Schmitt HHJ. Fusion Power from Lunar Resources. Fusion Technol 1992;21:2221–9. doi:10.13182/FST92-A29717.

[411] Wittenberg LJ, Santarius JF, Kulcinski GL. Lunar Source of ^{3}He for Commercial Fusion Power. Fusion Technol 1986;10:167–78. doi:10.13182/FST86-A24972.

[412] Sridhar KR, Finn JE, Kliss MH. In-situ resource utilization technologies for Mars life support systems. Adv Sp Res 2000. doi:10.1016/S0273-1177(99)00955-2.

[413] Zubrin R. In-Situ Propellant Production: The Key Technology Required for the Realization of a Coherent and Cost Effective Space Exploration Initiative. 42nd Congr. Int. Astronaut. Fed., 1991.

[414] Johnson-Freese J. Build on the outer space treaty. Nature 2017. doi:10.1038/550182a.

[415] Ghidini T. Materials for space exploration and settlement. Nat Mater 2018. doi:10.1038/s41563-018-0184-4.

[416] Abarbanel J, Aadeh W, Criswell M. Computer visualization analysis of a generic inflatable structure for a lunar/Martian base. Sp. Programs Technol. Conf., Reston, Virigina: American Institute of Aeronautics and Astronautics; 1995. doi:10.2514/6.1995-4062.

[417] Salehi H, Burgueño R. Emerging artificial intelligence methods in structural engineering. vol. 171. Elsevier; 2018. doi:10.1016/j.engstruct.2018.05.084.

[418] Naser MZ. Deriving temperature-dependent material models for structural steel through artificial intelligence. Constr Build Mater 2018;191:56–68. doi:10.1016/J.CONBUILDMAT.2018.09.186.

[419] Naser MZ. Properties and material models for modern construction materials at elevated temperatures. Comput Mater Sci 2019;160:16–29. doi:10.1016/J.COMMATSCI.2018.12.055.

[420] Seitllari A, Kutay ME. Soft Computing Tools to Predict Progression of Percent Embedment of Aggregates in Chip Seals. Transp Res Rec 2018:036119811875686. doi:10.1177/0361198118756868.

[421] Lai Z, Chen Q. Characterization and discrete element simulation of grading and shape-dependent behavior of JSC-1A Martian regolith simulant. Granul Matter 2017;19:69. doi:10.1007/s10035-017-0754-1.

[422] Chen Q, Lai Z, Moysey S, Shen M. Image-Based Shape Characterization and Three-Dimensional Discrete Element Modeling of a Granular Martian Regolith Simulant. Proc. GeoShanghai 2018 Int. Conf. Fundam. Soil Behav., 2018. doi:10.1007/978-981-13-0125-4_90.

[423] Papike JJ, Simon SB, Laul JC. The lunar regolith: Chemistry, mineralogy, and petrology. Rev Geophys 1982. doi:10.1029/RG020i004p00761.

[424] Gustafson RJ, White BC, Gustafson MA. Development of a high fidelity lunar soil simulant. AIP Conf. Proc., 2008. doi:10.1063/1.2844969.

[425] Freitas RA, Gilbreath WP, Freitas Jr R, Healy T, Long J. Advanced automation for space missions. J Astronaut Sci 1982;30:221. doi:10.1016/0165-6074(81)90105-8.

[426] Khoshnevis B, Bodiford MP, Burks KH, Ethridge E, Tucker D, Kim W, et al. Lunar contour crafting - A novel technique for ISRU-based habitat development. 43rd AIAA Aerosp Sci Meet Exhib - Meet Pap 2005:1–13. doi:10.2514/6.2005-538.

[427] Lietaert K, Thijs L, Neirinck B, Lapauw T, Morrison B, Lewicki C, et al. Meteorite as raw material for Direct Metal Printing: A proof of concept study. Acta Astronaut 2018. doi:10.1016/j.actaastro.2017.11.027.

[428] Mueller RP, Sibille L, Hintze PE, Lippitt TC, Mantovani JG, Nugent MW, et al. Additive Construction Using Basalt Regolith Fines, 2015. doi:10.1061/9780784479179.042.

[429] Tibbits S. 4D printing: Multi-material shape change. Archit Des 2014. doi:10.1002/ad.1710.

[430] Ge Q, Dunn CK, Qi HJ, Dunn ML. Active origami by 4D printing. Smart Mater Struct 2014. doi:10.1088/0964-1726/23/9/094007.

[431] Hager I, Golonka A, Putanowicz R. 3D Printing of Buildings and Building Components as the Future of Sustainable Construction? Procedia Eng., 2016. doi:10.1016/j.proeng.2016.07.357.

[432] Naser MZ. Space-native construction materials for earth-independent and sustainable infrastructure. Acta Astronaut 2019;155:264–73. doi:10.1016/J.ACTAASTRO.2018.12.014.

[433] Panda B, Paul SC, Mohamed NAN, Tay YWD, Tan MJ. Measurement of tensile bond strength of 3D printed geopolymer mortar. Measurement 2018;113:108–16. doi:10.1016/J.MEASUREMENT.2017.08.051.

[434] Zevalkink A, Smiadak DM, Blackburn JL, Ferguson AJ, Chabinyc ML, Delaire O, et al. A practical field guide to thermoelectrics: Fundamentals, synthesis, and characterization. vol. 5. 2018. doi:10.1063/1.5021094.

[435] Labeaga-Martínez N, Sanjurjo-Rivo M, Díaz-Álvarez J, Martínez-Frías J. Additive manufacturing for a Moon village. Procedia Manuf 2017;13:794–801. doi:10.1016/J.PROMFG.2017.09.186.

[436] Schmitt H. Return to the moon: exploration, enterprise, and energy in the human settlement of space. 2007.

[437] Mckay DS, Ming DW. Properties of Lunar Regolith. Dev Soil Sci 1990;19:449–62. doi:10.1016/S0166-2481(08)70360-X.

[438] White DC, Hirsch P. Microbial Extraction of Hydrogen from Lunar Dust. Lunar Bases Sp. Act. 21st Century. Houston, TX, Lunar Planet. Institute, Ed. by W. W. Mendell, 1985, p.591, 1985, p. 591.

[439] Kong P, Ebihara M, Palme H. Siderophile elements in Martian meteorites and implications for core formation in Mars. Geochim Cosmochim Acta 1999. doi:10.1016/S0016-7037(99)00030-7.

[440] Meinel C. Metal carbonyl refining and vaporforming for asteroidal ores. Sp. Manuf. 5 Eng. With Lunar Asteroidal Mater., 1985.

[441] Landis GA. Meteoritic steel as a construction resource on Mars. Acta Astronaut 2009;64:183–7. doi:10.1016/j.actaastro.2008.07.011.

[442] West MD, Clarke JDA. Potential martian mineral resources: Mechanisms and terrestrial analogues. Planet Space Sci 2010;58:574–82. doi:10.1016/J.PSS.2009.06.007.

[443] Sankar K, Sutrisno A, Kriven WM. Slag-fly ash and slag-metakaolin binders: Part II — Properties of precursors and NMR study of poorly ordered phases. J Am Ceram Soc 2019;102:3204–27. doi:10.1111/jace.16224.

[444] Sankar K, Stynoski P, Kriven WM. Sodium silicate activated slag-fly ash binders: Part III—Composition of soft gel and calorimetry. J Am Ceram Soc 2019;102:3175–90. doi:10.1111/jace.16219.

[445] Hardjito D, Rangan BV. Development and Properties of Low-Calcium Fly Ash-Based Geopolymer Concrete 2005.

[446] Hardjito D, Wallah SE, Sumajouw DMJ, Rangan BV. On the Development of Fly Ash-Based Geopolymer Concrete. ACI Mater J 2004;101:467–72. doi:10.14359/13485.

[447] Song G, Gu H, Mo YL. Smart aggregates: Multi-functional sensors for concrete structures - A tutorial and a review. Smart Mater Struct 2008. doi:10.1088/0964-1726/17/3/033001.

[448] Tsai S. Introduction to composite materials. Routledge; 2018.

[449] Jones R. Mechanics of composite materials. CRC Press; 2014.

[450] Leist SK, Zhou J. Current status of 4D printing technology and the potential of light-reactive smart materials as 4D printable materials. Virtual Phys Prototyp 2016;11:249–62. doi:10.1080/17452759.2016.1198630.

This is a preprint draft. The published article can be found at: https://doi.org/10.1016/j.pmatsci.2019.100577

Please cite this article as:
Naser M.Z. (2019). "Extraterrestrial Construction Materials." *Progress in Materials Science*. Vol. 105, 100577. https://doi.org/10.1016/j.pmatsci.2019.100577.

Vitae

M. Z. Naser is an assistant professor at the Glenn Department of Civil Engineering at Clemson University. His research interests cover the areas of cognitive and autonomous infrastructure, structural engineering in extreme conditions, materials science, and computational intelligence and mechanics. Dr. Naser is currently serving as a committee member in two ACI committees (216 and 447) as well as ASCE Fire Protection Committee. He is a registered professional engineer in the state of Michigan.

This is a preprint draft. The published article can be found at: https://doi.org/10.1016/j.pmatsci.2019.100577

Please cite this article as:
Naser M.Z. (2019). "Extraterrestrial Construction Materials." *Progress in Materials Science*. Vol. 105, 100577. https://doi.org/10.1016/j.pmatsci.2019.100577.

List of Figures

Please cite this article as:
Naser M.Z. (2019). "Extraterrestrial Construction Materials." *Progress in Materials Science*. Vol. 105, 100577. https://doi.org/10.1016/j.pmatsci.2019.100577.

This is a preprint draft. The published article can be found at: https://doi.org/10.1016/j.pmatsci.2019.100577

Please cite this article as:
Naser M.Z. (2019). "Extraterrestrial Construction Materials." *Progress in Materials Science*. Vol. 105, 100577. https://doi.org/10.1016/j.pmatsci.2019.100577.

This is a preprint draft. The published article can be found at: https://doi.org/10.1016/j.pmatsci.2019.100577

Please cite this article as:
Naser M.Z. (2019). "Extraterrestrial Construction Materials." *Progress in Materials Science*. Vol. 105, 100577. https://doi.org/10.1016/j.pmatsci.2019.100577.

List of Tables

This is a preprint draft. The published article can be found at: https://doi.org/10.1016/j.pmatsci.2019.100577

Please cite this article as:
Naser M.Z. (2019). "Extraterrestrial Construction Materials." *Progress in Materials Science*. Vol. 105, 100577. https://doi.org/10.1016/j.pmatsci.2019.100577.